Generation and Utilization of NADPH in the Endoplasmic Reticulum: Novel Insight into the Role of Luminal NADPH in Pathophysiological Processes

Inauguraldissertation

zur

Erlangung der Würde eines Doktors der Philosophie

vorgelegt der

Philosophisch-Naturwissenschaftlichen Fakultät

der Universität Basel

von

Balázs Legeza

aus Nyíregyháza, Ungarn

Basel, 2013

Genehmigt von der Philosophisch-Naturwissenschaftlichen Fakultät

auf Antrag von

Prof. Dr. Alex Odermatt

Prof. Dr. Martin Spiess

Basel, den 16.10.2012

Prof. Dr. Jörg Schibler

Dekan

Summary

Increasing evidence emphasizes the importance of the redox balance in the endoplasmic reticulum (ER). Disturbance of redox regulation can cause ER stress and contribute to the development of metabolic disease, cancer and neurodegenerative disorders. Nevertheless, the mechanisms underlying the well-regulated NADPH balance, and the generation and utilization of pyridine nucleotides in the luminal compartment are insufficiently understood. The aim of this work is to identify novel components involved in NADPH regulation in the ER.

Due to the observation that fructose-6-phosphate stimulates luminal NADPH generation, and enhances 11β-hydroxysteroid dehydrogenase 1 dependent glucocorticoid activation, we hypothesized the existence of a luminal hexose-6-phosphate isomerase. Using microsomal fractions, we characterized a novel luminal hexose-6-phosphate isomerase, which converts fructose-6-phosphate to glucose-6-phosphate. By further purification and protein sequencing, we try to identify the gene encoding this enzyme.

In order to identify additional genes encoding luminal enzymes involved in NAPDH generation in the ER (potential enzymes of the luminal pentose-phosphate pathway), we decided to apply a combination of classical activity-guided purification, mass-spectrometric analysis and sequence analysis. Furthermore, for promising candidate proteins, we attempt to confirm their intracellular localization and investigate their impact on luminal NADPH balance. To determine whether ER-associated and membrane proteins are facing the cytoplasmic or luminal compartment, we optimized the methods to determine membrane topology and intracellular localization. We used selective semi-permeabilization analysis using digitonin, followed by immunodetection and confocal microscopy, proteinase protection assays of microsomal preparations as well as glycosylation assays.

Furthermore, we determined the membrane topology of 17β-hydroxysteroid dehydrogenase 3, an enzyme responsible for the oxoreduction of androstenedione. We provide information on the functional impact of hexose-6-phosphate dehydrogenase, as well as the nutritional state of the cell on the formation of testosterone.

The findings are relevant regarding the understanding of the coupling between the cellular energy state, hormonal regulation, ER redox regulation and oxidative stress-induced damage in a cell.

Chapter I:

General introduction

The endoplasmic reticulum (ER) has a prominent role in protein and lipid synthesis, including phospholipids and steroids, metabolism of carbohydrates, regulation of calcium homeostasis and also importantly contributes to the metabolism of drugs and the detoxification of xenobiotics. The ER membrane allows to separate reactions in the luminal space from those in the cytoplasm, thus representing another level of regulation of metabolic processes.

Besides some nonspecific permeability of the ER membrane, which is mainly attributed to the translocon peptide channel (Heritage et al., 2001; Lizak et al., 2008), the specific luminal environment is maintained by the expression of selective transporters in the ER membrane. In the last decade, increasing evidence supported the hypothesis that these transmembrane traffic activities regulate important cytosolic and luminal metabolic processes (Csala et al., 2006). The membrane barrier preserves characteristic differences between the compositions of the two compartments. The composition of the major redox buffers, as well as the luminal Ca^{2+} concentration - due to a continuous inward ion pumping ATPase – is remarkably different the conditions in the cytoplasm. The luminal environment has been considered more oxidizing than the cytosol; however, the relatively oxidized state of the luminal thiol–disulfide system is generated by local oxidation rather than active transport activities.

Probably the most important functions of the ER are the synthesis and the post-translational modifications of secretory and membrane proteins. The lumen of the ER provides a powerful protein-folding machinery composed of chaperones, foldases, and sensors that are able to detect the presence of misfolded or unfolded proteins. Alterations of the luminal redox conditions, either in oxidizing or reducing direction or physiological and pathological effects as well as experimental agents that affect the synthesis and normal folding process, are sensed by the accumulation of misfolded/unfolded proteins. It induces ER stress and triggers unfolded protein response (UPR), an intracellular signaling pathway that coordinates the balance between ER protein-folding demand with protein-folding capacity. The UPR is essential for the cell to adapt to homeostatic alterations that cause protein misfolding and induce programmed cell death if these attempts fail.

The aim of this chapter is to summarize the intermediary metabolism pathways localized in the ER lumen and to give an overview of the major redox systems (thiol/disulfide and reduced/oxidized pyridine nucleotide couples), especially focusing on the connection between pyridine nucleotide redox homeostasis and the metabolic environment in this organelle.

1.1 The redox environment of the ER

The proteome and metabolome of the ER are characteristically different compartment from the other subcellular compartments. Separated by a membrane barrier, the ER contains cytosol-independent pools of the main electron carriers of the major redox systems *i.e.* the thiol/disulfide couple and the reduced and oxidized pyridine nucleotides. The redox potential in the ER lumen, defined by the oxidized state of the thiol/disulfide system is approximately -180 mV, which is much higher than that of the cytosol (-230 mV) (Hwang et al., 1992). In agreement with the presence of oxidative protein folding that requires oxidizing power the luminal environment has been considered more oxidizing than the cytosol. In the ER, the ratio of glutathione (GSH) to glutathione disulfide (GSSG) is much lower compared to that of the cytosol. This observation reflects the predominance of disulfide bridges in the ER and free cysteinyl thiols in cytosolic proteins (Bass et al., 2004; Dixon et al., 2008).

The disulfide bond formation in secretory and membrane proteins is catalyzed by an electron relay system. The key participants of this complex system are oxidoreductases, protein disulfide isomerase (PDI) and ER oxidoreductin 1-α (Ero1-α), and the ultimate electron acceptor is the oxygen (Appenzeller-Herzog et al., 2010; Depuydt et al., 2011). The thiol oxidase flavoprotein Ero1-α is oxidizing the active cysteinyl thiols of PDI and delivers the electrons to oxygen, converting it to hydrogen peroxide (Frand and Kaiser, 1998; Pollard et al., 1998; Cabibbo et al., 2000). In the absence of peroxidases, the generated H_2O_2 can also oxidize PDI, yielding two molecules of H_2O (Karala et al., 2009). On the other hand, GSH in the ER appears to be required for the reduction of non-native disulfide bonds and to maintain a pool of reduced PDI for catalysis of disulfide bond isomerization reactions (Molteni et al., 2004). In this context, the glutathione and protein thiols compete for oxidizing power during disulfide bond formation.

Until now, glutathione synthesis has not been reported in the ER. The luminal glutathione pool must be fueled from the cytosol and it is restricted by specific transport barriers. Since results of transport measurements showed that GSSG cannot pass through the ER membrane, it cannot efficiently counteract luminal oxidation of GSH (Bánhegyi et al., 1999). Therefore, the low luminal GSH/GSSG ratio can be defined as the consequence of oxidative protein folding, rather than the cause. The luminal GSSG is generated by PDI as a by-product of isomerization (Ellgaard and Ruddock, 2005) or via the action of H_2O_2 (Karala et al., 2009), produced by Ero1-α. In other terms, extensive thiol oxidation is necessary for appropriate protein processing but might come at the price of decreased antioxidant capacity of the ER lumen (Csala et al., 2010).

This hypothesis has been verified by recent observations. The reoxidation of PDI-family members and GSH after reductive challenge is rapid, while the GSSG-dependent PDI oxidation is able to occur in Ero1-deficient cells as a possible Ero1-independent pathway for disulfide generation and the oxidation

of PDI in the ER (Appenzeller-Herzog et al., 2010). In line with the transport measurements, this rapid recovery process could neither be explained through import of GSH or nascent proteins from the cytosol, nor by the escape of disulphide-bonded molecules from the ER through the secretory pathway. Appenzeller-Herzog and colleagues proposed that a dynamic equilibrium is existing between two oxidation mechanisms of substrate proteins through PDI-family members. In the Ero1-α-driven oxidation pathway for *de novo* disulfide formation, Ero1-α oxidizes PDI, thereby producing H_2O_2. The byproduct H_2O_2 can also oxidize PDI as mentioned *above*. In turn, GSH is oxidized to GSSG. The accumulation of GSSG will promote GSSG-driven oxidation of PDIs and also shutdown Ero1-α because of low availability of reduced PDI. Namely, Ero1-α is regulated by the oxidized state of PDI. Reduced PDI keeps Ero1-α in an active state (Appenzeller-Herzog et al., 2008). In the GSSG-driven oxidation pathway the PDIs will also then oxidize substrate proteins (Figure 1). The interplay between the two pathways depends on the redox state of the glutathione redox couple in the ER; it is required for the maintenance of its characteristic redox homeostasis and it is a prerequisite for appropriate oxidative protein folding. However, one should note that results from Ero1 double mutant cells provide strong evidence for the existence of another, Ero1-independent generation of disulfides (Zito et al., 2010a). Besides the contribution of other prominent redox couples in the ER and the recently identified peroxiredoxin IV (an Ero1-independent pathway (Zito et al., 2010b)), the Ero1- and GSSG-driven substrate protein oxidation through PDIs constitutes a central element of ER redox control and oxidative protein folding in the ER.

Fig.1. Different oxidation mechanisms of substrate proteins through PDI-family members (Appenzeller-Herzog et al., 2010).
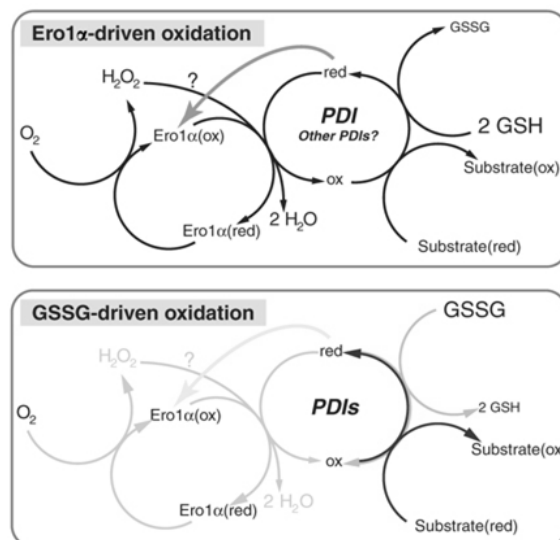
Similar to other subcellular organelles, the alternative major redox buffers in the ER lumen is the reduced/oxidized pyridine nucleotide couple. The phosphorylated nicotinamide adenine dinucleotide ($NADP^+$) and nicotinamide adenine dinucleotide (NAD) are the major water-soluble electron carriers in the metabolism (Pollak et al., 2007). Although the pyridine nucleotides are present in all subcellular compartments, they are only synthesized in the cytosol and the mitochondria (Nikiforov et al., 2011).

Because cellular membranes are impermeable for pyridine nucleotides, the origin of the luminal pyridine nucleotide pool is ambiguous. Bublitz and colleagues in early studies proposed the existence of enzymes in the ER for the synthesis of nucleotides, coenzymes and amino acids. They provided evidence for the existence of a luminal pentose-phosphate pathway (Bublitz and Steavenson, 1988). Most of the dehydrogenase enzymes participating in the main catabolic pathways of carbohydrate and lipid metabolism (glycolysis, citrate cycle, fatty acid oxidation) load NAD^+ with electrons, while only few cytosolic dehydrogenases (glucose-6-phosphate dehydrogenase (G6PDH), 6-phosphogluconate dehydrogenase (6PGDH), malic enzyme and isocitrate dehydrogenase) use $NADP^+$ as electron acceptor. On the other hand, NADH principally delivers electrons to the mitochondrial respiratory chain, whereas the main NADPH consumption occurs during biosynthesis, biotransformation and antioxidant defense.

The pyridine nucleotide redox system is tightly coupled to the thiol/disulfide system in the cytosol. The GSSG is mainly reduced by the NADPH-dependent enzyme glutathione reductase. In addition, the ascorbate/dehydroascorbate (DHA) system is influenced by the two main redox couple systems. Dehydroascorbate can be reduced by NADPH-dependent (Del Bello B et al., 1994) or GSH-dependent (Maellaro E et al., 1997) reductases. In the ER, the coupling has not been observed, because of the lack of NADPH-dependent DHA reductase and glutathione reductase (Piccirella et al., 2006). The addition of both GSH and GSSG does not influence the redox state of pyridine nucleotides in liver microsomes. Furthermore the reduced or oxidized pyridine nucleotides are unable to affect the redox state of microsomal thiols or influence oxidative protein folding (Piccirella et al., 2006; Marquardt et al., 1993.). These observations suggest that the pyridine nucleotide redox system is separated from the GSH/GSSG couple in the ER lumen. Nevertheless, one possible connection between the two redox systems might exist: there might be a competition between NADPH and thiols for H_2O_2 detoxification, and NADPH might be involved in disulfide bond reduction during the ERAD; however, these possibilities need further investigations to be verified.

Besides the two major redox systems (glutathione and pyridine nucleotides), other prominent redox couples, electron transfer compounds are presented in the ER, such as ascorbate (vitamin C) - dehydroascorbic acid (DHA) , tocopherol (vitamin E), flavin-adenin-dinucleotide (FAD), flavinmononucleotide (FMN), vitamin K, and ubiquinone. Although their presence in the ER is evident because of their requisite for various ER function, the role in redox homeostasis and protein folding - as well as their membrane transport and concentration - remains unclear. The ascorbate and dehydroascorbic acid redox couple contributes to the oxidative protein folding in the ER in the following way: ascorbate acts as an antioxidant and cofactor for enzymes in the lumen, while its oxidized form, dehydroascorbic acid, can accept electrons from PDI (Wells et al., 1990; Nardai et al., 2001) through glutathione (May et al., 1996) and also through substrate proteins (Saaranen et al., 2010).

1.2 Maintenance of the NADPH pool in the ER lumen

The ER contains a pyridine nucleotide pool that is independent of that of the cytoplasm. The luminal $NADPH/NADP^+$ ratio is lower than that in the cytoplasm. The cytosolic pentose-phosphate pathway is a well described mechanism for NADPH synthesis and generation. It generates ribose-phosphate, carbon dioxide and NADPH upon metabolism of glucose-6-phosphate (G6P). The oxidative steps of the pentose-phosphate pathway include the conversion of G6P to 6-phosphogluconate (catalyzed by glucose-6-phosphate dehydrogenase (G6PDH)), which is then further metabolized to ribulose-5-phosphate (catalyzed by 6-phosphogluconate dehydrogenase (6PGDH)). Ribulose-5-phosphate is essential for the synthesis of nucleotides, coenzymes and amino acids. The by-product NADPH is utilized for the reduction of various endogenous compounds (e.g. hormones, lipids, vitamins) and for biotransformation of xenobiotics. Several membrane-embedded biosynthetic and biotransforming enzymes (cytochrome P450 (CYP450) monooxygenases, 3-hydroxy-3-methyl-glutaryl-CoA reductase, biliverdin reductase) catalyze their reactions on the outer surface of the lipid bilayer and hence utilize cytosolic NADPH. On the other side, until now, only one enzyme, 11β-hydroxysteroid dehydrogenase type 1 (11β-HSD1) has been convincingly shown to be located in the ER (Ozols, 1995; Mziaut et al., 1999; Odermatt et al., 1999) and utilize NADPH (Bánhegyi et al., 2004; Atanasov et al., 2004). Another enzyme reported to face the ER and consume luminal NADPH is the NADPH cytochrome b5 oxidoreductase (NCB5OR) (Zhu et al., 2004). However, the luminal localization and function as well as the dependence on luminal NADPH remain to be confirmed.

While the cytosolic pentose-phosphate pathway has been extensively investigated, the luminal NADPH pool only recently received more attention due to the discovery of the ER-luminal NADPH generating enzyme hexose-6-phosphate dehydrogenase (H6PDH). This enzyme catalyzes the first two steps of the pentose-phosphate pathway by converting G6P and $NADP^+$ to 6-phosphogluconate and NADPH. H6PDH has a broad substrate specificity compared to G6PDH; it utilizes not only G6P but also other hexose-6-phosphates, such as galactose-6-phosphate, glucosamine-6-phosphate, 2-deoxyglucose-6-phosphate, as well as simple glucose although inefficiently (Beutler and Morrison; 1967). It was found that H6PDH has a wide tissue distribution (Gomez-Sanchez et al., 2008; Marcolongo et al., 2011), suggesting housekeeping function of the enzyme. H6PDH has been suggested to act as a nutrient sensor and as a prosurvival factor (Mandl J et al., 2009). The native substrate (G6P) supply is ensured by influx across the ER membrane mediated by specific G6P transporter (G6PT) (Gerin and Van Schaftingen, 2002). This transporter is part of G6Pase system in the ER. The G6Pase has its catalytic site oriented towards the lumen, and that it dependent on transporters that supply G6P, and export glucose and phosphate (Van Schaftingen and Gerin, 2002).

Growing interest in H6PDH is due to its major role in the maintenance of the NADPH/NADP$^+$ ratio in the lumen. H6PDH seems to be the major, but possibly not the only, enzyme responsible for NADPH generation within the ER. Recent studies showed that H6PDH deficiency decreased but did not eliminate NADPH content in liver and soleus microsomes (Rogoff et al., 2010). This observation corresponds with observations from H6PDH knock-out mice. No growth abnormalities were observed in mutant mice at birth (Lavery et al., 2006). Nevertheless, skeletal myopathy with activation of the UPR pathway was observed in mutant mice (Lavery et al., 2008).

Since the ER membrane is not permeable to pyridine nucleotides, the major function of H6PDH is to provide NADPH for luminal reductases. It is surprising that so little information is available on the use of NADPH for reductases in the ER. One of these enzymes, 11β-HSD1 is responsible for prereceptorial activation of glucocorticoids. Glucocorticoid hormones are essential for the coordinated regulation of metabolic and immune responses. They form an important component of adaptation environmental challenges. Glucocorticoids exert their effects mainly by activating glucocorticoid receptors (GR) and mineralocorticoid receptors (MR). Glucocorticoids regulate pathways leading to cellular proliferation, differentiation, or death, in response to infection, tissue damage, and inflammation. By converting intrinsically inert glucocorticoids (cortisone, 11-dehydrocorticosterone) into their active forms (cortisol, corticosterone), 11β-HSD1 increases the local availability glucocorticoids (Tomlinson et al., 2004). The activity of 11β-HSD1 has attracted increasing interest due to its role in the pathogenesis of various metabolic diseases. Increased expression and activity of 11β-HSD1 have been implicated in the pathomechanism of hypertension, type 2 diabetes, atherosclerosis, obesity, age-related cognitive dysfunction, osteoporosis and arthritis (Masuzaki et al., 2001; Hermanowski-Vosatka et al., 2005; Chapman and Seckl, 2008).

In our lab it was shown that the catalytic site of 11β-HSD1 is oriented into the ER lumen (Odermatt et al., 1999). Although the enzyme reaction is reversible *in vitro*, the enzyme acts as a reductase *in vivo*. The fact that the actual direction largely depends on the redox state of the pyridine nucleotides (Atanasov et al., 2004; Bánhegyi et al., 2004) and that the physiological direction of 11β-HSD1 is reductase suggests a high luminal NADPH/NADP$^+$ ratio in the ER, which has not yet been directly determined.

As mentioned above, this ratio is generated by H6PDH and probably other luminal enzymes. The functional cooperation of H6PDH with luminal reductases is based on common generation and utilization of luminal pyridine nucleotides, respectively (Figure 2). Furthermore, according to the present knowledge, the substrate source for H6PDH is ensured by G6PT. The availability of G6P reflects the nutritional and hormonal conditions of the cell. Therefore, the G6PT–H6PDH–11β-HSD1 triad can serve as an excellent candidate for a metabolic sensor connecting intermediary metabolism and hormone action in the ER. In line with this, measurements in intact cells suggested that the extracellular glucose levels influence 11β-HSD1 activity (Dzyakanchuk et al. 2008).

Lowering glucose in the culture medium dose-dependently decreased 11β-HSD1 reductase activity and diminished the cortisol/cortisone ratio (Dzyakanchuk et al. 2008). A NADPH/NADP$^+$ ratio of ten or higher was required for efficient microsomal 11β-HSD1 reductase activity. A significant increase in the activity started at a ratio 9:1 of NADPH/NADP$^+$ (Dzyakanchuk et al. 2008). Therefore, minor changes in the NADPH/NADP$^+$ ratio in a small compartment can lead to significant alterations in glucocorticoid activation. Recent observations indicate that not only G6P but also one other metabolite, fructose-6-phosphate (F6P) can maintain the high luminal NADPH/NADP$^+$ ratio (McCormick et al., 2008). Further chapters will discuss a series of experiments performed in our laboratories, regarding how F6P can enter the ER lumen and stimulate intraluminal NADPH formation via its isomerization to G6P.

Fig.2. Systemic model of the G6PT–H6PDH–11β-HSD1 triad in the ER lumen.
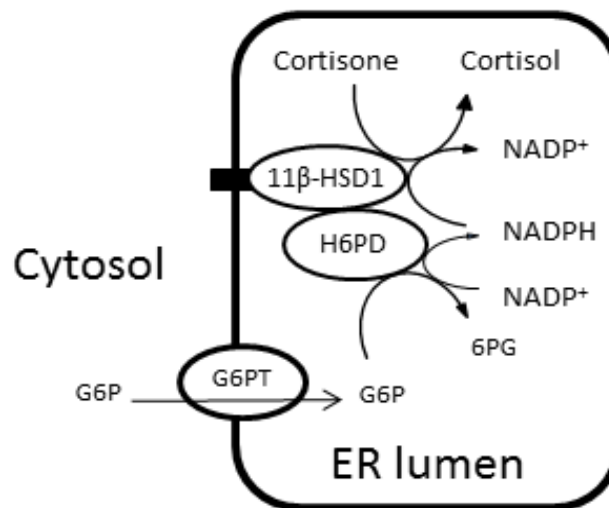
Further investigations of the functional cooperation between 11β-HSD1 and H6PDH revealed a direct physical interaction between the two enzymes. Coimmunoprecipitation, Far-Western and FRET techniques were applied to study recombinant H6PDH and 11β-HSD1 in HEK-293 cells (Atanasov et al., 2008). Furthermore, it was confirmed that the N-terminal 39 residues of 11β-HSD1 are sufficient for luminal orientation and that the N-terminal luminal residues of 11β-HSD1 are involved in the interaction with H6PDH. This direct interaction allows the direct supply of NADPH to 11β-HSD1 in a close proximity for the efficient reduction of cortisone to cortisol despite a rather oxidative environment within the ER lumen. Zhang and colleagues confirmed the physical interaction between 11β-HSD1 and H6PDH (Zhang et al., 2009). Moreover, they showed that the N-terminal domain of H6PDH can directly interact with 11β-HSD1, which was sufficient for the association. These findings provide explanation for the luminal localization of H6PDH, since there is no obvious retention signal in the H6PDH sequence. It suggests that the direct interaction with 11β-HSD1 might anchor H6PDH to the ER membrane.

1.3 Enzymatic reactions that require luminal NADPH

The current knowledge on the use of NADPH for enzymatic reactions in the ER is limited. Several enzymes involved in the metabolism of bile acids, cholesterol, triglyceride, oxysterols, steroids and xenobiotics are localized in the ER membrane. Therefore, it is important to solve the membrane topology of these enzymes. Particularly, it is crucial to know whether an enzyme faces the cytoplasm or the ER in order to understand its function, regulation and physiological role. The 11β-HSD1, whose NADPH consumption has been largely characterized, is a good example. The enzyme has other glucocorticoid-independent functions that require NADPH. Our group and others demonstrated that 11βHSD1 accepts various other substrates such as 7-oxocholesterol, 7-oxodehydroepiandrosterone (7-oxo-DHEA) and 7-oxolithocholic acid (7-oxo-LCA) (Nashev et al., 2007; Odermatt and Nashev, 2010; Schweizer et al., 2004; Odermatt et al., 2011; Hult et al., 2004; Muller et al., 2006). These findings suggest that this enzyme has additional functions in the metabolism of neurosteroids, oxysterols and bile acids as well as in the detoxification of various xenobiotics that contain reactive carbonyl groups. There are many studies on the effect of inhibitors of cortisone reduction and the consequences on circulating glucocorticoid levels as well as on the transcriptional regulation of 11β-HSD1 in obesity and diabetes. Nevertheless, it is important to investigate the role of 11β-HSD1 in the metabolism of the alternative substrate *in vivo*.

Beyond 11β-HSD1, the lumen of the ER might contain other NADPH-consuming reductase enzymes. One such candidate is the recently discovered NADPH cytochrome b_5 oxidoreductase (Ncb5or), which was suggested to be localized in the ER lumen (Zhu et al., 2004) and presumably transfers electrons from NADPH to the Δ9 fatty acid desaturase system (Larade et al., 2008). This unique soluble enzyme is a flavoheme reductase. It contains two domains: one 130-residue N-terminal domain that shares strong homology to cytochrome b_5, and the other one at the C-terminus that shows homology to classic microsomal cytochrome b_5 reductase flavoprotein. Nevertheless, the consequence of altered ER-luminal NADPH concentrations on Ncb5or activity and on subsequent fatty acid biosynthesis are unknown and the luminal presence of Ncb5or has not been proven unequivocally.

Another recently discovered enzyme possessing a NADPH binding site and facing the ER lumen is ERFAD (ER flavoprotein associated with degradation). It interacts with proteins involved in folding processes (Riemer et al., 2009); however, a functional read-out of ERFAD is not available and the role of NADPH on ERFAD activity could not yet be determined.

Another candidate enzyme suggested to catalyze the oxidation of NADPH in the ER lumen is the testosterone generating enzyme 17β-hydroxysteroid dehydrogenase type 3 (17β-HSD3). The main expression site of this enzyme is the Leydig cell in the testis, where it interconverts androstenedione and testosterone depending on the cofactor avaibility. Lower expression levels were found in other

tissues including prostate, bone and adipose. The protein contains well-conserved motifs present in all short-chain dehydrogenase/reductase (SDR) members. Recently, some studies hypothesized the functional interaction between 17β-HSD3-dependent testosterone formation and 11β-HSD1-mediated interconversion of glucocorticoids in the ER lumen of isolated mouse Leydig cells, suggesting that 11βHSD1 acts as a dehydrogenase in these cells using the $NADP^+$ produced during the conversion of androstenedione to testosterone catalyzed by 17β-HSD3 (Hu et al., 2008; Latif et al., 2011). It was proposed that the two enzymes compete for luminal NADPH. As a consequence of the interaction, high cortisone levels would inhibit testosterone formation, thereby affecting male sexual development. Mindnich and colleagues assigned the intracellular localization of 17β-HSD3 to the ER membrane (Mindnich et al., 2005); however, the membrane topology has not been determined. The functional coupling between 11β-HSD1 and 17β-HSD3 is only possible if 17β-HSD3 acts inside the ER lumen. Chapter IV describes studies on the dependence of the two enzymes on luminal and cytoplasmic NADPH and on the determination of the membrane topology of 17β-HSD3.

1.4 Alteration of the $NADPH/NADP^+$ ratio in pathophysiological processes

Many cellular processes including translation, energy metabolism, steroid homeostasis, inflammation, apoptosis and autophagy are controlled by the ER. The majority of secreted proteins go through the ER, where they fold and assemble properly. One main function of the ER is to exert quality control on the proteins formed. Only properly folded proteins can be released from this compartment, the improperly folded proteins are retained in the ER and delivered for subsequent proteasomal degradation, called ER-associated degradation (ERAD). Redox imbalance leads to the accumulation of unfolded proteins; ultimately causing ER stress and initiating ER-dependent signaling pathways to restore proper physiological conditions. Exhaustion of the protective mechanisms results in various ER-dependent forms of programmed cell death.

Little is known about sensing and signaling of the redox state of luminal pyridine nucleotides. It is possible that ER chaperones are responsible for sensing the redox state of luminal pyridine nucleotides. It is known that ER chaperones bind adenine nucleotides (Lamb et al., 2006), therefore it can be hypothesized that the structurally similar pyridine nucleotides are also potential ligands and probably they have different affinities towards the reduced and oxidized forms. This theory is supported by studies in H6PDH-knockout mice (Lavery et al., 2008). The pyridine nucleotide redox shift in these animals causes ER stress and can activate the UPR. Increased levels of ER chaperones affected by their redox state can regulate protein folding. Furthermore, the luminal $NADPH/NADP^+$ ratio defines the direction and rate of the prereceptorial metabolism of glucocorticoids, as mentioned

above. Prereceptorial activation of glucocorticoids caused by high NADPH/NADP$^+$ ratio results in autocrine and paracrine effects via the activation of the GR. This prereceptorial activation has been implicated in the pathomechanism of metabolic syndrome and related diseases (obesity, type 2 diabetes, polycystic ovary syndrome, apparent cortisone reductase deficiency).

It can be concluded that besides its prominent role in synthesis and processing of proteins, the luminal pyridine nucleotide source via the G6PT-H6PDH-11β-HSD1 triad also significantly contributes to carbohydrate metabolism, serving as a nutrient sensor for the cell. The carbohydrate metabolism in the ER lumen is mediated by the membrane-bound G6Pase (van Schaftingen and Gerin, 2002), which is responsible for hepatic glucose production and by H6PDH, which catalyzes the NADP-dependent oxidation of G6P. They compete for G6P, which is transported into the ER by the specific G6PT (van Schaftingen and Gerin, 2002). Lowering glucose in the culture medium of transfected HEK-293 cells dose-dependently decreased cortisol production and caused a pyridine nucleotide redox shift (Dzyakanchuk et al., 2008), reflecting the starvation of the cells. In agreement with this assumption, it has been recently reported in animal experiments that starvation decreased cortisone reduction, as a marker for luminal NADPH/NADP$^+$ ratio (Kereszturi et al., 2010). Additionally H6PDH knock-out mice have a reduced weight gain, a peripheral fasting hypoglycemia, an improved glucose tolerance, improved insulin sensitivity and an enhanced hepatic glycogen synthesis (Lavery et al., 2007; Rogoff et al., 2007). These results demonstrate that nutrient supply is mirrored by the redox state of the ER luminal pyridine nucleotides.

On the other hand, overfeeding either with carbohydrates or lipids results in elevated G6P levels, which via G6PT activates H6PDH. The generated and maintained high NADPH/NADP$^+$ ratio in the ER lumen supports glucocorticoid activation. High local glucocorticoid levels counter-regulate insulin action leading to insulin resistance and promoting nutrient storage, producing the most characteristic metabolic features of the metabolic syndrome. Furthermore, enhancement of local glucocorticoid production is an important event in preadipocyte differentiation. The capacity of the ER to convert cortisone to active cortisol is enhanced during preadipocyte differentiation by a remarkable induction of 11β-HSD1. Disturbance of this induction by pharmacological agent (Marcolongo et al., 2008) or by inhibiting 11β-HSD1 (Bujalska et al., 2008a) prevents preadipocyte differentiation. To conclude, it seems that a failure of the ER to adapt to changes in the nutrient availability can result in a pathological transition in ER functions, as observed in obesity-related diseases.

1.5 The short-chain dehydrogenase/reductase (SDR) superfamily

The short-chain dehydrogenases/reductases (SDRs) play important roles in carbohydrate, lipid, amino acid, hormone, cofactor and xenobiotic metabolism. Besides, some SDRs serve as a redox sensors. The SDR superfamily is one of the largest, most heterogenous family, with more than 47.000 members listed in sequence databases and found in all life forms (Kallberg et al., 2010). They catalyze NAD(P)(H)-dependent reactions with a wide substrate spectrum ranging from polyols, steroids, retinoids, fatty acids, sugars and xenobiotics. Although the sequence identities are low (15-30%), they all have a conserved "Rossmann-fold" structural element. This "Rossmann-fold" motif is composed of a central, twisted parallel β-sheet consisting of 6–7 β-strands, which are flanked by 3–4 α-helices from each side (Branden et al., 1975; Lesk, 1995). The long crossover between strands 3 and 4 creates a characteristic binding site for the nicotinamide. This structural motif is characterized by a highly variable Gly-rich sequence pattern, which is critical for structural integrity, accomodation and binding of the pyrophosphate portion to the nucleotide cofactor (Lesk, 1995). Among this structurally conserved N-terminal region, which binds NAD(H) or NADP(H) cofactors, they also have a structurally variable C-terminal region that is responsible for the substrate diversity (Kavanagh et al., 2008). The reactions catalyzed by SDRs appear to proceed through an ordered mechanism. The coenzyme binds first, extending the proper conformational changes and leaves last. They not only interconvert hydroxyl/carbonyl groups, but also catalyze reductions of C=C and C=N double bonds, thereby mediating dehydratase, epimerase, sulfotransferace, isomerase and decarboxylation reactions (Jörnvall et al., 1995). SDR proteins can use NAD(H) and NADP(H) cofactors depending to the performed catalysis. The enzymes preferring NAD(H) contain an acidic residue at the C-terminus of the second core β-strand that interacts with 2` and 3`-hydroxyl group of the adenine ribose part of the cofactor, whereas NADP(H) preferring enzymes contain a basic residue one position further along the sequence responsible for the stabilization of the additional phosphate group of the cofactor. An additional feature for NADP(H) preferences is a basic residue in the glycine rich motif of the enzyme (Kallberg et al., 2002). According to the sequence and predicted secondary structure analysis it is possible to divide three main sequence clusters among the human SDRs (Bray et al., 2009). Cluster C1 contains mostly non-membrane bound proteins with a wide range of substrates including prostaglandings, coenzyme A related compounds and quinine-like molecules. The cluster C2 and C3 consists of membrane-associated proteins that typically catalyze reactions using retinoids and steroids as substrate (Bray et al., 2009).

An additional function of SDRs is to serve as a redox sensor. The CC3/TIP30 proapoptotic oncogene (Shtivelman, 1997) and the fungal transcriptional regulator NmrA (Zheng et al., 2007) are suggested to have clear relationships to SDRs, demonstrating that the nucleotide binding scaffold can adopt other roles and functions. However, to clarify the role of SDRs in redox sensing additional experiments need to be performed.

Although nowadays 82 human SDR genes and 77 SDR proteins have been identified only 14 members of human SDRs have been well characterized. The function of about half of the human SDR enzymes are completely unknown and the knowledge about the subcelullar localization and membrane topology of the many poorly characterized enzymes is not well established (Bray et al., 2009; Persson et al., 2009; Kallberg et al., 2010). Based on experimental observations, we proposed the existence of SDRs other than 11β-HSD1 that are oriented to the luminal side of the ER and are dependent on the luminal NADPH pool. Elucidation of the function of such SDRs may help to understand the mechanisms underlying UPR activation in H6PDH knock-out mice (Semjonous et al., 2011) and impaired autophagy upon knock-down of H6PDH in cultured cells (Száraz et al., 2010).

1.6 Aims of this thesis

The general aim of this thesis was to identify novel enzymes or mechanisms affecting the pyridine nucleotide balance in the ER. The proposed research contributes to the understanding of how luminal NADPH is regenerated and should enhance the current knowledge on disturbances of luminal NADPH homeostasis regarding the development of metabolic diseases. Discovering enzymes generating or utilizing luminal NADPH should provide novel insight into the role of luminal NADPH in pathophysiological redox processes and mechanisms of the antioxidant defense system in the ER. The expected findings could be relevant to understand the coupling between the cellular energy state, hormonal regulation and ER redox regulation.

This thesis addressed the following topics:

Due to the observation that F6P stimulated luminal NADPH generation and enhanced 11β-HSD1 dependent glucocorticoid activation, we characterized a luminal hexose-6-phosphate isomerase. Using microsomal fractions, we found that this enzyme can convert F6P to G6P.

Upon functional characterization, we initiated a classical activity-guided purification strategy combined with mass spectrometry with the ultimate goal to identify the gene encoding this enzyme.

In order to identify additional luminal enzymes involved in NAPDH generation in the ER (potential enzymes of the luminal pentose-phosphate pathway), we applied a combination of classical activity-guided purification, mass-spectrometric analysis and sequence analysis.

To determine whether ER-associated and membrane proteins are facing the cytoplasmic or luminal compartment we optimized the methods to determine the topology and intracellular localization of each enzyme. We used selective semi-permeabilization of the plasma membrane with digitonin, followed by immunodetection and confocal microscopy, as well as proteinase K protection assays of microsomal preparations as well as glycosylation assays.

The optimized conditions were applied to determine the membrane topology of 17β-HSD3. The results demonstrate a cytoplasmic orientation of 17β-HSD3 and a lack of functional coupling with 11β-HSD1 dependent glucocorticoid metabolism.

Chapter II:

Contribution of fructose-6-phosphate to glucocorticoid activation in the endoplasmic reticulum

2.1 Introduction

Old times man`s ancestors obtained their food from hunting and gathering. At this time fruits were the major source of carbohydrates; however, their nutritional intake was primarily composed of meat. The modern Western society lifestyle with its tremendous technological improvement to process food led to extensive changes in food intake and composition. Sugar intake has dramatically increased during the last decades, due to the excessive consumption of high-sugar drinks and the increased use of sucrose, a disaccharide consisting of fructose and glucose units. As a monosaccharide, fructose naturally occurs in many fruits as well as in honey; however, in the human diet it is present primarily as a component of sucrose and in high-fructose corn syrup, a mixture of 55% free fructose and 45% free glucose (Elliott et al., 2002).

Both fructose (Havel, 2005; Montonen et al., 2007; Stanhope, 2008; Stanhope, 2009a) and increased intracellular glucocorticoid production (Tomlinson et al., 2008; Bujalska et al., 2008b) have been suggested to contribute to the pathogenesis of the metabolic syndrome. Furthermore, increasing fructose and sugar-sweetened drink intake has been associated with the occurrence of hypertension and hyperuricemia in adolescents (Gao et al., 2007; Nguyen et al., 2009). Physiological studies suggested that fructose consumption is elevating the blood pressure, whereas glucose has noeffect on it after acute ingestion (Brown et al., 2008).

Upon ingestion fructose is taken up by the intestine and metabolized in the liver to fructose-1-phosphate by fructokinase and subsequently to triose phosphates (Fig. 1). By this metabolic pathway fructose bypasses phosphofructokinase, which is the key regulatory enzyme of glycolysis, and subsequently enters lipogenesis. Fructose can also increase glucose phosphorylation in the liver because fructose-1-phosphate binds to the glucokinase regulatory protein and decreases its affinity for glucokinase, thereby allowing translocation of glucokinase from the nucleus to the cytoplasm (Agius, 1998; Van Schaftingen et al., 1994). Postprandial hypertriglyceridemia due to increased hepatic *de novo* lipogenesis is one of the earliest metabolic derangements following fructose ingestion. Unregulated supply of glycerol-3-phosphate and acetyl-CoA derived from fructose strongly stimulate lipogenesis (Fig. 1).
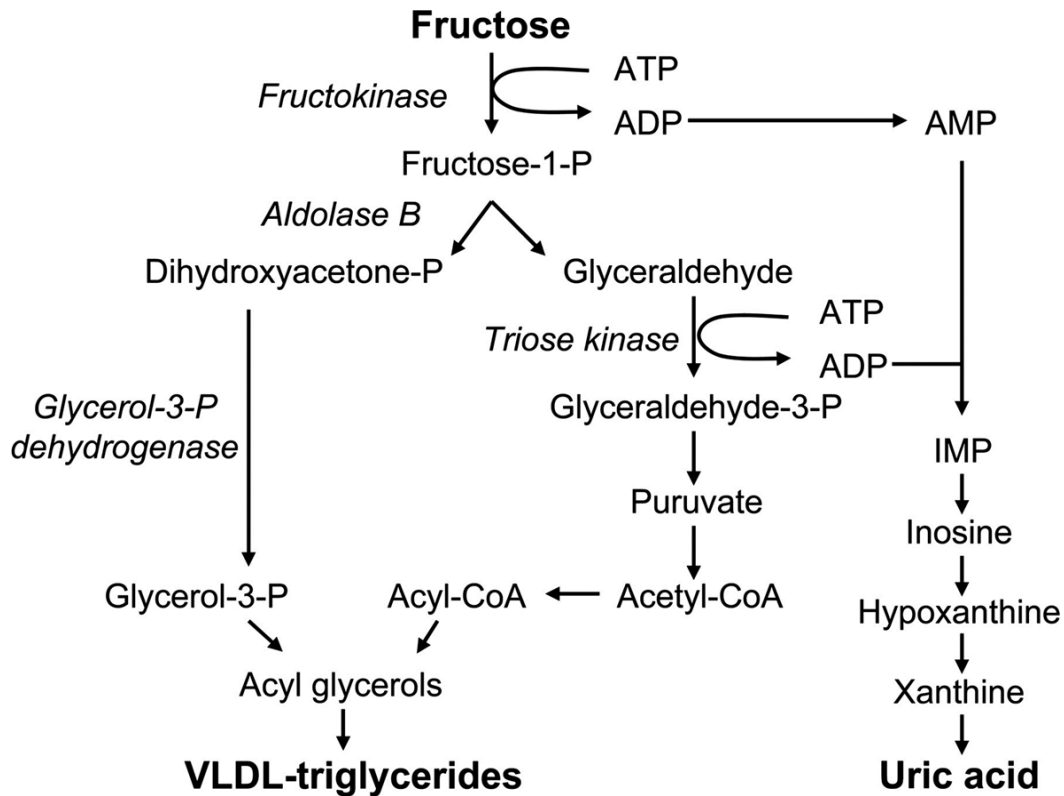
Fig.1. Metabolism of fructose and the formation of triglycerides and uric acid.

Hypertriglyceridemia increases visceral lipid deposition, hepatic triglyceride accumulation and insulin resistance. Consequently, VLDL production is upregulated and increases lipid delivery to muscle and adipose tissue (Stanhope, 2008). The pathway of fructose utilization in adipose tissue largely differs from that in the liver. Adipocytes lack fructokinase and are equipped with a hexokinase, which catalyzes phosphorylation of fructose thereby leading to formation of F6P (Froesch, 1962).

Elevated intracellular activation of glucocorticoids has been shown to stimulate preadipocyte differentiation, which results in enhanced expression of lipoprotein lipase, and increased glycerol production and triglyceride synthesis (Tomlinson et al., 2008; Bujalska et al., 2008b). Active glucocorticoids (cortisol in humans and corticosterone in rodents) are generated by the reductase activity of 11β-hydroxysteroid dehydrogenase type 1 (11β-HSD1), an intraluminal enzyme of the endoplasmic reticulum (ER) (Mziaut et al., 1999; Odermatt et al., 1999). Reducing equivalents for the reaction ultimately derive from glucose-6-phosphate (G6P) by the concerted action of glucose-6-phosphate translocase (G6PT) and hexose-6-phosphate dehydrogenase (H6PDH). H6PDH, localized in the lumen of the ER and physically interacting with 11β-HSD1, generates NADPH for the reduction of active glucocorticoids (Atanasov et al., 2008; Stanhope et al., 2009b; Bánhegyi et al., 2004; Marcolongo et al., 2007; Atanasov et al., 2004).

It is likely, however, that compounds other than G6P can contribute to the generation of NADPH in the ER-lumen and thus would be able to influence the direction of the reaction catalyzed by 11β-HSD1. In this chapter, we examined whether the presence of F6P is sufficient to maintain 11β-HSD1 reductase activity in isolated microsomes. We attempted to show that F6P is transported across the ER membrane through a route distinct from that of G6P. Furthermore, we propose that F6P can be converted to G6P in the lumen of microsomes, thus providing substrate for the activity of H6PDH. Moreover, we investigate whether purified H6PDH does neither act as a F6P dehydrogenase nor as a hexose-phosphate isomerase.

Based on our results, we postulate the existence of a presently unidentified ER luminal hexose-phosphate isomerase distinct from the well characterized cytosolic enzyme (Fig. 2), and provide a possible mechanism for the role of fructose consumption in the development of metabolic syndrome.
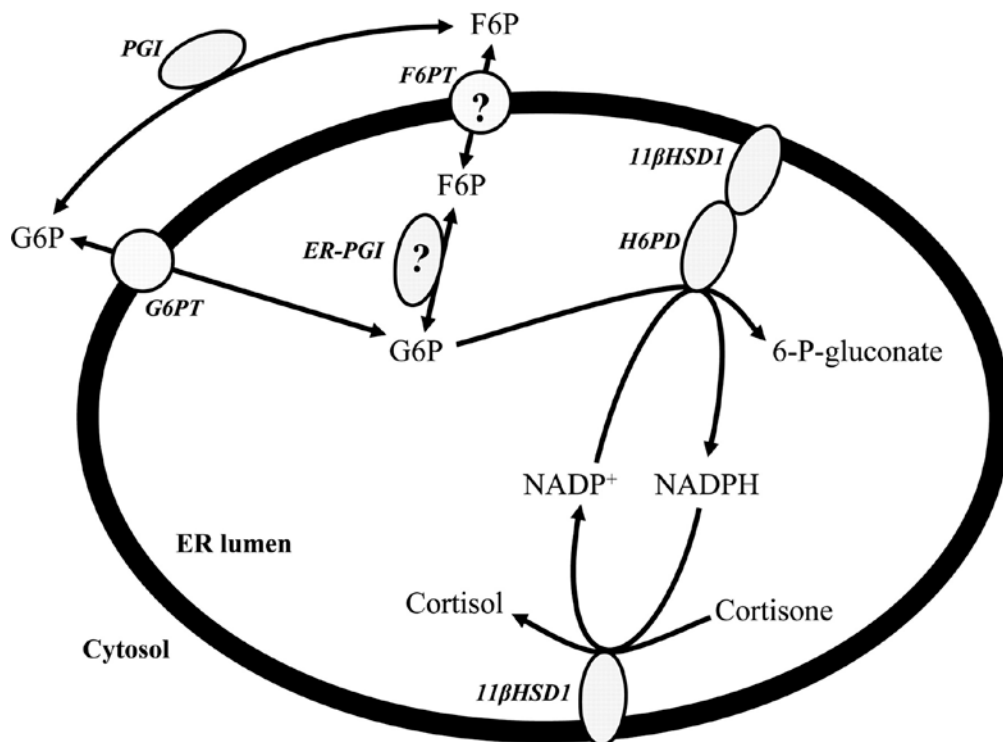
Fig.2. Contribution of F6P to NADPH generation and cortisol production in the ER. Abbreviations: ER, endoplasmic reticulum; F6P, fructose-6-phosphate; G6P, glucose-6-phosphate; G6PT, G6P translocase; H6PDH, hexose-6-phosphate dehydrogenase; 11β-HSD1, 11β-hydroxysteroid dehydrogenase type 1; NADPH, reduced nicotinamide adenine dinucleotide phosphate; PGI, phosphoglucose isomerase; ER-PGI, luminal hexose-phosphate isomerase.

Glucocorticoids play an important role in preadipocyte differentiation, since active glucocorticoids are required for terminal adipogenesis (Hauner et al., 1987) and limit cell proliferation (Tomlinson et al., 2002). From experiments with transgenic mice it is known that global deletion of 11β-HSD1 caused reduced visceral fat accumulation and improved insulin sensitivity on a high-fat diet. These mice are protected from obesity, diabetes, and dyslipidemia (Kotelevtsev et al., 1997). At an early stage of differentiation the expression of 11β-HSD1 is very low in preadipocytes, whereas it strongly increases during the late phase. Inhibition of 11β-HSD1 activity by pharmacological agents or shRNA constructs blocked the capability of inactive oxidized glucocorticoids to promote differentiation (Bujalska et al., 1999; Liu et al., 2008). Depletion of luminal pyridine nucleotides in the endoplasmic reticulum also attenuated 11β-HSD1 activity and the accumulation of lipid droplets during preadipocyte differentiation (Marcolongo et al., 2008).

Recently, we found that replacing glucose by fructose in the culture medium was sufficient to drive 11β-HSD1 oxoreductase activity in transfected HEK-293 cells. In fact, fructose was even somewhat more efficient than glucose to stimulate 11β-HSD1 activity (unpublished observations). These findings support our hypothesis that fructose as the only carbohydrate in the medium could be sufficient for differentiation of preadipocytes to adipocytes. We investigated the amount of lipids, differentiation markers and 11β-HSD1 gene expression in 3T3-L1 cells that were incubated and differentiated in medium with fructose as the only source of carbohydrates.

2.2 Materials and Methods

2.2.1 Isolation of subcellular fractions

Rat liver microsomes and epididymal fat pad microsomes were prepared from male Sprague-Dawley rats (200–250 g) as described earlier (Bánhegyi et al., 2004; Simpson et al., 1983). HEK-293 microsomes were prepared as described (Bánhegyi et al., 2003; Dzyakanchuk et al., 2009). Microsomes were resuspended in 100 mM KCl, 20 mM NaCl, 1 mM $MgCl_2$, and 20 mM MOPS, pH 7.2 (KCl-MOPS buffer), snap frozen and stored in liquid N_2 until further processing. The intactness of the vesicles was verified by measuring the latency of UDP-glucuronosyltransferase activity (Fulceri et al., 1994), which was found to be higher than 95% in each microsomal preparation. The protein concentration of microsomes was determined using the BCA method (Pierce, Piscataway, NJ).

To further remove possible cytosolic contaminants, i.e. the cytosolic enzymes, prior to each experiment, microsomes were rapidly washed as previously reported (Bánhegyi et al., 1996). Briefly, 0.5 mg/ml of microsomal suspensions in KCl-MOPS buffer containing 4.5% polyethylene glycol 8000 (w/v) were centrifuged at 6'000 × g for 30 sec. Microsomal pellets were resuspended in KCl-MOPS buffer for subsequent assays.

2.2.2 Glucose production

Liver microsomes (0.5 mg protein/ml) were incubated in KCl-MOPS buffer at 37°C in the presence of 2 mM G6P or F6P. The reaction was stopped by heat-denaturation (100°C, 5 min). After centrifugation (20'000 × g for 10 min at 4°C), glucose content of the supernatants was measured by using Glucose (GO) Assay Kit according to the manufacturer's instruction.

2.2.3 11β-HSD1 reductase activity

The reduction of cortisone to cortisol was measured by incubating 0.25 mg/ml of liver microsomes in 150 µl of KCl-MOPS buffer at 37°C for 20 min in the presence of 5 µM of cortisone and 50 µM of G6P or F6P. The reaction was stopped with 150 µl of ice-cold methanol and the samples were stored at -20°C until analysis. After centrifugation (20.000 × g for 10 min at 4°C), cortisol and cortisone contents of the supernatants were measured by HPLC (Waters Alliance 2690) using a Nucleosil 100 C18 column (5 µm 25 µ 0.46) (Teknokroma. Barcelona, Spain). The mobile phase was isocratic methanol–water (58:42, v/v) at 0.7 ml/min flow rate and absorbance was detected at 245 nm

wavelength (Waters Dual l Absorbance Detector 2487). The retention times of cortisone (14.1 min) and cortisol (16.8 min) were determined by injecting standards.

2.2.4 H6PDH dehydrogenase activity

Microsomes were incubated in KCl-MOPS buffer at 37°C. H6PDH activity was measured by fluorometric detection of NADPH upon addition of 2 mM NADP$^+$ and 50 μM G6P or F6P. Subsequently, microsomes were permeabilized by the addition of Triton X-100 (1% final concentration), to allow the entry of the cofactor in the luminal space. In some experiments, 1 IU (international unit) of 6-phosphogluconate dehydrogenase was added to measure 6-phosphogluconic acid, generated by the lactonase activity of the H6PDH dual enzyme. NADPH formation was monitored at 350-nm excitation and 460-nm emission wavelengths.

2.2.5 Hexose-6-phosphate isomerase activity

The isomerase activity was indirectly evaluated by incubating washed microsomes or cytosolic fraction in KCl-MOPS buffer at 22°C. The formation of G6P upon the addition of F6P was measured enzymatically with G6PDH. For this assay we used G6PDH isolated from *Leuconostoc mesenteroides*, which is NAD$^+$-dependent, so that we could distinguish isomerase activity from H6PDH dehydrogenase activity (which is prevalently NADP$^+$-dependent, see below). The production of NADH by the G6P-dependent dehydrogenase reaction was monitored fluorimetrically at 350 nm excitation and 460 nm emission wavelengths. To investigate pH sensitivity, the pH of the reaction buffer was adjusted with HCl and NaOH, respectively. Addition of Triton X-100 did not affect the enzymatic activity.

2.2.6 Transport measurements

The microsomal uptake of F6P and G6P was evaluated by a rapid filtration technique (15). Briefly, microsomes (1 mg protein/ml) were incubated in KCl-MOPS buffer in the presence of 10 to 1000 μM F6P/G6P plus D-[14C]-F6P/D-[14C]-G6P (20 μCi/ml) at 22°C. At 30 sec of incubation, samples were rapidly filtered through cellulose acetate/nitrate filter membranes (pore size 0.22 μm), and filters were washed with 4 ml of HEPES (20 mM) buffer (pH 7.2) containing 250 mM sucrose and 1 mM 4,4-diisothiocyanostilbene-2,2-disulfonic acid. This latter compound was added to reduce the eventual efflux of vesicular F6P/G6P during the washing procedure.

Total radioactivity associated with microsomes retained by the filters was measured by liquid scintillation counting. To distinguish intravesicular and bound radioactivity, 0.1% deoxycholate was added to the incubation mixture. The deoxycholate-releasable portion of radioactivity was regarded as intravesicular.

2.2.7 Affinity purification of H6PDH

H6PDH was affinity purified as described previously (Atanasov et al., 2008). Briefly, HEK-293 cells were transfected with a C-terminally myc-tagged H6PDH construct (Atanasov et al., 2004) using the calcium-phosphate precipitation method. At 48 h post-transfection, cells were rinsed twice with a phosphate buffered saline solution (pH 7.4), followed by lysis in lysis buffer for 1 h at 4°C. After centrifugation, the protein containing supernatant was immunopurified with anti-myc antibody-coupled agarose beads (Sigma-Aldrich) following the manufacturer's protocol. Bound protein was eluted from the beads with 100 μg/ml c-myc peptide in 0.1 M ammonium hydroxide for 30 sec at 25°C. Coomassie-stained SDS-PAGE analysis revealed a single protein band of approximately 90 kDa, corresponding to H6PDH (see below, Fig. 6A). The purified protein was snap frozen in liquid N_2 and stored at -70°C. The dehydrogenase activity of H6PDH was measured by fluorometric detection of NADPH formation in the presence of 100 μM G6P and 250 μM $NADP^+$ as described previously (Bánhegyi et al., 2004). The putative hexose-phosphate isomerase activity was measured by fluorometric detection of NADH in the presence of 100 μM G6P or 100 μM F6P plus 250 μM NAD^+ in the presence of 1 UI of *Leuconostoc mesenteroides* G6PDH.

2.2.8 PGI immunoblot

Total protein amounts of microsomal and cytosolic fractions corresponding to comparable PGI activity (30 μg for microsomal and 3 μg for cytoplasmic fraction) of HEK 293 cells were separated on 8% SDS-PAGE and blotted on PVDF membrane. After overnight blocking in blocking buffer [5% milk in tris-buffered saline (TBS)] the membrane was incubated with the primary antibody (diluted 1:8.000 in blocking buffer) for 6 h, followed by intense washing with TBS containing 0.05% Tween-20 for 1 h. Horseradish peroxidase–conjugated goat anti-rabbit antibody was used as secondary antibody (diluted 1 to 10.000 in blocking buffer). HRP activity was detected using enhanced chemiluminescence and a Fuji LAS-4000 detection system.

2.2.9 Cell culture

Murine 3T3-L1 fibroblasts (American Type Culture Collection, Rockville, MD, USA) were cultured and differentiated in a humidified incubator at 5% CO_2 and 37°C as described earlier (Frost, 1985). Briefly, preadipocytes were allowed to reach 2-day postconfluence – referred to as day 0 – prior to induction of adipogenesis by the addition of DMEM containing 10% FBS, 5 μg/ml insulin, 0.5 mM 3-isobuthyl-1-methylxanthine and 0.5 μM dexamethasone. Two days later, the medium was removed and cells were cultured for another 2 days in adipocyte growth medium (DMEM containing 10% FBS and 5 μg/ml insulin). Cells were then maintained in DMEM containing 10% FBS until use, normally at the 7th day after initiation of adipogenesis.

2.2.10 RNA isolation and analysis

Total RNA was extracted from adherent 3T3-L1 cells using the Trizol method (Invitrogen, Carlsbad, CA). Total mRNA (2 µg) was reverse transcribed to cDNA using the Superscript-III First-Strand Synthesis System and oligo-dT (Invitrogen). Relative quantification of mRNA expression levels was performed by RT-PCR on a RotorGene 6000 (Corbett, Australia) using the KAPA SYBR® FAST qPCR Kit (Kapasystems, Boston, MA). Specific primers and sequence probes for each gene were obtained as assay-on-demand gene expression products (11β-HSD1, PPARγ). Relative gene expression compared with the internal control GAPDH was determined using the delta-delta-CT method (Vandesompele et al., 2002).

2.2.11 Oil Red O staining

3T3-L1 adipocytes were washed with PBS and fixed with 4% paraformaldehyde in PBS for 60 min at room temperature. After washed in PBS, cells were rinsed with 60% isopropanol and stained for 30 min in freshly diluted Oil Red O solution (three parts Oil Red O stock solution and two parts of H_2O; Oil Red O stock solution contains 0.25% Oil Red O in isopropanol). The stain was then removed and cells were immediately washed with H_2O four times. For OD measurement, the cells were incubated with 100% isopropanol for 10 min and the collected solution was measured at 520 nm in spectrophotometer.

2.3 Results

2.3.1 F6P-dependent cortisone reduction and glucose production in liver microsomes

In intact microsomes G6P can stimulate the reduction of cortisone to cortisol catalyzed by 11β-HSD1 in the ER lumen utilizing NADPH as a cosubstrate. The phospho-sugar enters the luminal compartment by means of the action of G6PT and fuels local NADPH generation as a substrate for H6PDH (Bánhegyi et al., 2004). A more recent observation that microsomal cortisone reduction can be enhanced also by F6P (McCormick et al., 2008) indicates that this hexose-phosphate can somehow contribute to luminal NADPH generation. However, the transport processes and enzymatic reactions involved are unknown.

Here, we first measured whether F6P can be isomerized to G6P in the ER lumen by means of measuring glucose production following F6P addition in rat liver microsomes, taking advantage of the presence of the glucose-6-phosphatase enzyme in the lumen. F6P proved to be nearly as good a source of glucose production as G6P (Table 1), which strongly suggests the isomerization of F6P to G6P in this system. The isomerase activity may be due to the cytoplasmic enzyme phospho-glucose isomerase (PGI). This protein (which is also called autocrine motility factor, neuroleukin and maturation factor) can be also secreted by an unconventional (i.e. ER/Golgi-independent) mechanism and has an ER membrane-bound receptor named autocrine motility factor receptor/ubiquitin ligase 3 (Fairbank et al., 2009). Alternatively, the observed isomerization might be catalyzed by an enzyme localized in the ER lumen. This question was first addressed by washing the microsomal vesicles by multiple sedimentation and buffer replacement to eliminate the membrane-adherent cytosolic proteins. The first such cleansing resulted in a 9-fold decrease in the rate of glucose production from F6P in intact microsomes, although, as expected, it modestly affected glucose production from G6P, i.e. glucose-6-phosphatase activity (Table 1). This suggests that a major part of the total hexose-6-phosphate isomerase activity, probably corresponding to PGI, is loosely associated to the outer surface of the microsomal vesicles. However, the remaining capacity of the microsomes to utilize F6P as a glucose precursor could not be eliminated by subsequent washing steps and hence seems to be based on a tightly membrane-associated or luminal hexose-6-phosphate isomerase activity. The higher latency of glucose production in the case of F6P (approx 85%, compare intact and permeabilized microsomes in Table 1) with respect to the case of G6P (approx 40%), might be due to the lower rate of entry of F6P as compared to that of G6P into liver microsomal vesicles (see below, Fig. 5).

Efficiency of F6P (and of G6P for comparison) to stimulate the conversion of cortisone to cortisol was also investigated in washed microsomes. In this case, the first washing step caused only a moderate decrease in cortisone reductase (32% and 11% when F6P and G6P was used, respectively), and the

subsequent washing steps did not affect the rate of cortisone reduction significantly (Table 1). It can be concluded that an irremovable intrinsic hexose-6-phosphate isomerase activity of the microsomes can provide the dehydrogenase enzymes with G6P at a sufficient rate. Nevertheless, to avoid any interference of the extravesicular (cytosolic) isomerase activity, only washed microsomes were used in all further experiments.

Table 1. Glucose production and cortisone reduction in liver microsomes.

| Substrate | Microsomes | Times washed | | | |
		0	1	2	3
Glucose production (nmol/min mg protein)					
G6P	Intact	80.15 ± 4.37	45.56 ± 3.82[1]	41.60 ± 5.19	40.31 ± 4.73
	Permeabilized	156.23 ± 9.37	72.74 ± 5.82[1]	70.14 ± 7.02	67.54 ± 3.91
F6P	Intact	30.11 ± 5.12	3.58 ± 1.31[1]	3.35 ± 0.95	3.22 ± 1.06
	Permeabilized	54.28 ± 4.73	23.39 ± 2.70[1]	21.74 ± 1.99	20.83 ± 2.12
Cortisone to cortisol conversion (pmol/min mg protein)					
G6P	Intact	50.58 ± 0.37	44.80 ± 1.60[1]	45.77 ± 1.99	43.05 ± 1.00
F6P	Intact	51.98 ± 1.31	35.16 ± 1.60[1]	36.15 ± 0.81	33.98 ± 1.72

Rat liver microsomes (1 mg protein/ml) were washed by sedimentation and buffer replacement as many times as indicated. The microsomal membrane was permeabilized by using alamethicin (0.05 mg/mg protein). Glucose production was measured after addition of 2 mm G6P or F6P. Conversion of cortisone (5 μm) to cortisol was assessed in the presence of 50 μm G6P or F6P. Data are means ± SD of five separate experiments.

[1]Statistically different from the previous washing step (*column to the left*) at $P < 0.005$, determined by Student's t test for two-group comparison.

2.3.2 F6P-dependent NADPH generation and 6-phosphogluconate production in hepatic and adipose tissue microsomes

F6P acts like G6P in liver microsomes, i.e. stimulates cortisol formation. We collected further evidence that its microsomal isomerization provides G6P, which feeds NADPH generation by H6PDH, both in hepatic and adipose tissue microsomes. Due to the luminal localization of H6PDH and the poor permeability of microsomal membrane to NADP$^+$, when microsomes are incubated in the presence of NADP$^+$ and G6P, NADPH generation cannot be detected until the membrane barrier is eliminated. Once the lipid bilayer is permeabilized with a detergent, the linear increase in fluorescence indicates the progress of the redox reaction both in hepatic and adipose tissue microsomes (Fig. 2 A and Fig. 2 C, respectively). In line with the results shown in Table 1, F6P proved to be also efficient in stimulating NADPH generation in this system (Fig. 2 B and 2 D, in liver and adipose tissue microsomes, respectively).

Fructose-1,6-bisphosphate (F1,6BP), a known inhibitor of the cytoplasmic PGI, also significantly reduced the rate of F6P-driven NADPH generation (Fig. 2 B and Fig. 2 D), while it did not interfere with the process in microsomes using G6P (Fig. 2 A and Fig. 2 C).
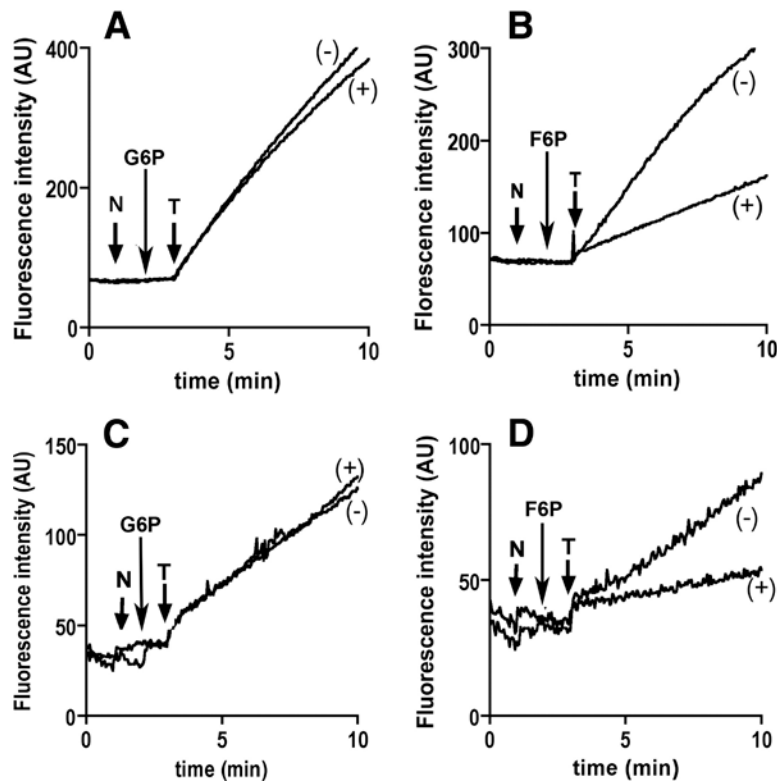
Fig.2. F6P-dependent NADPH generation in hepatic and adipose tissue microsomes. Liver (panel A and B) and adipose tissue (panel C and D) microsomes, prepared as describe in the "Materials and Methods" section, were incubated at 37°C in the KCl/MOPS buffer at a protein concentration of 0.5 mg/ml. The NADPH formation was measured fluorimetrically (excitation and emission wavelengths at 350 and 460 nm, respectively) following the subsequent addition (arrows) of 2 mM NADP$^+$ (N), 50 µM G6P or F6P, and 1% Triton X-100 (T). Microsomes were indicated by (-) and (+) no or 10 mM F1,6BP was present in the incubation mixture as an inhibitor of PGI. One of five representative experiments is shown.

Besides functioning as a dehydrogenase, H6PD possesses lactonase activity, converting G6P ultimately to 6-phosphogluconate (Clarke, 2003). Formation of 6-phosphogluconate from F6P could be also demonstrated in our experimental model by measuring further NADPH generation in the presence of exogenous 6-phosphogluconate dehydrogenase to the hepatic or adipose tissue microsomes (Fig. 3 A and 3 B, respectively). Since F6P-driven NADPH generation could be inhibited by F1,6BP and was accompanied by 6-phosphogluconate formation, we conclude that F6P is indeed isomerized to G6P providing H6PDH with substrate.
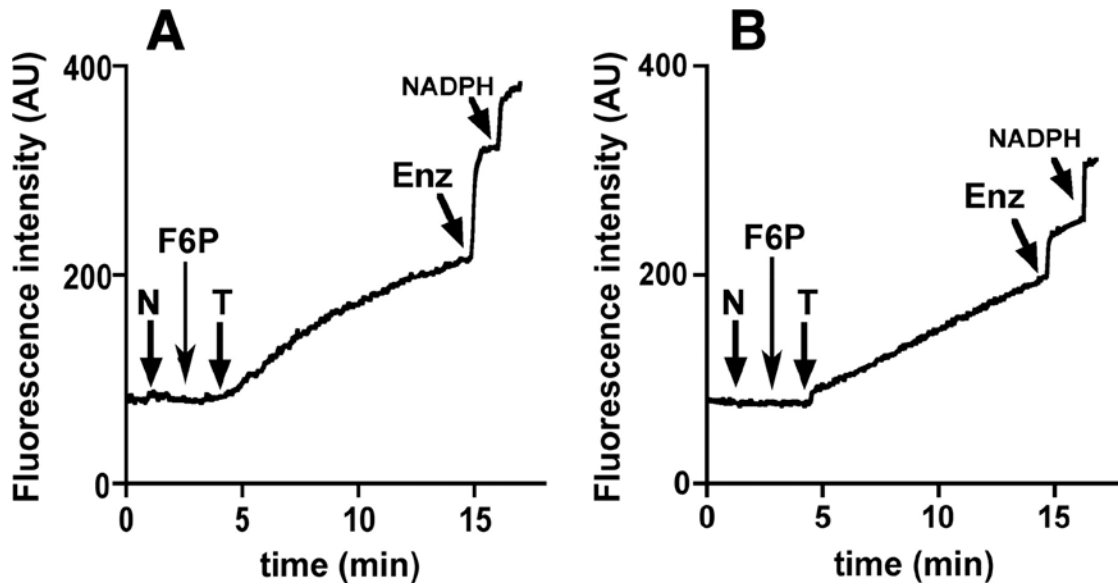
Fig.3. F6P-dependent 6-phosphogluconate production in hepatic and adipose tissue microsomes. Liver (panel A) and adipose tissue (panel B) microsomes, prepared as reported in the "Materials and Methods" section were incubated at 37°C in the KCl/MOPS buffer in a fluorimeter cuvette, at a protein concentration of 0.5 mg/ml. The dehydrogenase activity of H6PDH was monitored on the basis of NADPH formation following the subsequent addition (*arrows*) of 2 mM $NADP^+$ (N), 10 µM F6P, and 1% Triton X-100 (T). The production of 6-phosphogluconate was measured on the basis of the further increase in NADPH signal, upon the addition of 6-phosphogluconic acid dehydrogenase (1 U/ml, indicated by *arrows* as Enz) to the reaction mixture. NADPH (5 µM) was subsequently added for calibration. One of three representative experiments is shown.

2.3.3 Luminal localization of microsomal hexose-6-phosphate isomerase activity

Although our findings convincingly demonstrated the formation of G6P from F6P in hepatic and adipose tissue microsomes, it still remained to be elucidated whether this conversion occurs on the outer surface (i.e. representing the cytoplasmic side) of the vesicular membrane or inside the vesicles. To answer this question, formation of G6P was compared in intact and permeabilized microsomes, i.e. the latency of the hexose-6-phosphate isomerase was investigated. The experimental conditions were similar to those in the previous set of measurements but $NADP^+$ was substituted by NAD^+. In preliminary experiments a slow reduction of NAD^+ to NADH was observed in the presence of G6P in permeabilized microsomes, indicating, under our experimental conditions, a lower (approximately ten-fold) preference of H6PDH for NAD^+. Accordingly, in the presence of NAD^+ and F6P, the permeabilization of hepatic or adipose tissue microsomes resulted in a very slow NADH generation (Fig. 4 A and Fig. 4 B, respectively). The subsequent addition of the NAD^+-specific *Leuconostoc mesenteroides* G6PDH to the samples greatly increased the rate of NADH generation (Fig. 4 A and Fig. 4 B), indicating the efficient isomerization of F6P to G6P in the permeabilized microsomes. The PGI inhibitor, F1,6BP (10 mM) remarkably repressed this process both in hepatic and adipose tissue microsomes.

The addition of F6P to intact (non-permeabilized) microsomes caused no NADH generation, since the membrane is impermeable to pyridine nucleotides (Fig. 4 C and 4 D).

Most importantly, the subsequent addition of the *Leuconostoc mesenteroides* G6PDH poorly stimulated NADH generation, indicating a negligible isomerization of F6P by intact microsomes (Fig. 4 C and 4 D). These findings clearly demonstrate the luminal localization of hexose-6-phosphate isomerase activity.
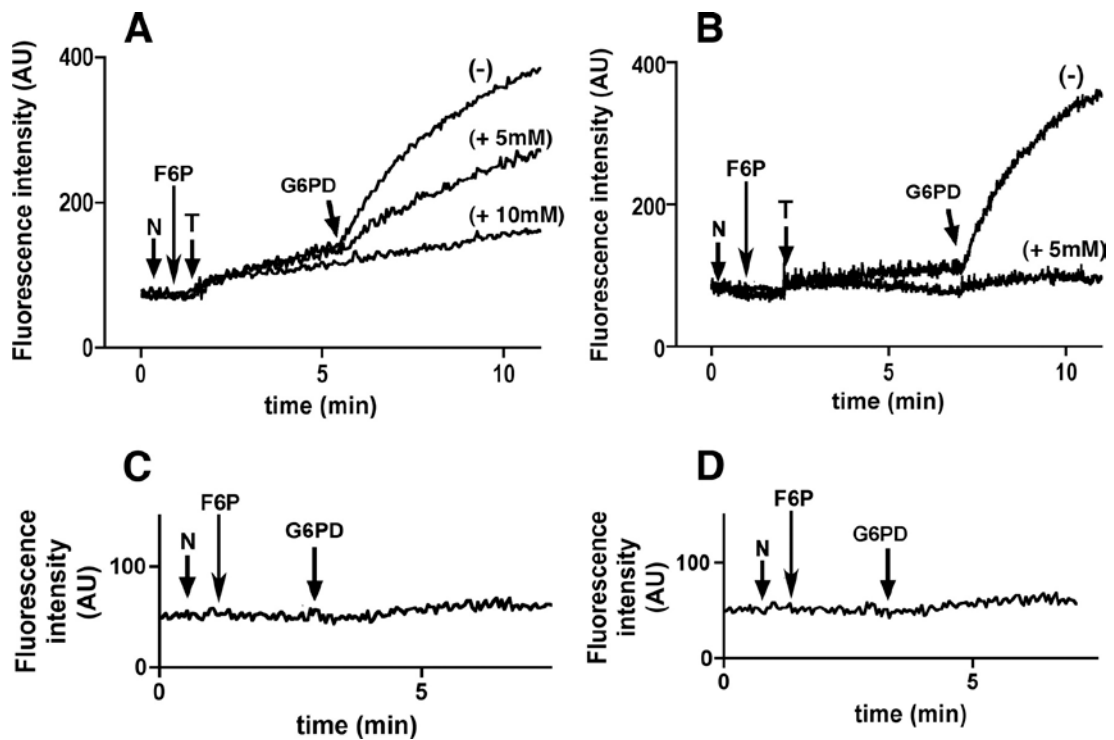
Fig.4. Luminal localization of microsomal hexose-6-phosphate isomerase activity. Liver (panel A and C) and adipose tissue (panel B and D) microsomes, prepared as reported in the "Materials and Methods procedures" section, were incubated at 22°C in the KCl/MOPS buffer in a fluorimeter cuvette, at a protein concentration of 0.5 mg/ml. The isomerization of F6P to G6P was evaluated by measuring the G6P-dependent reduction of NAD^+ upon the addition of the NAD^+-dependent *Leuconostoc mesenteroides* G6PDH both to permeabilized (panel A and B) and intact (panel C and D) microsomes. NADH production is evident in permeabilized microsomes only, indicating the luminal localization of isomerase activity. The additions indicated by *arrows* are: 500 μM NAD^+ (N) 50 μM F6P, 1% Triton X-100 (T) and 1 U/ml G6PDH. One of three representative experiments is shown.

2.3.4 Transport of F6P across the microsomal membrane

Glucose-6-phosphate transport across the ER membrane has been thoroughly characterized (Gerin, 2002). Although the membrane traffic of F6P has not been investigated in the ER, the luminal utilization in intact microsomes was proposed after our findings. The uptake of F6P and G6P was investigated in hepatic and adipose tissue microsomes by using a rapid filtration transport assay. The initial rate of transport was determined at 30 sec; to minimize the contribution of the intravesicular accumulation of metabolites of G6P (radiolabeled glucose and phosphogluconic acid, respectively) (Bánhegyi et al., 1997).

The transport activity was found to be concentration-dependent in both hepatic and adipose tissue microsomes, for both F6P and G6P, in the investigated range of extravesicular hexose-phosphate concentrations (10 μM to 1 mM see Fig. 5 A-C). The rate of influx of F6P was approximately 1.7 fold higher in adipose tissue compared to liver microsomes (Fig. 5 A), whilst G6P was transported at a higher rate (approximately 3.7 folds) in liver than in adipose tissue microsomes (Fig. 5 B). This latter observation is consistent with our previous results (Marcolongo et al., 2007), and is very likely due to the higher representation of G6PT in liver microsomes (Marcolongo et al., 2007). On the other hand, in adipose tissue microsomes, G6P was transported at a higher rate (approximately 1.4) than F6P (Fig. 5 C).
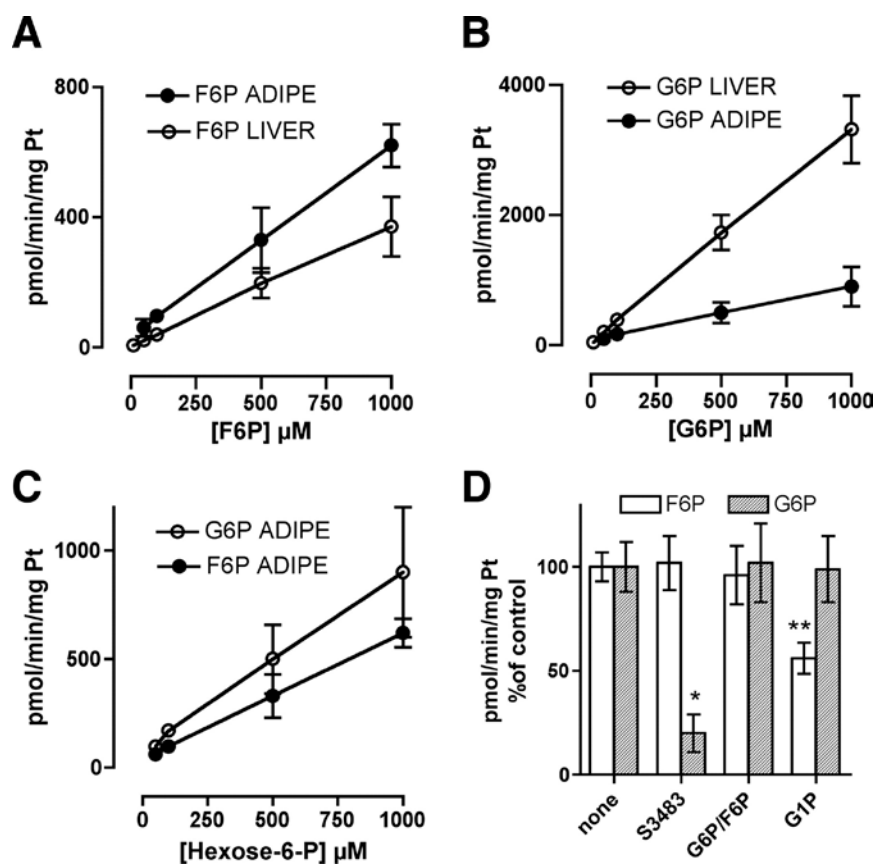
Fig.5. Transport of F6P across the microsomal membrane. The initial rate of transport of F6P (A) as well as that of G6P (B) was measured by a rapid filtration technique with [^{14}C]-F6P/[^{14}C]-G6P at different extravesicular concentrations of the hexose phosphates (10-1000 μM) in liver and in adipose tissue microsomes as described in the "Materials and Methods". The comparison between F6P and G6P uptake in adipose tissue microsomes is shown in panel C. The effect of the G6PT inhibitor S3483 (40 μM) and of the other phosphoester (5 mM), as well as of G1P (5 mM) on the microsomal uptake of F6P and G6P (D), expressed as percentage of control, was measured liver microsomes, in the presence of 50 μM extravesicular F6P/G6P. Data are means ± SD of five separate experiments. Values statistically different from control are indicated: *P>0,001; **P>0,01.

The possibility that F6P permeates the microsomal vesicles trough the G6P transporter G6PT (Gerin et al., 1997) was investigated in liver microsomes by using the selective inhibitor of the transporter S3483 (Arion et al., 1998). As shown in Fig 5 D, the G6PT inhibitor markedly reduced the transport of G6P but did not affect the transport of F6P, suggesting a different route of entry for F6P.

Moreover, the transport activity for each phosphohexose was unaffected by the other phosphohexose at a high (competitive) concentration (10 mM), which strengths the hypothesis that the phosphoesters do not share the same transporter. Furthermore we also observed that S3483 did not inhibit F6P transport in adipose tissue microsomes, and we previously reported that the inhibitor reduces G6P entry in adipose tissue microsomes by approximately 70% (Marcolongo et al., 2007). The possibility that the route of entry of F6P is via the nonspecific glucose-phosphate transporter (GPT) previously described in human fibrocytes was also tested by measuring the transport of F6P (50 µM) in the presence of competitive concentrations of glucose-1-phosphate (G1P, 5 mM), a known substrate of GPT (Leuzzi et al., 2001). Results demonstrated, that G1P significantly inhibited the transport of F6P by approximately 50%, whilst did not interfere with G6P transport. The results are consistent with the role of GPT in F6P transport. The apparent lack of effect on G6P transport, which is also mediated by GPT, is very likely due to the high representation of G6PT in liver microsomes that allows a massive entry of G6P.

2.3.5 F6P does not serve as substrate for H6PDH, which has neither intrinsic isomerase activity

To prove the assumption that H6PDH cannot use F6P as a substrate, we overexpressed the myc-tagged human enzyme in HEK-293 cells followed by subsequent affinity purification. Cells transfected with the empty pcDNA3.1 vector were used as control. After SDS-PAGE analysis and Coomassie-blue staining a single protein band at approximately 90 kDa, corresponding to H6PDH, was detected (Fig 6 A). The identity of H6PDH was further confirmed by immunoblot analysis using a rabbit primary antibody raised against the myc peptide. Next, we measured NADPH generation by the purified enzyme upon supplying G6P or F6P and NADP$^+$ as substrates. NADPH was produced in the presence of G6P, but not of F6P (Fig. 6B). This result confirms our assumption that F6P is not directly utilized by H6PDH to generate NADPH. Moreover to investigate whether H6PDH possesses intrinsic isomerase activity and can interconvert F6P and G6P, we used G6PDH from *Leuconostoc mesenteroides* as an indicator enzyme to measure NADH production from NAD$^+$ with G6P or F6P as substrates. As shown in Fig 6 C, G6PDH could generate NADH from G6P only, independently whether it was supplied with or without F1,6BP, an inhibitor of the isomerase activity. H6PDH was not able to generate G6P from F6P. These results indicate that human H6PDH itself cannot function as a hexose-phosphate isomerase.
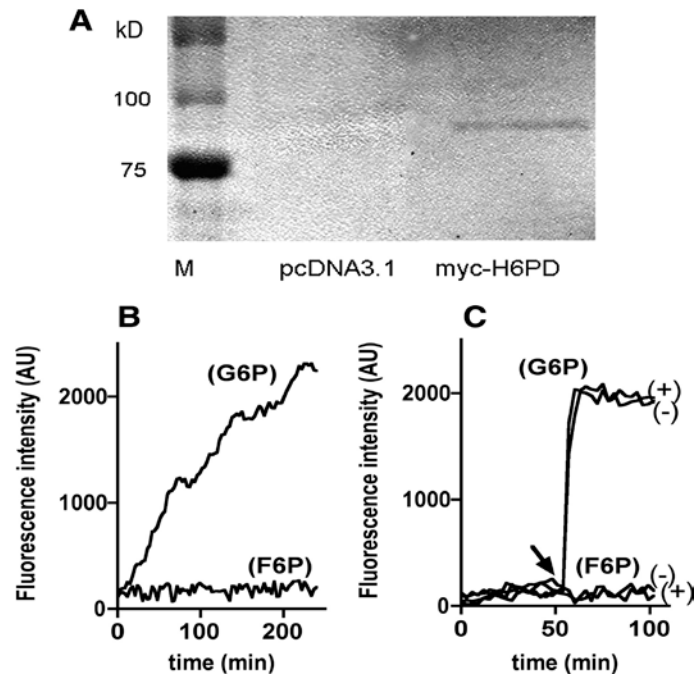
Fig.6. Characterization of H6PDH activity. (A) SDS-PAGE analysis of the purified H6PDH. Recombinant human H6PDH was purified from transfected HEK-293 cells as described in the "Materials and Methods" section. The eluate after purification was separated by 10% SDS-PAGE under nonreducing conditions and Coomassie Brilliant Blue staining was performed. M: molecular mass marker (kDA). The protein band at 90 kDa represents H6PDH. No signal could be detected in the eluate after the purification procedure performed with cells transfected with the pcDNA3.1 vector only. (B) F6P does not serve as substrate for H6PDH. The purified H6PDH was incubated in the presence of 100 μM glucose-6-phosphate (G6P) or fructose-6-phosphate (F6P) and 250 mM NADP$^+$. Dehydrogenase activity was detected by fluorimetric detection of NADPH. (C) H6PDH does not catalyze isomerization of F6P to G6P. The purified H6PDH was incubated with 100 μM G6P and 100 μM F6P as well as 500 μM NAD$^+$ as a cofactor. Where indicated by the *arrow*, G6PDH (1 U) (from *Leuconostoc mesenteroides*) was added to evaluate the possible isomerization of F6P to G6P. It acts only on G6P was used as an indicator of H6PDH isomerase activity. To inhibit the possible isomerase activity, fructose-1,6-bisphosphate (F1,6BP) (10 mM) was added to the indicated samples. The time course of NADH formation was determined fluorimetrically.

2.3.6 Evidence for the existence of an intrinsic microsomal hexose-phosphate isomerase enzyme

To rule out that the cytoplasmic PGI was responsible for the conversion of F6P to G6P in microsomes, we subjected total proteins that correspond to comparable hexose-phosphate isomerase activity, i.e. 30 μg of washed microsomes or 3 μg of cytosolic fraction (proteins present in the supernatant after the ultracentrifugation step in the microsome isolation procedure) from HEK-293 cells, or 100 μg of washed microsomes or 2 μg of cytosolic fraction from rat liver to SDS-PAGE and subsequent immunoblot analysis using an antibody raised against the cytosolic PGI. As shown in Figure. 7 A and D, we could detect a single protein band at 63 kDa in the cytosolic but not in the microsomal fraction of HEK 293 cells (Fig. 7 A) and rat liver preparations (Fig. 7 D), even if ten or fifty times more microsomal protein was loaded respectively, indicating the absence of the cytosolic PGI in the lumen of the microsomes. The hexose-phosphate isomerase activity of the two protein preparations was practically the same.

To further strengthen this evidence, we incubated microsomes (30 μg protein) as well as the cytosolic fraction (3 μg protein) of HEK-293 cells in the presence of erythrose-4-phosphate (E4P), a known potent inhibitor of the human cytosolic PGI (Chirgwin et al., 1975), followed by measurement of NADH production by the G6PDH from *Leuconostoc mesenteroides* as described in the "Materials and Methods" section. Without the addition of E4P, both incubations showed comparable, time-dependent activity. The microsomal hexose-phosphate isomerase activity; however, was more efficiently inhibited by E4P than the cytosolic PGI (Fig. 7 B). We obtained similar results using 2 μg of rat liver cytoplasmic and 100 μg of microsomal protein with F1,6BP as an inhibitor (Fig 7 E). Upon incubation with F1,6BP instead of E4P, we detected similar differences between the cytosolic and microsomal enzymes in HEK-293 cells. These results indicate that the microsomal phosphohexose isomerase possesses kinetic properties distinct from the cytosolic PGI. We also investigated whether the enzymes in the two subcellular fractions might differ in their sensitivity towards changes in the pH of the reaction buffer. As depicted in Fig. 7 C, the microsomal enzyme was less sensitive to pH changes and showed approximately two-fold higher catalytic activity at low pH compared with the cytoplasmic enzyme, suggesting different pH sensitivities of the cytoplasmic and the luminal phosphohexose isomerases.
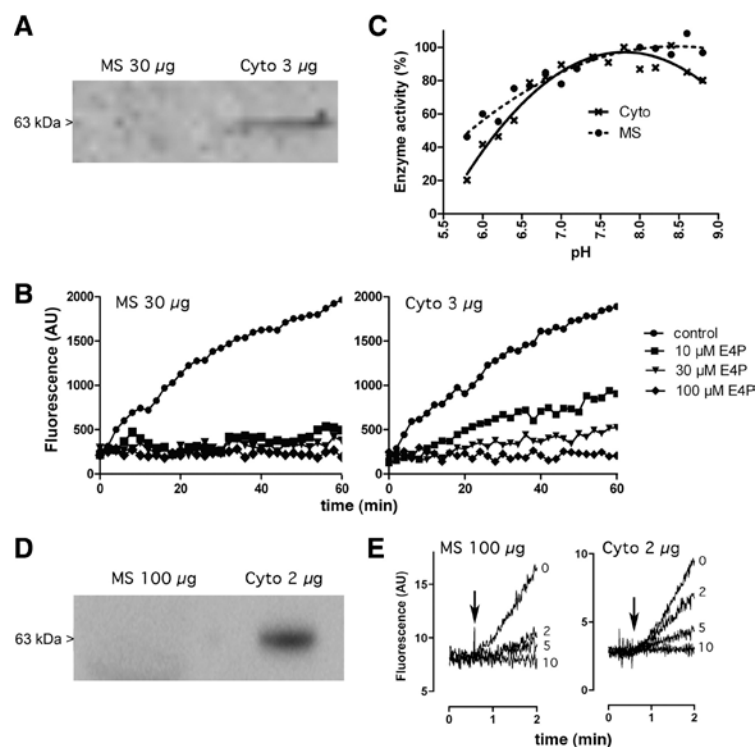
Fig.7. The microsomal (MS) hexose-phosphate isomerase is distinct to the cytoplasmic (Cyto) phosphoglucose isomerase. (A) Immunoblot analysis of the human phosphoglucose isomerase. Amounts of 30 μg microsomal and 3 μg cytoplasmic proteins, corresponding to comparable phosphoglucose isomerase activities, were separated by SDS-PAGE and analyzed by immunoblotting using an anti-human cytoplasmic phosphoglucose isomerase antibody. A 63 kDa protein band was detected in the cytosolic (Cyt) but not in the microsomal (MS) fraction of HEK-293 cells. (B) Microsomal protein (30 μg, MS) and cytosolic protein (3 μg, Cyto) from HEK-293 cells were subjected to measurement of hexose-phosphate isomerase activity in the absence or presence of increasing concentrations of erythrose-4-phosphate (E4P). NADH production by the G6PDH from *L. mesenteroides* is shown.

(C) The microsomal hexose-phosphate isomerase was less sensitive to pH changes than the cytoplasmic enzyme. Activities of the cytoplasmic (Cyto) and microsomal (MS) hexose-phosphate isomerase were compared in reaction buffers of the pH indicated on the X-axis after 50 min of incubation. (D) Immunoblot analysis of the rat phosphoglucose isomerase. Amounts of 100 μg of microsomal and 2 μg of cytoplasmic proteins were loaded, followed by SDS-PAGE and immunoblot using the anti-rat cytoplasmic phosphoglucose isomerase antibody. (E) Microsomal proteins (100 μg, MS) and cytosolic proteins (2 μg, Cyto) from rat liver were subjected to measurement of hexose-phosphate isomerase activity in the absence or presence of increasing concentrations of fructose-1,6-bisphosphate (F1,6BP). NADH production by the G6PDH from *L. mesenteroides* is shown.

2.3.7 Fructose can substitute glucose as a carbohydrate source for adipocyte differentiation

The ER luminal NADPH/NADP$^+$ ratio and the prereceptorial glucocorticoid regulation has an important role in preadipocyte differentiation. Disturbance of 11β-HSD1-mediated glucocorticoid activation results in modified lipogenesis and reduced lipid droplet formation. First, we investigated whether fructose can substitute glucose and serve as efficient carbohydrate source to generate active glucocorticoids and stimulate the differentiation of mouse 3T3-L1 fibroblasts into mature adipocytes. In our preliminary experiments we differentiated 3T3-L1 preadipocytes in medium containing only fructose as a carbohydrate source and compared the effects with cells grown in glucose containing medium as describe *above*. We observed that fructose is sufficient to maintain viability, and the capacity of cells to initiate differentiation and form lipid droplets was comparable to that of cells grown in glucose medium. At the end of differentiation (day 8), the amount of lipids in the cells was comparable with that found in cells differentiated in glucose containing medium (Fig 8 A). To test the differentiation stage of mature adipocytes we investigated FABP4 and PPARγ gene expression, as differentiation marker proteins. We found that FABP4 and PPARγ expression was slight elevated comparedto cells differentiated in glucose containing medium (Fig 8 B C).
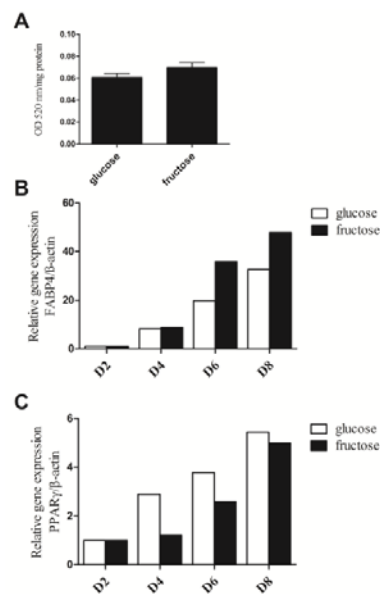
Fig.8. Fructose can substitute glucose during preadipocyte differenciation. At the end of differentiation the total lipid content was determined by Oil-Red O staining (A), and the mRNA expression of FABP4 (B) and PPARγ (C) was measured by RT-PCR.

2.4 Discussion

Fructose, a sugar present in very low quantities in the human diet a few hundred years ago, became a major constituent of present-day nutrition. The increase of fructose consumption and the incidence of metabolic syndrome show a thought-provoking correlation. Although there is compelling evidence that high fructose intake can have deleterious metabolic effects such as dyslipidemia and impaired insulin sensitivity, the role of fructose in the development of the current epidemic of metabolic disorders remains controversial. Several mechanisms – increased de novo hepatic lipogenesis, lipotoxicity, oxidative stress, and hyperuricemia – have been forwarded to explain the adverse metabolic effects of fructose (Tappy, 2010). Our observations suggest a novel pathomechanism: fructose, via its intracellular metabolite F6P, can stimulate prereceptorial activation of glucocorticoids that are regarded to be a principle factor in the development of obesity-related metabolic disorders.

F6P-promoted glucocorticoid activation can be especially important in cells lacking fructokinase activity, i.e. in cells of non-hepatic tissues, particularly in adipocytes. Skeletal muscle and white adipose cells express GLUT5, mediating insulin-independent fructose transport (Darakhshan et al., 1998; Hajduch et al., 1998) and F6P is the obligatory intermediate of fructose metabolism therein. Investigating the metabolic pathway between F6P and cortisone reduction, we revealed that the last steps – from H6PDH – are the same as in the "classic", G6P-dependent route. However, our observations indicate that in this case two new entities – a microsomal F6P transporter and a luminal hexose-phosphate isomerase – are required for the substrate supply of H6PDH.

The existence of a microsomal F6P transport was demonstrated by rapid filtration assay and was also indirectly supported by F6P-dependent microsomal glucose production and cortisone reduction. The transport was not inhibited by G6P or by G6PT inhibitor showing that a transporter other than G6PT is responsible for the microsomal permeation of F6P. The observed competition with G1P transport suggests that F6P may be transported by GPT previously described in fibrocytes (Leuzzi et al., 2001). As expected, due to the high representation of G6PT in the liver, G6P can be transported much better into liver microsomes than F6P. This observation, together with the fact that the concentration of G6P is several fold higher than that of F6P in the liver cytoplasm (Hems, 1979), minimizes the possible role of F6P in the glucocorticoid activation in the intact liver. Theoretically, a notable exception might be the inherited deficiency of G6PT, i.e., the glycogen storage disease Type 1 b (van Schaftingen E, 2002). It should be noted, however, that G6P and F6P are transported at similar rates in microsomes isolated from adipose tissue.

It could be hypothesized, that fructose is sufficient to maintain energy supply for adipocyte survival and differentiation, which requires intracellular glucocorticoid activation. We tested lipid content and differentiation marker gene expression after differentiating preadipocytes in medium containing fructose as the only carbohydrate source. Interestingly, these adipocytes showed similar morphology and number of lipid droplets. After measuring the lipid content with Oil-red staining, there was no significant difference compared to the lipid content in cells differentiated in glucose containing medium. Two differentiation marker genes, FABP4 and PPARγ gene expression showed similar or even elevated levels in cells incubated with fructose containing medium. However, under physiological conditions these sugars are both present. The observation that fructose could be transported more efficiently into adipocytes and the similar effects on preadipocyte differentiation may provide an explanation for the adverse metabolic effects of excessive fructose consumption.

We also observed a microsomal hexose-phosphate isomerase activity, which is definitely distinct from the cytosolic enzyme. Besides the activity of a resident yet undefined enzyme, microsomal hexose-phosphate isomerase activity may theoretically also derive from the adherence or entrapment of the cytosolic enzyme to/in the microsomal vesicles during the homogenization procedure. The first assumption can be ruled out since repeated wash could not remove the activity. The increased latency of the residual activity clearly shows the intraluminal positioning. Concerning the second assumption, the entrapment of the cytosolic PGI is unlikely, since the well measurable enzymatic activity was not accompanied by the presence of the immunodetectable protein, and the cytosolic and microsomal activities showed different sensitivity towards inhibitor and pH. It is noteworthy furthermore, that the cytosolic PGI does not contain an ER targeting or retention signal sequence, making it unlikely that this enzyme translocates into the ER lumen. The gp78/AMFR protein, which has been reported to bind PGI, is an ER membrane protein, but its ligand binding site faces the cytosol (Fairbank, 2009). Thus, our results provide strong evidence for the existence of a novel phosphohexose isomerase that is located in the lumen of the ER. Taken together, experimental evidence shows that these presently unidentified proteins are not identical with G6PT or the cytosolic PGI. Further work is described in this thesis for the molecular identification and definition of these entities.

The extent of *in vivo* contribution of fructose for glucocorticoid activation as a reducing equivalent donor is presently difficult to estimate. Although several groups investigated the effect of macronutrients on glucocorticoid activation both in humans and in animal models (Basu et al., 2006; Stimson et al., 2010), similar studies with fructose are still missing. Additional studies are needed to verify the effect of fructose on glucocorticoid activation in living animals. As discussed above, it is unlikely that fructose contributes at a relevant extent to glucocorticoid activation in the liver. By contrast, such a role can be hypothesized in non-hepatic tissues, especially in the white adipose tissue. The possibility that the blood fructose concentration can increase near the millimolar range after fructose/sucrose enriched meals in humans (Johnson et al., 2009) and in rats (Prieto et al, 2004),

and our observation that F6P and G6P are transported at a similar rate across the ER membrane of adipocytes makes this a reasonable hypothesis. The role of fructose in the maintenance of glucocorticoid activation can be even more important in the already developed metabolic syndrome, where insulin resistance hinders glucose uptake. In conclusion, we propose that F6P-dependent glucocorticoid activation in the adipose tissue is a possible factor in the pathogenesis of the metabolic syndrome.

Chapter III:

Towards the identification of new components of the pyridine nucleotide homeostasis in the ER

3.1 Introduction

The aim of this part of the thesis project was the identification of novel components of the luminal NADPH balance. The recent discovery of H6PDH provided an explanation for the generation and maintenance of the luminal NADPH pool. However, some studies suggested the existence of additional enzymes that contribute to the maintenance of the NADPH pool in the ER (Rogoff et al., 2010; Margittai and Bánhegyi, 2008; Wang et al., 2011). Furthermore, microsomes of *H6PDH* knock-out mice were able to reduce cortisone (Lavery et al., 2006), although at a low rate suggesting the existence of a H6PDH-independent source of NADPH. Moreover, biochemical evidence also argues for the presence of a pentose-phosphate pathway in the ER (Bublitz and Steavenson, 1988). The H6PDH enzyme catalyzes the first two reactions of the pentose-phosphate pathway which produces 6-phosphogluconate (6PG) in the ER. Despite the recent biochemical characterization of H6PDH, nothing is known about the fate of its product 6PG. It is not envisageable that 6PG can cross the ER membrane since no transport mechanism is known, or that it might accumulate in the ER due to end-product inhibition of H6PDH. Bublitz and colleagues provided evidence for the existence of a 6-phosphogluconate dehydrogenase (6PGDH) in rat liver microsomes (Bublitz et al., 1987). However, the luminal 6PGDH has not yet been identified. The enzymatic reaction of 6PGDH generates one molecule of NADPH; thereby this reaction would contribute to luminal NADPH generation. Our preliminary results showed that a latent 6PGDH activity was present in microsomes isolated from rat liver, but not in microsomes from HEK-293 cells. We aim to identify the gene encoding the luminal 6PGDH, which would further strengthen the hypothesis that this enzyme may contribute to the maintenance of NADPH in the ER lumen.

Surprisingly, very little information is available on the utilization of NADPH for enzymatic reactions in the ER. Hypothetically, the NADPH pool in the ER may be necessary for the metabolism of steroids, lipids, carbohydrates and xenobiotics, although at present, 11β-HSD1 is the only thoroughly characterized NADPH-dependent enzyme in the ER. Several observations indicated the existence of other NADPH-dependent luminal enzymes (McCormick et al., 2008; Semjonous et al., 2011; Latif et al., 2011); however, there is a lack of experimental evidence for the identity of such enzymes and their membrane topology.

Therefore, our current aim is to further characterize the mechanisms of NADPH generation in the ER and to search for enzymes that utilize NADPH in the luminal compartment. To identify luminal enzymes we used rat and mouse liver microsomes and followed an activity-guided purification strategy. We applied the combination of fractionation, affinity purification, gel-electrophoretic separation and mass spectrometry methods to generate a list of potential candidates.

The difficulty of investigating microsomal enzymes is reason why the exact membrane topology of most microsomal membrane proteins has not yet been determined. A proper determination of the intracellular localization and determination of membrane topology of luminal proteins or epitopes requires a semi-permeabilization of the plasma membrane to allow the access of antibodies to the cytoplasmic but not the luminal compartment. The semi-permeabilization assay can be combined with electron microscopy detection or a glycosylation assay. This assay reveals whether a luminal protein is glycosylated and therefore the protein was modified when it passed the ER compartment.

As discussed in the previous chapter, we observed that fructose can stimulate the generation of luminal NADPH. In experiments with washed intact microsomes from rat liver and adipose tissue, we characterized a novel luminal hexose-phosphate isomerase activity (Senesi et al., 2010). This enzyme converts F6P to G6P, thereby generating substrate supply for H6PDH and promoting the production of luminal NADPH. Identification of the gene encoding this luminal isomerase would allow further investigations regarding its transcriptional regulation and its potential role in metabolic diseases. In order to identify the genes encoding the luminal hexose-6-phosphate isomerase and 6PGDH and other genes coding for luminal enzymes utilizing NADPH we plan to apply a combination of classical activity-guided purification, mass-spectrometric analysis and sequence-based bioinformatics analysis as mentioned above.

3.2 Materials and Methods

3.2.1 Preparation of rat liver microsomes

Liver microsomes were prepared from Sprague-Dawley rats. The livers were homogenized in sucrose-HEPES buffer (0.3 M sucrose, 0.02 M HEPES, pH 7.2) with a glass-Teflon homogenizer. The microsomal fraction was then isolated with fractional centrifugation. After centrifugation of liver homogenates for 10 min at $1´000 \times g$, the supernatant was then spun twice for 15 min at $12´000 \times g$. The resulting supernatant was centrifuged for 60 min at $100´000 \times g$; the pellet resuspended in MOPS buffer (20 mM MOPS, pH 7.5) and centrifuged again for 60 min at $100´000 \times g$. The final microsomal pellet was resuspended in MOPS buffer.

3.2.2 Glycoprotein isolation kit

Glycoproteins were purified using the Glycoprotein Isolation Kit from Thermo Scientific. The columns bind glycoproteins using the lectin concanavalin A (ConA) or wheat germ agglutinin (WGA) immobilized on agarose beads. The ConA lectin preferentially recognizes α-linked mannose whereas the WGA lectin preferentially binds N-acetyl glucosamine (GlcNAC) and also has affinity for sialic acid. The permeabilized microsomes, containing up to 1.5 mg of total protein, are first diluted with binding/wash buffer and applied to the ConA or WGA resin bed. Following incubation, the resin is washed several times and bound glycoproteins are eluted as described by the manufacturer.

3.2.3 Hexose-6-phosphate isomerase and 6-phosphogluconate dehydrogenase activities

The isomerase activity was indirectly evaluated by incubating washed microsomes or separated fractions in KCl-MOPS buffer at 22°C. The formation of G6P upon addition of F6P was measured enzymatically with G6PDH, isolated from *Leuconostoc mesenteroides*. This enzyme is NAD^+-dependent. The production of NADH was measured fluorimetrically at 350 nm excitation and 460 nm emission wavelengths. The isomerase activity was measured in the presence of 100 µM F6P and 500 µM NAD^+ as cofactor and reactions were initiated by the adding of 1 IU of G6PDH from *Leuconostoc mesenteroides*. The 6PGDH activity was measured by fluorometric detection of NADPH in the presence of 250 µM $NADP^+$ and 1 µM 6-PG. The microsomes were permeabilized by addition of 0.5% Triton X-100. The production of NADPH was measured fluorimetrically at 350 nm excitation and 460 nm emission wavelengths.

3.2.4 Enzyme purification

To identify the luminal hexose isomerase and 6PGDH enzymes we applied an affinity-guided purification strategy. In a first step, the microsomal preparation was optimized. After differential centrifugation the microsomal pellets were washed to remove proteins attached to the cytoplasmic surface of the ER vesicles. To partially solubilize the microsomal fraction we incubated it with a buffer containing 20 mM octylglucoside (OG). This treatment permeabilized the membrane and released luminal proteins. The remaining membranous fraction could still be pelleted by further centrifugation. Using this method we separated total microsomal proteins, octylglucoside solubilized proteins and ER membrane pellet fraction (Mathias et al., 2011) (Fig 1).
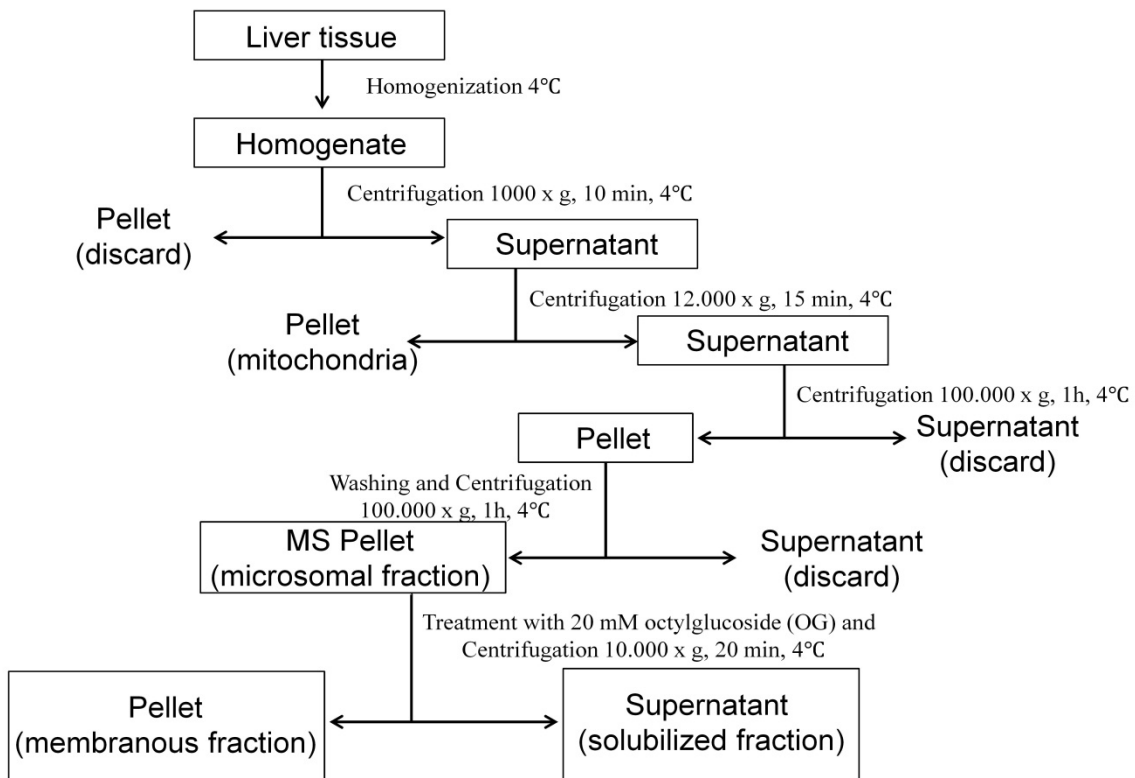
Fig.1. Preparation of different fractions by centrifugation and solubilization with OG

Aliquots (30 µg) of each of the membrane fractions were resuspended in sample buffer containing 50 mM dithiothreitol (DTT), boiled at 95 °C for 5 min, and loaded onto a 8–12% SDS-PAGE. Electrophoresis was performed in running buffer at 120 V (constant voltage) until the tracking dye reached the bottom of the gel. Proteins were visualised using SimplyBlue SafeStain (Invtrogen).

Individual gel lanes were excised into 1 mm gel slices, and gel slices were reduced, alkylated, and subjected to in-gel tryptic digestion. Digests were then subjected to protein identification by mass-spectrometry analysis (kindly performed by Dr. Reto Portmann, Forschungsanstalt Agroscope Liebefeld-Posieux ALP, Bern; and Dr. Paul Jenö Biozentrum, Basel).

For protein fractionation we applied ion exchange chromatography and size exclusion chromatography methods. We used Q Sepharose Fast Flow (strong anion exchanger) and SP Sepharose Fast Flow (strong cation exchanger) from GE Healthcare according to the manufacture`s instruction. We applied size exclusion using an FPLC system and XK16/70 column containing Superose 6 or a XK16/60 column containing Superdex 200. Finally, we separated the samples using ionic exchange columns, first through anion-exchange UNO Q column (Bio-RAD) with a 1 ml/min flow rate of 20 mM MOPS buffer (pH 7.2), and second through a cation-exchange UNO S column (Bio-RAD) with 20 mM Tris buffer (pH 8.0) and increasing concentrations of sodium-chloride.

3.3 Results

3.3.1 Both luminal hexose-6-phosphate isomerase and 6PGDH activity recovered after octlyglucoside solubilization of microsomes

We started our investigation by incubating washed microsomes with a buffer containing the detergent octylglucoside (OG) (20 mM final concentration). With this treatment we expected recovery of luminal hexose-6-phosphate isomerase and 6PGDH activities by collecting the supernatant after centrifugation. The pelleted fraction contains the total ER membranes. Both activities effectively appeared in the supernatant (solubilized fraction (Fig. 2)), as it was demonstrated by our collaborators at the University of Siena University, Italy (Senesi el al., 2010).
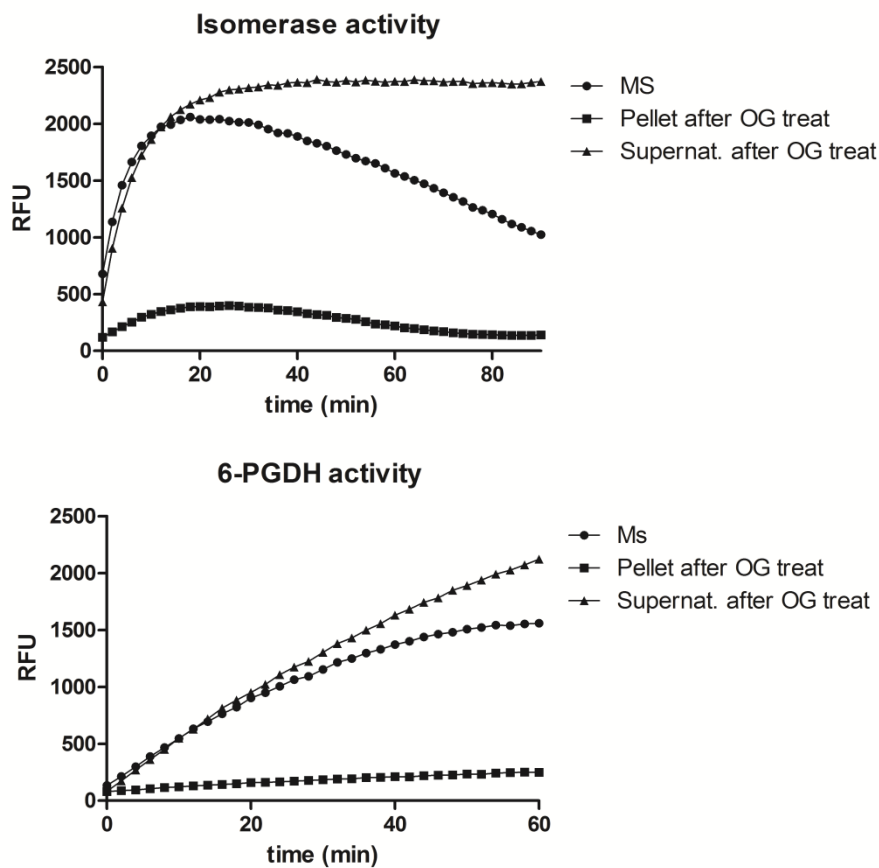
Fig.2. Both hexose-6-phosphate isomerase (*upper*) and 6PGDH activity (*lower*) were observed in octlyglucoside (OG) solubilized microsomal fractions. Fractions were permeabilized by addition of Triton X-100 prior to measurement of NADH production. Abbreviations: MS, microsomal fraction; Supernat., supernatant following $10´000 \times g$ centrifugation step., RFU, relative fluorescence units.

Upon incubation of the total microsomal fraction (MS) with a buffer containing 20 mM OG, further fractions were obtained: one with solubilized proteins (supernatant), which contained the activities of interest, and one with the remaining membranous fraction (PELLET).

These samples were subjected to SDS-PAGE, and after separation the corresponding lanes were subjected to protein identification by mass-spectrometry (performed by Dr. Portmann) (Figure 3). The total microsomal fraction contained about 500 different proteins. The microsomal pellet after OG treatment (PELLET) typically contained ER membrane proteins such as cytochrome P450 enzymes and other multi-span membrane proteins. The OG solubilized fraction contained about 200 different soluble and single-span membrane proteins. Some of them were expected, such as H6PDH, 11β-HSD1 and several single-span membrane anchored short-chain dehydrogenase (SDR) enzymes, retinol dehydrogenases and alcohol dehydrogenases (Appendix II). On the other hand, the solubilized fraction contained some interesting candidates, revealed by sequence analysis. However, further research is required to confirm their intracellular localization and investigate their association with luminal NADPH. Since the number of potential candidates for the unidentified luminal hexose-6-phosphate isomerase is too large after this step, further purification was necessary. Therefore, we started to investigate the solubilized fraction of proteins by further separation using size and/or ion exchange chromatography.

MS   PELLET   SUPERNAT
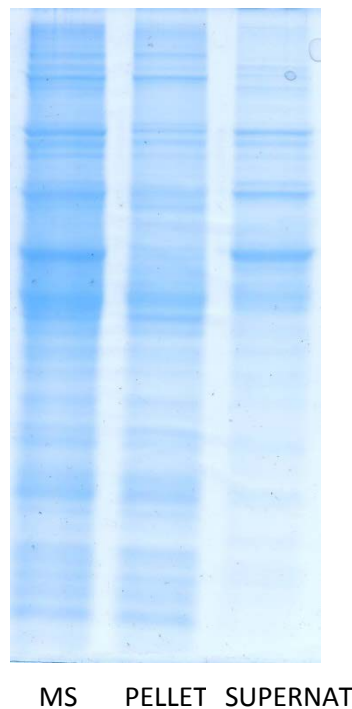
Fig.3. SDS-PAGE gel electrophoresis with SimplyBlue Stain. The first lane contains the total microsomal fraction (MS), the second lane contains the pelleted fraction after treatment of microsomes with OG (PELLET), while the third line is the solubilized supernatant fraction (SUPERNAT) containing the activities of hexose-6-phosphate isomerase and 6PGDH.

3.3.2 Fractionation of the luminal hexose-6-phosphate isomerase and 6PGDH

We attempted to separate the OG solubilized proteins by ion exchange chromatography. First, we applied Q Sepharose Fast Flow (strong anion exchanger) and SP Sepharose Fast Flow (strong cation exchanger) chromatography systems.

After loading the column, we increased the salt concentration in the elution buffer by 25 mM in each step. During the gravity forced separation, we collected the different fractions. As a result we could detect an enrichment in hexose-6-phosphate isomerase activity, whereas we observed a loss of 6-PGDH activity during increasing the salt concentration. We combined the fractions with highest hexose-6-phosphate isomerase activity and performed a gel-electrophoretic separation of proteins. After separation the lanes were sent to mass spectrometric analysis, which was performed by Dr. Portmann (Fig. 4). The gel lanes were cut into slices, followed by trypsinization of the proteins. The proteins were identified with Mascot software using the UniProt database (Appendix III). From the two separated fractions we were able to identify 74 proteins. Some of the identified proteins are members of the SDRs superfamily (methylenetetrahydrofolate dehydrogenase; alcohol dehydrogenase; 17β-hydroxysteroid dehydrogenase), others are potential candidates with yet unknown isomerase function (catalase; liver carboxylesterase 4; transketolase; fructose-bisphosphate aldolase B; arginase-1) (Appendix III). Because of the large number of possible candidates for the hexose-6-phosphate isomerase among the identified proteins and the fact that we could not find similarities with other isomerases or identify a sugar binding site, we decided to continue the protein separation by adding size exclusion chromatography.

Fig.4. Gel-electrophoretic separation of the fraction proteins stained by SimplyBlue Stain.
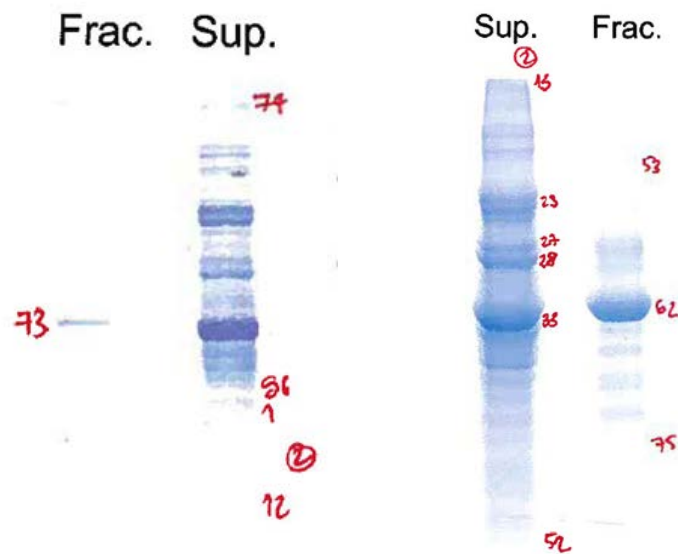
For further fractionation we applied Superose 6 and then the more precise Superdex 200 size exclusion chromatography columns. Furthermore, we used a Gel Filtration Calibration Kit assay to detect the approximate size of the luminal isomerase activity that was eluted from the column. In our first experiments we could see a clear activity peak (Fig. 5).
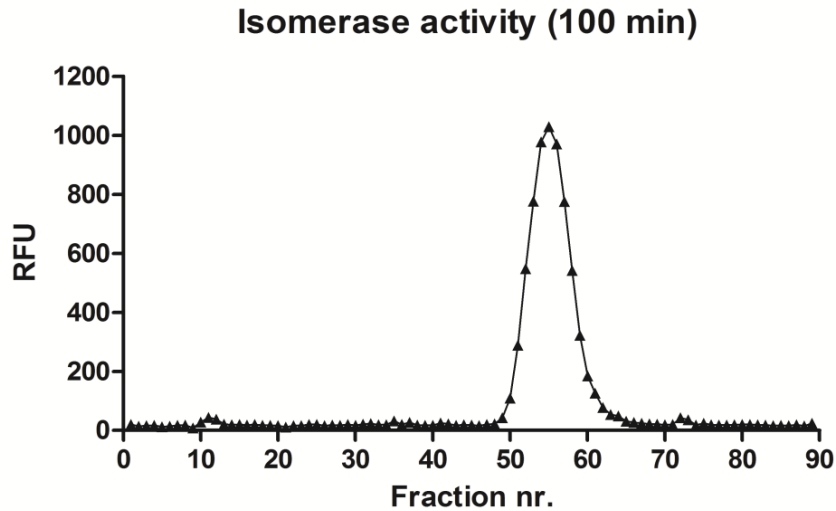
Fig.5. Hexose-6-phosphate isomerase activity measurement after size exclusion fractionation.

However, when we mixed the cytosolic and the microsomal fractions we failed to detect two separate peaks that would suggest separated luminal and cytosolic enzyme activities. Thus, either we had contaminated cytosolic enzyme in the microsomal fraction or, alternatively, the cytoplasmic and luminal enzymes are of similar size. According to the Gel Filtration Calibration Kit that includes known proteins (ovalbumin, conalbumin, aldolase, ferritin and thyroglobulin) we estimated a size of the luminal isomerase enzyme of 82 – 97 kDa.

The purchase of a BioLogic Chromatography Systems (Bio-RAD) with UNO Q and S ion exchange columns allowed to optimize the protein purification system. After initial optimization steps we applied samples from the previous size exclusion for further separation by anion exchange chromatography. The fraction with the highest enzyme activity was then analysed using a mass-spectrometry by Dr. Paul Jenö at the Biozentrum (Basel, Switzerland). Only few proteins were contained in this fraction (Table 1). Following mass-spectrometric analysis sequence-based bioinformatics was performed using "DAVID Bioinformatics Resources 6.7" and UniProt databases in order to search for potential Rossmann-folds, sugar binding sites and ER retention sites in the sequence of the identified proteins.

Table 1. Mass-spectrometric analysis of the activity enriched fraction. Accession, Protein accession number, gene name, and description obtained from the IPI database, Score; MASCOT protein score, Unique Peptides, Number of unique significant peptides identified.

Accession	Description	Score	Coverage	# Proteins	# Unique Peptides	# Peptides	# PSMs	# AAs	MW [kDa]	calc. pI
P02535	RecName: Full=Keratin, type I cytoskeletal 10;AltName: Full=Cytokeratin-10;	526.73	4.91	11	2	3	15	570	57.7	5.11
P19001	RecName: Full=Keratin, type I cytoskeletal 19;AltName: Full=Cytokeratin-19;	247.08	6.20	16	2	3	9	403	44.5	5.39
Q921I1	RecName: Full=Serotransferrin; Short=Transferrin;AltName: Full=Sideror	206.81	6.17	1	4	4	7	697	76.7	7.18
Q3TTY5	RecName: Full=Keratin, type II cytoskeletal 2 epidermal;AltName: Full=Cytoke	136.15	1.98	1	1	1	4	707	70.9	8.06
P04104	RecName: Full=Keratin, type II cytoskeletal 1;AltName: Full=Cytokeratin-1;	126.65	1.73	1	1	1	3	637	65.6	8.15
Q91Y97	RecName: Full=Fructose-bisphosphate aldolase B; EC=4.1.2.13;AltName	115.99	7.69	1	2	2	3	364	39.5	8.27
P24270	Catalase OS=Mus musculus GN=Cat PE=1 SV=4 - [CATA_MOUSE]	69.97	2.47	1	1	1	2	527	59.8	7.88
P14206	RecName: Full=40S ribosomal protein SA;AltName: Full=Laminin receptor 1;	63.01	4.41	1	1	1	1	295	32.8	4.87
P40142	RecName: Full=Transketolase; Short=TK; EC=2.2.1.1;AltName: Full	53.23	1.28	1	1	1	1	623	67.6	7.50
P11679	RecName: Full=Keratin, type II cytoskeletal 8;AltName: Full=Cytokeratin-8;	48.47	2.04	4	1	1	1	490	54.5	5.82
Q61176	RecName: Full=Arginase-1; EC=3.5.3.1;AltName: Full=Type I arginase;A	46.03	2.48	1	1	1	1	323	34.8	7.01
P30115	RecName: Full=Glutathione S-transferase A3; EC=2.5.1.18;AltName: Full	45.06	4.98	3	1	1	1	221	25.3	8.73
P10853	RecName: Full=Histone H2B type 1-F/J/L;AltName: Full=H2B 291A; - [H2B1F_N	39.45	7.14	12	1	1	1	126	13.9	10.32

3.3.3 Isolation of glycosylated proteins from the ER

Alternatively, presuming that the luminal hexose-6-phosphate isomerase and other potential enzymes playing an important role in the luminal generation and utilization of NADPH might be glycosylated, we loaded the OG treated microsomal fraction to concanavalin A (ConA) and wheat germ agglutinin (WGA) affinity columns. The aim of this approach was to isolate glycosylated proteins. Non-glycosylated proteins attached to microsomes at the cytoplasmic surface and proteins with transmembrane helices but facing the cytoplasm are expected not to bind to these columns. The eluted proteins from these columns (glycoproteins) were collected; followed by gel-electrophoretic separation and mass-spectrometric analysis (Appendix IV). The aim of this experiment was to obtain a list of glycosylated ER proteins for the subsequent identification of various luminal enzymes that may participate in the utilization or generation of the luminal NADPH pool and to identify the putative hexose-6-phosphate isomerase. We also tested whether our initial hypothesis was correct, that means to test whether the luminal isomerase may be glycosylated. Surprisingly, the enzyme activity was recovered from the flow fraction, meaning that the putative hexose-6-phosphate isomerase is not glycosylated (Fig.7).
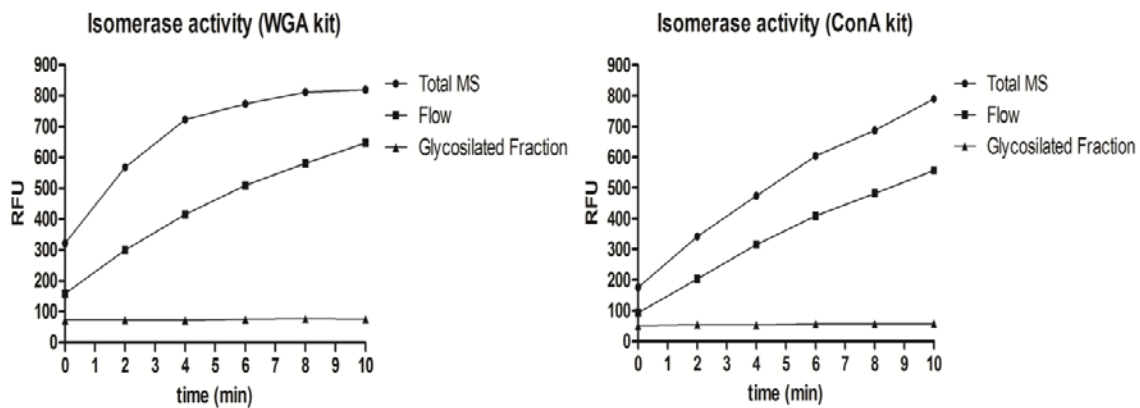
Fig.7. Recovery of the hexose-6-phosphate isomerase activity in the flow through fraction of ConA and WGA columns.

Upon subjecting the microsomal fractions concanavalin A (ConA) and wheat germ agglutinin (WGA) affinity columns, we identified 321 different proteins, of which 163 were bound by both columns (Appendix IV). Unfortunately we detected about 20% of these proteins in both glycosylated and flow through fractions, which can be explained either by unspecific binding to the column or saturation of the column or weak affinity and recovery in the flow. Nevertheless, we received a valuable list of potentially glycosylated proteins, which may be helpful for the identification of potentially important factors for luminal NADPH homeostasis. We run our list of proteins through databases to find Rossmann-fold pyridine nucleotide binding sites, or possible functions in the ER. Various SDRs turned up in this list (Retinol dehydrogenase 7 (Rdh7, CRAD-2); 17β-hydroxysteroid dehydrogenase 13 (17β-HSD13); 17β-HSD6; as well as the expected glycosylated proteins 11β-HSD1 and H6PDH. However it needs to be mentioned that we also recognized cytochrome P450 reductase enzymes (not known to be glycosylated) and peroxisomal and mitochondrial resident proteins (Appendix IV). This may indicate the contamination of the ER fraction by peroxisomal and mitochondrial proteins, emphasizing the difficulties of pure preparations of the subcellular organelles.

To conclude, we identified promising candidates with yet unidentified membrane localization and function that now can be further investigated for potential hexose-6-phosphate isomerase activity. Such candidate proteins can be modified by attaching an epitope tag for further functional analysis and subcellular localization studies. Epitope tagging also allows affinity purification of the candidate proteins.
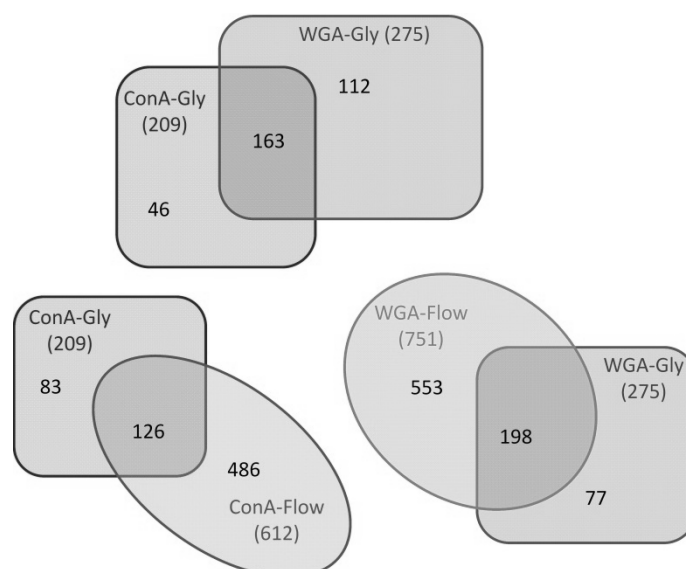
Fig.8. Summary of the result from experiments using the Glycosylation Kit. In total, 321 potential glycoproteins bound ConA and WGA columns were identified. Of those, 163 proteins were found in both concanavalin A (ConA) and wheat germ agglutinin (WGA) affinity columns.

3.4 Discussion

Our main goal of protein purification was to identify the luminal hexose-6-phosphate isomerase, which we functionally can clearly distinguish from the phosphoglucose isomerase (PGI) activity of the cytoplasm (Senesi et al., 2010). We observed some chemical diversity for the cytoplasmic and luminal activity. The activity in washed microsomes was clearly latent. Furthermore, using the antibody against the cytosolic enzyme did not detect a band in the microsomal fraction that had comparable isomerase activity.

For further characterization we tried to identify the luminal enzyme by classical activity-guided purification using a combination of size and ion exchange chromatography. With this effort, we obtained a list of potential candidates. The mass-spectrometry analysis confirmed the absence of the cytoplasmic PGI from our sample, supporting the evidence for separate isomerase enzymes. However, the final identification is still missing. Three candidates are of interest. One of these candidates is the fructose-bisphosphate aldolase B, catalyzing the conversion of D-fructose 1,6-bisphosphate to glycerone phosphate and D-glyceraldehyde 3-phosphate. It is a cardinal enzyme of the glycolysis pathway, while its genetic defect causes hereditary fructose intolerance. The second candidate is the transketolase. It catalyzes the transfer of a two carbon ketol group from a ketose donor to an aldose acceptor, via a covalent intermediate with the cofactor thiamine pyrophosphate. Transketolase is involved in the pentose phosphate pathway in all organisms and also plays a role in the Calvin cycle of photosynthesis in plans (Kochetov, 1982) and catalyzes different reactions (Figure 9).
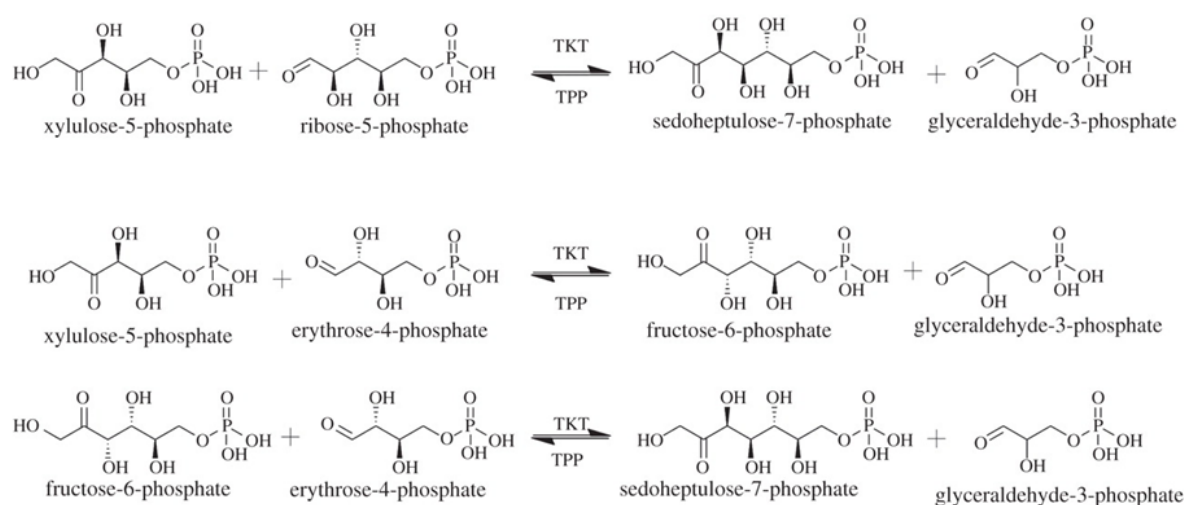
Fig.9. Transketolase enzyme catalysed reactions.

Interestingly, it acts in opposite directions in the two pathways. The first reaction accepts a 2-carbon fragment from a 5-carbon ketose (D-xylulose-5-P) and transfers this 2-carbon group to a 5-carbon aldose (D-ribose-5-P) to form a 7-carbon ketose (sedoheptulose-7-P). This yields the 3-carbon aldose glyceraldehyde-3-P from the D-xylulose-5-P. The second reaction catalyzed by transketolase in the pentose phosphate pathway involves the transfer of a 2-carbon fragment from D-xylulose-5-P to the aldose erythrose-4-phosphate, leading fructose 6-phosphate and glyceraldehyde-3-P. In the Calvin cycle, exactly the same two reactions occur, but in the opposite direction. Both enzymes take an important part in the known intermediate metabolism in the cytoplasm. But it could be hypothesized that an analog of this enzyme may function as an isomerase or may produce pentose or triose intermediates, which then leads to the NADH production during indirect measurement of the isomerase activity. However, the activity was missing in the absence of the *Leuconostoc mesenteroides* G6PDH enzyme. This indicates the formation of G6P from F6P, because the *Leuconostoc mesenteroides* G6PDH enzyme is able to use only G6P as a substrate. Thus, it is unlikely that an intermediate metabolite itself with NAD^+ potentiates the measured isomerase activity and leads to NADH formation. The third candidate is the catalase. It catalyzes the decomposition of hydrogen peroxide to water and oxygen (Chelikani et al., 2004). It is a specific marker protein, typically related to peroxisomes. The catalase may be bound to the ER membrane, and possibly has other functions.

Our future plan is to clone the cDNAs of these candidate proteins, and test whether the expressed proteins have isomerase activity upon expression in HEK-293 cells. Using epitope tagged constructs we will assess the intracellular localization and attempt to purify the enzymes followed by activity measurements.

In addition to the effort to identify the role of these enzymes, the novel aspect of the proposed research is to enhance the current knowledge on ER enzymes affecting the luminal $NADPH/NADP^+$ ratio and on enzymes anchored in the ER membrane and facing the luminal compartment. With the list of glycosylated proteins, we opened a new field of interest regarding potential new enzymes utilizing NADPH, and how they might influence the physiological redox status in the ER. Hopefully, this will help to understand how the ER pyridine nucleotide pool is regulated and how it is associated with the nutritional level of cells and the hormone regulation. In future experiments, several interesting genes (SDRs, membrane proteins) will be cloned for further functional characterization.

The critical issue that became obvious during this work is the difficulty of proper "inside-out" microsome isolations and determination of the membrane topology of microsomal enzymes. There is a concern that during microsomal preparations the microsomal membrane partially opens and reconnects in a reversed way, forming an "inside-in" microsomal vesicle. Such "insdide-in" microsomes would also show latency. Furthermore, the contamination with peroxisomal, mitochondrial and plasma membrane proteins cannot be fully prevented. Therefore, the ultimate determination of the intracellular localization and determination of membrane topology has to be performed.

The missing part in our experiments –which we also plan to accomplish - is to shave washed microsomal preparation with Protainase K. In this way we "clean" the membrane from proteins the bound to the outside part of the vesicle. If we cannot detect known cytosolic-oriented enzymes any longer by these methods, then a contamination with a small percentage of the "wrong-oriented" microsomes can be minimized.

Chapter IV:

Membrane topology of the microsomal enzyme 17β-hydroxysteroid dehydrogenase 3

4.1 Introduction

Androgens play a key role in the regulation of male sexual development. In the testis the conversion of the weak androgen 4-androstene-3,17-dione (AD) to the potent androgen testosterone is catalyzed by 17β-HSD3 (Geissler et al., 1994). The formation of testosterone is essential for further activation by 5α-reductase, leading to the most potent androgen dihydrotestosterone, and also for generation of estradiol by aromatase. In humans and rodents 17β-HSD3 is highly expressed in testis and at a lower level in other tissues including prostate, bone and adipose (Geissler et al., 1994; Sha et al., 1997; Mustonen et al., 1997). The consequences of impaired 17β-HSD3 function are seen in patients with loss-of-function mutations who suffer from male pseudohermaphroditism (Geissler et al., 1994; Andersson et al., 1996). Besides genetic defects, 17β-HSD3 activity may be decreased by the presence of environmental chemicals or endogenous modulators that either directly inhibit enzyme activity or suppress its expression (Nashev et al., 2010; Lo et al., 2003; Ohno et al., 2005; Yuan et al., 2012). Glucocorticoids are important modulators of androgen action. Elevated glucocorticoid levels caused by stress have been associated with reduced male fertility in humans and rodents (Orr et al., 1990; Orr and Mann, 1992; Fenster et al., 1997) with a negative correlation between circulating glucocorticoid and testosterone concentrations (Smals et al., 1977; Nakashima et al., 1975; Monder et al., 1994; Hardy et al., 2002). Experiments with isolated rat Leydig cells showed that glucocorticoids can directly inhibit testosterone synthesis by a glucocorticoid receptor (GR)-dependent mechanism (Orr et al., 1994; Hales et al., 1989).

Recently, a functional coupling between 17β-HSD3 and the glucocorticoid metabolizing enzyme 11β-hydroxysteroid dehydrogenase 1 (11β-HSD1) was proposed as a possible mechanism by which glucocorticoids might interfere with testosterone production in Leydig cells (Hu et al., 2008; Latif et al., 2011). 11β-HSD1 catalyzes the oxoreduction of inactive 11-ketoglucocorticoids (cortisone, 11-dehydrocorticosterone) into their active forms (cortisol, corticosterone) and of some other carbonyl containing steroidal and non-steroidal compounds into their respective hydroxyl forms (Odermatt and Nashev, 2010). 11β-HSD1 has been shown to function predominantly as a reductase in intact hepatocytes, adipocytes and macrophage (Balazs et al., 2009; Jamieson et al., 1995; Thieringer et al., 2001). Controversial observations were reported for the reaction direction in Leydig cells (Ge and Hardy 2000; Leckie et al., 1998; Ferguson et al., 1999). Recently, some investigators proposed that 11β-HSD1 may function as a dehydrogenase, thereby generating NADPH upon cortisol/corticosterone oxidation and stimulating 17β-HSD3-dependent reduction of AD (Hu et al., 2008; Latif et al., 2011). This hypothesis implies that 11β-HSD1 and 17β-HSD3 are both localized within the endoplasmic reticulum (ER) and are dependent on the luminal NADPH/NADP$^+$ pool.

We and others demonstrated that 11β-HSD1 has an N-terminal transmembrane helix with the catalytic moiety facing the ER-lumen (Odermatt et al., 1999; Mziaut et al., 1999; Frick et al., 2004; Ozols 1995). Importantly, the oxoreductase activity of 11β-HSD1 depends on NADPH supply in the ER-lumen by hexose-6-phosphate dehydrogenase (H6PDH) (Atanasov et al., 2008; Atanasov et al., 2004; Bánhegyi et al., 2004). Since the ER membrane has a low permeability for pyridine nucleotides, the luminal NADPH/NADP$^+$ pool is independent of that in the cytoplasm and its ratio determines the reaction direction of 11β-HSD1 and other luminal enzymes utilizing NADPH. H6PDH is fueled by glucose-6-phosphate (G6P) via a glucose-6-phosphate transporter (G6PT) in the ER membrane, or alternatively, by fructose-6-phosphate which can be converted to G6P in the ER by an enzyme that remains to be identified (Senesi et al., 2010).

The hypothesized functional coupling between 17β-HSD3 and 11β-HSD1 is based on the assumption that the catalytic domain of 17β-HSD3 is oriented toward the ER-lumen. Mindnich et al. assigned the intracellular localization of 17β-HSD3 to the ER membrane (Mindnich et al., 2005); however, they did not solve its membrane topology. Here, we investigated a potential functional coupling between 17β-HSD3 and 11β-HSD1 by using mouse MA-10 Leydig cells expressing endogenous levels of the two enzymes as well as transfected HEK-293 cells. We studied the dependence of the two enzymes on luminal and cytoplasmic NADPH and determined the membrane topology of 17β-HSD3.

4.2 Materials and Methods

4.2.1 Expression constructs

The plasmid for expression of C-terminally myc epitope-tagged 17β-HSD3 was constructed by PCR using a forward primer containing a *Bam*HI restriction endonuclease site followed by a Kozak consensus sequence (Kozak 1987) upstream of the ATG to initiator codon (5'-ATCGGATCCGCCATGGGGGACGTCCTGGAAC-3') and a reverse primer containing a myc epitope tag for facilitated detection at the C-terminus followed by the stop codon and a *Xba*I restriction endonuclease site (5'-ACTTCTAGATCAATCATCATCATCTTTATAATCCATACCTGAACCCCTGACCTTGGTGTTG AGCTTCAG-3') (Nashev et al., 2010). Attachment of the C-terminal myc epitope did not affect enzyme activity. The chimeric constructs, where the N-terminal transmembrane segment was exchanged, were obtained by PCR amplification. Sequences were exchanged at the beginning of the conserved Rossmann-fold at residue Lys36 of 11β-HSD1 and at Lys37 of 17β-HSD3. Chimeric construct N17-11HSD1 containing amino acids 1-36 of 17β-HSD3 followed by amino acids 36-292 of 11β-HSD1 was obtained using the forward primer 5'-GAGGATCCGCCATGGGGGACGTCCTGGAACAGTTCTTCATCCTCACAGGGCTGCTGGTGT GCCTGGCCTGCCTGGCGAAGTGCGTGAGATTCTCCAGATGTGTTTTACTGAACTACTGGA AAGTGATTGTCACAGGGGCCAGCAAAGG-3` and the reverse primer 5`-GTTTCTAGACTAATCATCATCATCTTTATAATCCATTCCGCTTCCGCTTCCGCTTCCGCTTC CGCTTCCGCTTCCGCTTCCGCTTCCGCTTCCGCTCTTGTTTATGAATCTGTCCATATTATAG CTCG-3'. Chimeric construct N11-17HSD3 containing amino acids 1-35 of 11β-HSD1 followed by amino acids 37-310 of 17β-HSD3 was obtained using the forward primer 5'-GAGGATCCGCCATGGCTTTTATGAAAAAATATCTCCTCCCCATTCTGGGGCTCTTCATGGC CTACTACTACTATTCTGCAAACGAGGAATTCAGACCAGAGATGCTCCAAGGAAAGAAAG TTTTGCCAAAGTCTTTCTTGCGG-3' and the reverse primer 5`-GTTTCTAGACTAATCATCATCATCTTTATAATCCATTCCGCTTCCGCTTCCGCTTCCGCTTC CGCTTCCGCTTCCGCTTCCGCTTCCGCTTCCGCTCCTGACCTTGGTGTTGAGCTTCAGG-3'. The chimeric proteins were tagged with a FLAG-epitope at the C-terminus to allow facilitated detection. All constructs were verified by sequencing.

4.2.2 Cell culture and transfection

HEK-293 cells were grown in Dulbecco's modified Eagle's medium (DMEM) supplemented with 10% fetal calf serum (FCS), 4.5 g/L glucose, 50 U/mL penicillin/streptomycin, 2 mM glutamine, and 10 mM HEPES, pH 7.4. The mouse Leydig cell line MA-10 (kindly provided by Prof. Mario Ascoli, University of Iowa, (Ascoli 1981)) was cultivated on 0.1% gelatin-coated cell culture dishes in DMEM/F12 medium containing 20 mM HEPES, pH 7.4, 15% horse serum and 50 μg/ml gentamicin. MA-10 cells were transfected using Lipofectamine reagent as described by the manufacturer (Life technologies, Zug, Switzerland).

4.2.3 Measurement of 17β-HSD3 and 11β-HSD1 enzyme activity

Endogenous 17β-HSD3 activity of MA-10 cells was measured by incubating cells in serum- and steroid-free (doubly charcoal-treated) DMEM/F12 medium containing 200 nM [1,2,6,7-^{3}H]-AD for 2–4 h. Reactions were terminated by adding 2 mM unlabeled AD and testosterone dissolved in methanol, followed by steroid extraction with ethylacetate and separation of steroids by TLC using chloroform:methanol at a ratio of 9:1 as solvent system. Product formation was detected by scintillation counting. Endogenous 11β-HSD1 activity in intact MA-10 cells was determined by adding radiolabeled cortisone at a final concentration of 200 nM. Following incubation at 37°C for 12-24 h, the amount of converted cortisone was assessed by ethylacetate extraction of steroids from the medium, TLC separation and scintillation counting.

Activities of recombinant enzymes expressed in HEK-293 cells were measured essentially as described earlier (Nashev et al., 2010; Atanasov et al., 2008). Cells were transiently transfected by the calcium-phosphate precipitation method with human recombinant 11β-HSD1 or 17β-HSD3 containing a C-terminal FLAG or myc epitope, respectively. The rates of conversion of cortisone to cortisol and AD to testosterone were determined. Reactions were terminated after 6 h by adding 2 mM unlabeled cortisol and cortisone and after 90 min by adding 2 mM unlabeled AD and testosterone dissolved in methanol.

4.2.4 Down-regulation of H6PDH and G6PDH by small interfering RNA (siRNA)

MA-10 cells were cultured in 12-well plates. At 48 h after transfection with 10 nM of H6PDH siRNA (QIAGEN; Entrez Gene ID:100198) or G6PDH siRNA (Dharmacon; Entrez Gene ID:2539) total RNA was extracted from adherent cells using Trizol reagent, followed by reverse transcription using Superscript II reverse transcriptase (Invitrogen). The mRNA levels were analyzed on a Rotor-Gene 6000 light cycler (Sydney, Australia). Reactions were performed in a total volume of 10 μL containing 20 ng cDNA, KAPA SYBR Master Mix (Kapasystems, Boston, MA), and specific primers and probes from assay on demand (Invitrogen). Expression levels relative to that of the internal control glyceraldehyde-3-phosphate dehydrogenase (GAPDH) were determined. Data represent triplicates of at least three independent experiments.

4.2.5 Selective permeabilization and immunofluorescence analysis

For immunofluorescence analysis HEK-293 cells were transfected with the corresponding construct, fixed 48 h post-transfection with 4% paraformaldehyde for 10 min, followed by washing 3 times with NAPS buffer (150 mM sodium phosphate, pH 7.4, 120 mM sucrose) as described earlier with few modifications (Frick et al., 2004). For complete permeabilization of membranes, cells were incubated with 0.5% Triton X-100 in NAPS buffer for 30 min. For selective permeabilization of the plasma membrane cells were incubated for 1 min with 25 µM digitonin. After washing 3 times with NAPS cells were incubated in blocking solution (NAPS containing 3% FBS) for 30 min. Enzymes were detected upon incubation with mouse monoclonal anti-FLAG antibody and rabbit polyclonal anti-myc antibody overnight at 4°C, washing three times, and incubation with ALEXA-488 goat anti-mouse and ALEXA-594 goat anti-rabbit antibody, respectively, for 1 h at 25°C. After washing, samples were mounted and analyzed on an Olympus FV1000-IX81 confocal microscope (Olympus, Volketswil, Switzerland) or on a Cellomics high-content imaging system according to the manufacturer's protocol (Cellomics ThermoScientific, Pittsburgh, PA).

4.2.6 Preparation of microsomes

HEK-293 cells (five 10 cm dishes each transfected with 5 µg of the corresponding expression plasmid) were collected 48 h post-transfection, washed twice with PBS and resuspended in 1.5 mL of ice-cold lysis buffer (10 mM MOPS, pH 7.5, 0.5 mM $MgCl_2$, and Complete protease inhibitor (Roche Diagnostics, Rotkreuz, Switzerland) and kept on ice for 5 min for cell lysis. The lysate was transferred into a Potter-Elvehjem homogenizer. Samples were homogenized by 20 strokes, followed by addition of 2 mL of solution A (0.5 M sucrose, 10 mM MOPS, pH 7.5, 20 mM NaCl, 100 mM KCl, 1 mM dithiothreitol) and centrifugation at $11,000 \times g$ for 15 min at 4°C. The supernatant was transferred into a new tube and centrifuged at $8,800 \times g$ for 20 min at 4°C. After centrifugation of the supernatant at $100,000 \times g$ for 1 h at 4°C, the pellet was resuspended in 500 µl of buffer A and centrifuged again at $100,000 \times g$ for 1 h at 4°C. The washed microsomal pellet fraction was resuspend in buffer B containing 10 mM MOPS, pH 7.5, 250 mM sucrose, 10 mM NaCl, 50 mM KCl and 0.5 mM dithiothreitol. The protein concentration was determined by BCA protein detection assay. Microsomal preparations were shock-frozen and stored at –70°C until analysis.

4.2.7 Proteinase K protection assay and immunoblotting

The proteinase K protection assay was performed as described earlier (Frick et al., 2004). Microsomes (30 µg of total proteins) were incubated in a total volume of 25 µL with 0.5 µg/µL of proteinase K (Roche Diagnostics) for 15 min on ice in the presence or absence of 0.5% Triton X-100.

Proteinase K was inactivated by adding 0.6 µL of 200 mM phenylmethylsulfonyl fluoride in isopropyl alcohol solution for 2 min, followed by adding SDS-PAGE sample buffer and immediate boiling for 5 min. Proteins were subjected to SDS-PAGE and Western blot analysis using anti-FLAG antibody M2 or anti-myc antibody as primary antibodies and horseradish peroxidase-conjugated secondary antibody.

4.2.8 Deglycosylation assay

For deglycosylation of luminal proteins microsomes (5 µg total proteins) were permeabilized with 0.5% Triton X-100, followed by boiling for 10 min in glycoprotein denaturation buffer. After cooling, microsomes were incubated for 1 h at 37°C in a final volume of 20 µl containing 500 U of Peptide:N-Glycosidase F (PNGaseF, New England Biolabs, Beverly, MA). The reaction was stopped by adding SDS-PAGE sample buffer and samples were analyzed by SDS-PAGE and subsequent immunoblotting.

4.3 Results

4.3.1 Lack of a direct functional interaction between 17β-HSD3 and 11β-HSD1

The hypothesized functional interaction between 17β-HSD3 and 11β-HSD1 and competition for the same NADPH/NADP$^+$ pool is based on the assumption of a luminal orientation of the catalytic moiety of 17β-HSD3. To test the existence of a functional coupling between the two enzymes, we coexpressed 17β-HSD3 and 11β-HSD1 either alone or in combination in HEK-293 cells and measured the respective enzyme activity. At a physiologically relevant concentration of 200 nM, neither cortisone nor cortisol affected the 17β-HSD3-dependent conversion of AD to testosterone upon incubation for 90 min in cells expressing 17β-HSD3 alone or upon coexpression with 11β-HSD1 (Fig. 1A). Also inhibition of 17β-HSD3 by the known inhibitor benzophenone-1 (BP1) (Nashev et al., 2010) was not affected upon coexpression with 11β-HSD1. Similar observations were made in MA-10 mouse Leydig cells expressing endogenous levels of the two enzymes (Fig. 1B). Due to the longer incubation time (2 and 4 h), 1 µM of cortisone and cortisol were used to avoid a substantial decrease in concentrations due to metabolism. Similarly, at 200 nM final concentration, neither AD nor testosterone affected the 11β-HSD1-dependent reduction of cortisone in HEK-293 cells in the presence or absence of 17β-HSD3 (Fig. 1C).
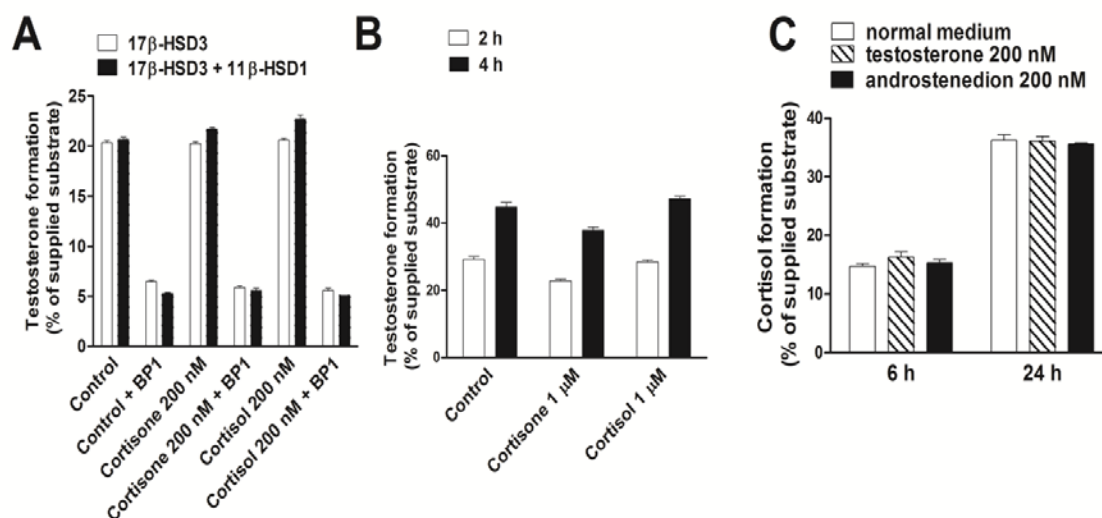
Fig 1. 17β-HSD3 and 11β-HSD1 do not functionally interact in MA-10 cells and in transfected HEK-293 cells. A, HEK-293 cells were transfected with 17β-HSD3 alone or together with 11β-HSD1. At 48 h post-transfection, 17β-HSD3-dependent conversion of 200 nM AD to testosterone (90 min incubation) was determined in the presence of vehicle, 200 nM cortisone or cortisol, and 5 µM of the 17β-HSD3 inhibitor benzophenone-1 (BP1), respectively. B, 17β-HSD3-dependent conversion of 200 nM AD to testosterone (2 and 4 h incubation) was determined in MA-10 mouse Leydig cells in the absence or presence of 1 µM cortisone or cortisol. C, HEK-293 cells were transfected with 11β-HSD1, followed by measuring the conversion of 200 nM cortisone to cortisol (incubation 6 and 24 h) in the presence of vehicle, 200 nM testosterone or 200 nM AD. Data represent mean ± SD from three independent experiments.

4.3.2 H6PDH does not modulate 17β-HSD3 activity

To investigate the impact of H6PDH on 17β-HSD3 activity we expressed 17β-HSD3 in the absence or presence of H6PDH in HEK-293 cells and determined the conversion of AD to testosterone. Coexpression with H6PDH did not affect 17β-HSD3 activity (Fig. 2A). We tested also whether overexpression of H6PDH in MA-10 cells might affect the activity of endogenous 17β-HSD3 (Fig. 2B). The fact that we could not detect an increased 17β-HSD3 activity might be due to substantial endogenous H6PDH expression. Therefore, we treated MA-10 cells with siRNA against H6PDH. 17β-HSD3-dependent reduction of AD was not altered (Fig. 2C); however, 11β-HSD1-dependent reduction of cortisone was significantly decreased as expected (Fig. 2D). These experiments suggested that 17β-HSD3 either has a luminal orientation but is independent of H6PDH-generated NADPH or that it is oriented toward the cytoplasm.
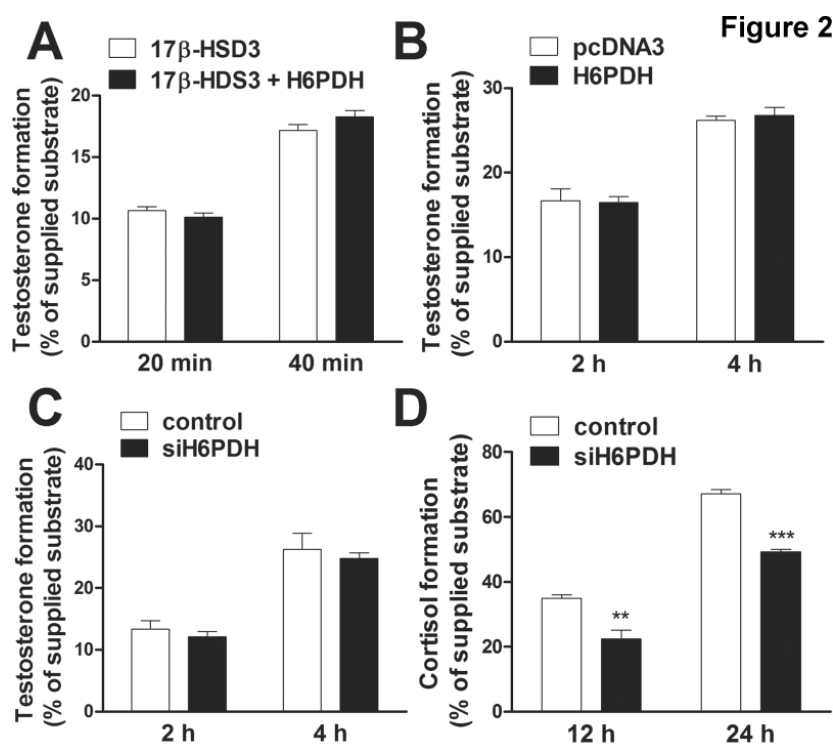
Fig. 2. Coexpression with H6PDH does not affect 17β-HSD3 activity. A, HEK-293 cells were transfected with 17β-HSD3 and either pcDNA3 vector control or H6PDH. At 48 h post-transfection, 17β-HSD3-dependent reduction of AD (200 nM) to testosterone was measured for 20 and 40 min. B, MA-10 cells with endogenous 17β-HSD3 expression were transfected with pcDNA3 control or H6PDH. Conversion of AD (200 nM) to testosterone was determined after 2 and 4 h. To investigate the impact of H6PDH knock-down, MA-10 cells were transfected with scrambled control siRNA or siRNA against H6PDH. At 48 h post-transfection 17β-HSD3 activity (C) and 11β-HSD1 (D) was determined. Data represent mean ± SD from three independent experiments. * $p < 0.05$, ** $p < 0.01$, *** $p < 0.001$.

4.3.3 Determination of the membrane topology of 17β-HSD3

To determine the orientation in the ER membrane of 17β-HSD3 we transfected HEK-293 cells with C-terminally myc epitope-tagged 17β-HSD3 and analyzed the intracellular localization by fluorescence microscopy. As controls FLAG-tagged 11β-HSD2 (with cytoplasmic orientation) and myc-tagged H6PDH (with luminal localization) were used. Analysis of 5'000 cells per well and measurement by Cellomics ArrayScan high-content imaging revealed a transfection rate of approximately 30% with comparable numbers of positive signals upon selective permeabilization of plasma membrane with 25 µM digitonin and complete permeabilization of membranes using 0.5% Triton X-100 (Fig. 3A). These observations indicate that the catalytic moiety of 17β-HSD3 protrudes into the cytoplasm. 11β-HSD2 and H6PDH showed cytoplasmic and luminal orientation, respectively, as previously reported (Odermatt et al., 1999; Atanasov et al., 2004). To assess the role of the N-terminal transmembrane helix, we constructed two chimeric proteins. 17N-11HSD1 consisted of the N-terminal membrane anchor of 17β-HSD3, followed by the cytoplasmic moiety of 11β-HSD1. 11N-17HSD3 had the N-terminal helix of 11β-HSD1 fused to the catalytic domain of 17β-HSD3. As shown in Figure 3A, the C-terminal tag of N17-11HSD1 was accessible to antibody in digitonin-treated cells, whereas N11-17HSD3 was protected. Thus, the N-terminal transmembrane sequence of 17β-HSD3 and 11β-HSD1 determines the cytoplasmic and luminal orientation, respectively. In addition to high-content imaging, cells treated with either Triton X-100 or digitonin were also analyzed by confocal microscopy by counting fluorescence positive cells among 500 cells randomly chosen in phase-contrast. Despite differences in the transfection rates and/or threshold of fluorescence detection with the different constructs, similar rates of positive cells than with high-content imaging were obtained (Table 1).

Table 1. Topology of 17β-HSD3, chimeric proteins and controls

Expressed protein	Triton X-100	Digitonin	Relative rate of positive cells with digitonin
11β-HSD2, C-terminal FLAG	28 ± 2	28 ± 1	100 ± 1
H6PDH, C-terminal myc	12 ± 1	1.3 ± 0.2	11 ± 1
17β-HSD3, C-terminal myc	10 ± 1	7 ± 1	67 ± 1
11N/17HSD3, C-terminal FLAG	20 ± 3	7 ± 1	34 ± 2
17N-11HSD1, C-terminal FLAG	20 ± 2	14 ± 2	69 ± 1

Transfected HEK-293 cells were either fully permeabilized with 0.5% Triton X-100, or the plasma membrane was selectively permeabilized with 25 µM digitonin, allowing restricted access of the antibody to the cytosolic compartment. Cells were incubated with primary anti-tag and fluorescence labeled secondary antibody, followed by analysis of fluorescent cells using confocal microscopy. Numbers represent the percentage of fluorescent cells relative to total cells from three independent experiments. In each experiment 500 cells were counted. Data represent mean ± SD.

To confirm the membrane topology of 17β-HSD3 and the chimeric proteins, we incubated microsomal vesicles expressing the respective protein for 15 min with proteinase K in the absence or presence of 0.5% Triton X-100. In the absence of detergent the chimera 11N-17HSD3 was protected from degradation by proteinase K as expected (Fig. 3B). 11β-HSD1 and H6PDH were also protected from degradation (not shown, (Odermatt et al., 1999)). In contrast, both 17β-HSD3 and 17N-11HSD1 were readily degraded, indicating cytoplasmic orientation. Additionally, since luminal but not cytoplasmic proteins can be glycosylated, we employed a deglycosylation assay. Treatment of microsomal preparations with PNGaseF for 1 h at 37°C did not alter the mobility of 17β-HSD3 and 17N-11HSD1 protein on SDS-PAGE but led to a band which migrated faster in case of H6PDH (not shown), 11β-HSD1 and 11N-17HSD3 (Fig. 3C).
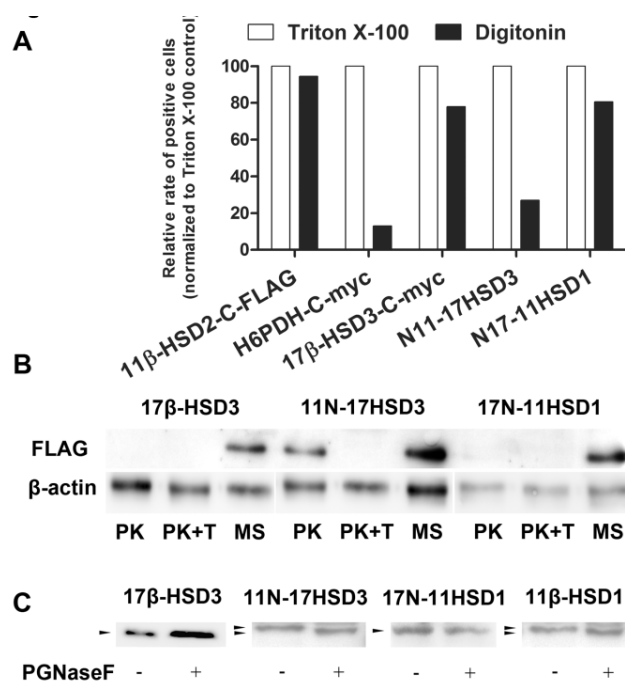
Fig 3. Determination of the membrane topology of 17β-HSD3. HEK-293 cells were transfected with different constructs. A, after 48 h cells were fixed with 4% paraformaldehyde, followed by selective permeabilization of the plasma membrane by incubation for 1 min with 25 μM digitonin or full permeabilization of membranes by incubation for 30 min with 0.5% Triton X-100. Fluorescence was analyzed using Cellomics ArrayScan high-content screening system by staining nuclei with Hoechst 33342 and counting cells yielding a positive signal with the respective anti-tag antibody. Results were normalized to Triton X-100 positive control. B, Microsomal preparations of cells expressing the respective C-terminally myc- or FLAG-tagged wild-type or chimeric protein were incubated for 15 min on ice with 0.5 μg/μL proteinase K in the absence or presence of 0.5% Triton X-100. Proteins were analysed by Western blotting using mouse monoclonal anti-tag antibody and secondary anti-mouse horseradish peroxidase antibody. C, For deglycosylation of proteins, microsomes were incubated with 500 U of PNGaseF for 1 h at 37°C, followed by analysis of samples by SDS-PAGE and Western blotting. Representative experiments are shown.

4.3.4 Glucose and cytoplasmic NADPH generation stimulate testosterone formation in MA-10 Leydig cells

A cytoplasmic orientation of 17β-HSD3 implies a dependence of the enzyme on the cytoplasmic NADPH pool. To test this assumption, we incubated MA-10 cells in normal medium containing 1 g/L glucose and in low glucose (0.1 g/L) medium. A significantly decreased 17β-HSD3-dependent testosterone formation was found under low glucose conditions (Fig. 4). Moreover, knock-down of the cytoplasmic NADPH generating enzyme glucose-6-phosphate dehydrogenase (G6PDH) by siRNA significantly reduced 17β-HSD3 activity both under high and low glucose conditions.
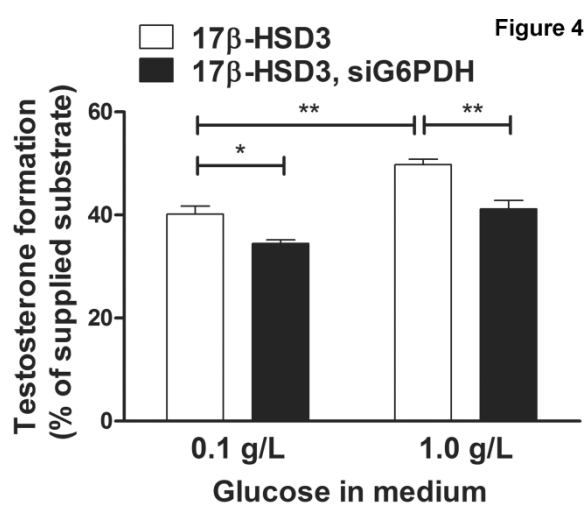
Fig 4. Modulation of 17β-HSD3 activity by glucose and cytoplasmic NADPH. HEK-293 cells were transfected with 17β-HSD3 and either scrambled control siRNA or siRNA against the cytosolic NADPH generating enzyme G6PDH. Prior to incubation with the respective medium, cells were preincubated with carbohydrate-free medium for 2 h, followed by incubation in low (0.1 g/L) or high (1 g/L) glucose medium and determination of 17β-HSD3 activity for 30 min at a supplied AD concentration of 200 nM.

4.4 Discussion

In the present study, we could not observe a functional coupling between 17β-HSD3 and 11β-HSD1. Coexpression with 11β-HSD1 and/or the addition of glucocorticoids did not alter 17β-HSD3 activity. Furthermore, 17β-HSD3-dependent reduction of AD was not affected by overexpression or knock-down of the luminal NADPH generating H6PDH but was decreased by knock-down of the cytoplasmic NADPH source G6PDH, suggesting cytoplasmic orientation of 17β-HSD3.

The intracellular localization of human and zebrafish 17β-HSD3 has been localized to the ER (Mindnich et al., 2005); however, the membrane topology was not resolved. Using selective permeabilization of the plasma membrane, proteinase K digestion and analysis of glycosylation patterns of wild-type and chimeric enzymes, we demonstrate a cytoplasmic orientation of 17β-HSD3. Importantly, we could show that the N-terminal membrane anchor sequences of 17β-HSD3 and 11β-HSD1 are sufficient to determine their cytoplasmic and luminal orientation, respectively. This resembles previous observations with 11β-HSD2 (Odermatt et al., 1999) and Rdh1 and Crad1 (Zhang et al., 2004). Thus, 17β-HSD3 and 11β-HSD1 are facing different compartments and utilize distinct NADPH pools (Fig. 5).
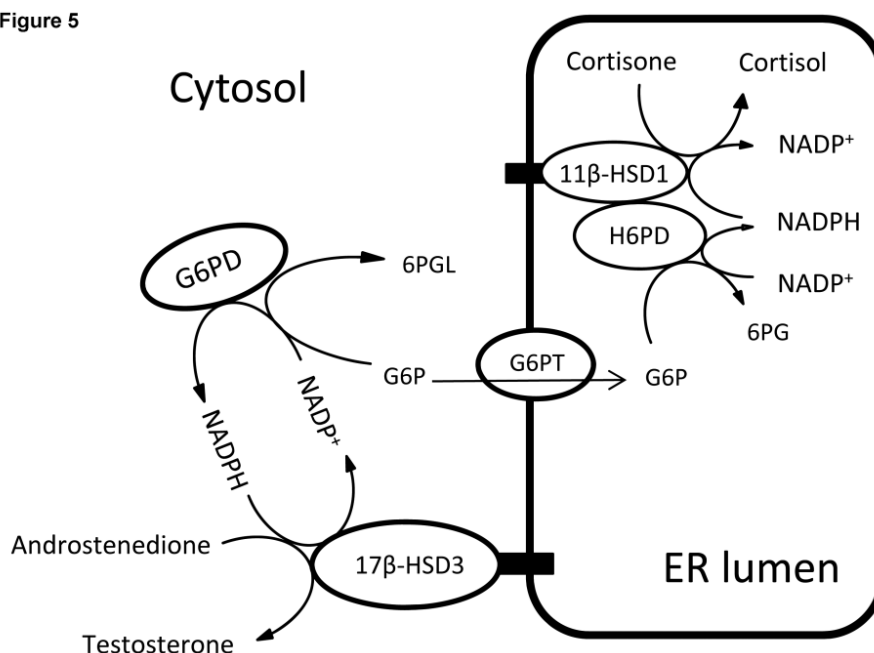
Fig 5. Model of 17β-HSD3 and 11β-HSD1 localization and their respective NADPH supplying enzymes. The cytoplasm and ER maintain independent NADPH/NADP+ pools that are dependent on cytoplasmic G6PDH and luminal H6PDH, respectively. 17β-HSD3 is anchored by its N-terminal transmembrane helix in the ER membrane, protrudes into the cytoplasm, and its activity is stimulated by G6PDH-generated NADPH, whereas 11β-HSD1 faces the ER-lumen and interacts with the NADPH supplying H6PDH.

That 17β-HSD3 is dependent on cytoplasmic and not luminal NADPH is supported by the fact that both H6PDH-deficient mice and H6PDH/11β-HSD1 double knock-out mice are fertile and do not seem to have impaired male development (Lavery et al., 2006; Lavery et al., 2008; Semjonous et al., 2011). Patients with cortisone reductase deficiency have increased rather than decreased androgen production (Draper et al., 2003), indicating that 17β-HSD3 function is not abolished by impaired H6PDH/11β-HSD1 activity.

The present study emphasizes the importance of the knowledge of intracellular localization and membrane topology to understand enzyme function. Nevertheless, this information is available only for very few of the microsomal short-chain dehydrogenase/reductase enzymes (Skarydova and Wsol, 2012; Bray et al., 2009), and resolving the membrane topology might provide further insight into the physiological roles of these enzymes.

To further study a potential interference of glucocorticoids with 17β-HSD3-dependent testosterone formation, we recently began to investigate its transcriptional regulation. Despite the known suppressive effect of elevated glucocorticoids on testosterone production, we did not observe any effect of 100 nM of the potent glucocorticoid dexamethasone on 17β-HSD3 expression in MA-10 Leydig cells and on a *HSD17B3* promoter-driven luciferase reporter in transfected HEK-293 cells (data not shown). Therefore, the suppressive effect of glucocorticoids on androgen production is probably mainly caused by inhibition of steroidogenesis. Reduced expression of steroidogenic acute regulatory protein (StAR) (Wang et al., 2000), cytochrome P450 side-chain cleavage enzyme (P450scc) (Hales and Payne, 1989) and cytochrome P450-17 (CYP17) (Orr et al., 1994) upon treatment with elevated glucocorticoids have been reported. Also, glucocorticoid-dependent apoptosis of testosterone producing Leydig cells has been reported (Gao et al., 2002; Gao et al., 2003). In conclusion, glucocorticoids do not seem to modulate 17β-HSD3 expression and activity. Reduced steroidogenesis may be responsible for the observed glucocorticoid-mediated suppression of androgen production.

Chapter V:

General discussion, conclusions and outlook

5.1 General discussion and conclusions

The ER plays a central role in the cellular adaptation to pathophysiological changes. It can function as a metabolic sensor to responsed to an overload of sugars and fatty acids as well as to a shortage of energy supply. Since the synthesis and the post-translational modifications of secretory and membrane proteins occur in the ER, this function can be coupled to anabolic and catabolic processes and the luminal redox environment. The response of the ER to these environmental changes is an activation of the unfolded protein response (UPR) pathway. If the ER-mediated UPR fails to cope with the challenge, this leads to ER-associated autophagy and ER-associated degradation of proteins or apoptosis. Therefore, maintenance of the balance of the luminal redox environment is essential for the cell to adapt to homeostatic alterations that cause protein misfolding and can induce programmed cell death if the repair attempts fail.

The thiol/disulfide redox system has been extensively studied and described in detail (Cuozzo and Kaiser, 1999; Ellgaard and Ruddock, 2005; Csala et al., 2010; Ramming and Appenzeller-Herzog, 2012;). In contrast, less information is known on another important redox system, the $NADPH/NADP^+$ pyridine nucleotide couple in the ER. It still remains a mystery how pyridine nucleotides reach the ER, since currently no transport is known across the ER membrane. The luminal pyridine nucleotide pool is separated from the cytosolic pool, because cellular membranes are impermeable for pyridine nucleotides. The cytosolic NADPH is generated by the widely investigated pentose-phosphate cycle, by the activity of G6PDH. The luminal NADPH pool only recently received greater attention due to the discovery of the ER-luminal NADPH generating enzyme hexose-6-phosphate dehydrogenase (H6PDH). This enzyme is the luminal analog of the cytosolic G6PDH. In contrast with the latter, the H6PDH catalyzes the first two steps of the pentose-phosphate pathway by converting G6P and $NADP^+$ to 6-phosphogluconate and NADPH (Beutler and Morrison, 1967). The native substrate G6P is transported into the ER compartment by a specific G6P-transporter (G6PT) (Gerin and Van Schaftingen, 2002). The main reason of the growing interest in H6PDH is its major role in the maintenance of the $NADPH/NADP^+$ ratio in the ER lumen. H6PDH is the only enzyme discovered so far that is generating NADPH in the ER. Evidence from cell-based studies suggests that other enzymes in the ER might contribute to NADPH formation, such as 6-phosphogluconate dehydrogenase ((Bublitz and Steavenson, 1988), sodium isocitrate dehydrogenase (Margittai and Bánhegyi, 2008) or malic enzyme (Wang et al., 2011). However, these enzymes need to be identified. Moreover, in *vivo* studies also suggested the existence of other ER luminal NADPH sources (Rogoff et al., 2010; Lavery et al., 2006; Semjonous et al., 2011). Primarily, it is important to maintain a high luminal $NADPH/NADP^+$ ratio for luminal redox reactions required in protein folding processes (Lavery et al., 2008). On the other side, this ratio determines the reaction direction of the luminal 11β-HSD1 dehydrogenase (Bánhegyi et al., 2004; Atanasov et al., 2004).

Several enzymatic reactions involved in the metabolism of bile acids, cholesterol, triglycerides, oxysterols, steroids and xenobiotics can be localized to the ER membrane. Some of these reactions may be dependent on luminal NADPH. However, the current knowledge on the utilization of NADPH for enzymatic reactions in the ER is limited. Until now, only one enzyme, 11β-HSD1, has been convincingly shown to be located and function in the ER (Ozols, 1995; Mziaut et al., 1999; Odermatt et al., 1999). 11β-HSD1 is responsible for the prereceptorial activation of glucocorticoids by converting intrinsically inactive cortisone and 11-dehydrocorticosterone into their active forms cortisol and corticosterone. Increased expression and activity of 11β-HSD1 have been implicated in the pathogenesis of metabolic diseases such as hypertension, type 2 diabetes, atherosclerosis, obesity, age-related cognitive dysfunction, osteoporosis and arthritis (Masuzaki et al., 2001; Hermanowski-Vosatka et al., 2005; Chapman and Seckl, 2008). Although the enzyme reaction is reversible *in vitro*, the enzyme acts as a reductase *in vivo*. As mentioned above, the direction of the enzyme reaction largely depends on the redox state of the pyridine nucleotides (Atanasov et al., 2004; Bánhegyi et al., 2004), and the high luminal $NADPH/NADP^+$ directly determines the physiological direction of 11β-HSD1. This ratio is generated by H6PDH and probably other luminal enzymes. Furthermore, a direct physical interaction between 11β-HSD1 and H6PDH allows the direct supply of NADPH to 11β-HSD1 in a close proximity for the efficient reduction of cortisone to cortisol despite a rather oxidative environment within the ER lumen (Atanasov et al., 2008). The physical interaction of the N-terminal domain of H6PDH with 11β-HSD1 might anchor H6PDH to the ER membrane, since H6PDH is associated with the ER membrane despite the absence of an obvious retention signal in its sequence (Zhang et al., 2009).

11β-HSD1 catalyzes other enzymatic reactions besides the activation of glucocorticoids. It has glucocorticoid-independent functions that require NADPH. We and others demonstrated that 11β-HSD1 can metabolize other substrates such as 7-oxocholesterol, 7-oxo-DHEA and 7-oxolithocholic acid (Nashev et al., 2007; Odermatt and Nashev, 2010; Schweizer et al., 2004; Odermatt et al., 2011; Hult et al., 2004; Muller et al., 2006). These findings suggest that this enzyme has additional functions in the metabolism of neurosteroids, oxysterols and bile acids as well as in the detoxification of various xenobiotics that contain reactive carbonyl groups. However, we hypothesize that beyond 11β-HSD1, the lumen of the ER might contain other NADPH-consuming reductases.

Recently 17β-HSD3 was suggested to catalyze the oxidation of NADPH in the ER lumen for the generation of testosterone from its precursor androstenedione. 17β-HSD3 contains well-conserved motifs such as the NADPH binding site (Rossmann-fold) that are present in all short-chain dehydrogenase/reductase (SDR) members. It is mainly expressed in Leydig cells of the testes, and lower expression levels were found in other tissues, including prostate, bone and adipose. Some studies hypothesized the functional interaction between 17β-HSD3-dependent testosterone formation and 11β-HSD1-mediated interconversion of glucocorticoids in the ER lumen of isolated mouse Leydig cells, suggesting that 11β-HSD1 may act as a dehydrogenase in these cells by using the $NADP^+$

produced during the conversion of androstenedione to testosterone catalyzed by 17β-HSD3 (Hu et al., 2008; Latif et al., 2011). It was proposed that the two enzymes compete for luminal NADPH. Mindnich and colleagues assigned the intracellular localization of 17β-HSD3 to the ER membrane (Mindnich et al., 2005); however, the membrane topology has not been determined. A functional coupling between 11β-HSD1 and 17β-HSD3 is only possible if 17β-HSD3 is oriented toward the ER lumen. As a consequence of the interaction, high cortisone levels would inhibit testosterone formation, thereby affecting male sexual development. In our experiments, we solved the question whether 17β-HSD3 may depend on luminal or cytoplasmic NADPH and determined the membrane topology of 17β-HSD3.

The current knowledge on the use of NADPH for enzymatic reactions in the ER is limited. Members of the large family of SDRs (73 proteins in human) play important roles in the metabolism of carbohydrates, lipids, amino acids, hormones, vitamins and xenobiotics. They all contain a conserved NAD(P)(H)-cofactor binding site, the Rossmann-motif. The functions of many human SDR enzymes remain unknown and the knowledge on their subcelullar localization and membrane topology may help to uncover the physiological roles of the poorly characterized enzymes (Bray et al., 2009; Persson et al., 2009; Kallberg et al., 2010). Particularly, it is crucial to know whether an enzyme faces the cytoplasm or the ER in order to understand its dependence on the redox environment. Thus, it is important to solve the membrane topology of these enzymes. We optimized the conditions to determine the topology and intracellular localization of microsomal enzymes. We applied selective semi-permeabilization of the plasma membrane, followed by immunodetection and confocal microscopy, as well as proteinase K protection assays and glycosylation assays.

According to the present knowledge, H6PDH is the only well-characterized luminal NADPH generating enzyme. It can utilize galactose-6-phosphate, glucosamine-6-phosphate, 2-deoxyglucose-6-phosphate, as well as simple glucose, although it uses G6P most efficiently (Beutler and Morrison; 1967). The availability of the substrate for H6PDH is ensured by G6PT. Recent observations indicated that not only G6P but also fructose-6-phosphate (F6P) can maintain a high luminal NADPH/NADP$^+$ ratio (McCormick et al., 2008). In the present work, we studied how F6P can enter the ER lumen and whether H6PDH can use F6P as a substrate and, if not, whether F6P is able to isomerized to G6P and thereby stimulates intraluminal NADPH formation.

In the present work, we addressed some of the open question regarding the generation and utilization of NADPH in the ER.

The first part of the present work showed that F6P can substitute for G6P and is sufficient to maintain the reductase activity of 11β-HSD1 in isolated microsomes. Moreover, using a rapid filtration transport assay we showed that F6P is transported across the ER membrane. This transport activity was found to be concentration-dependent both in hepatic and adipose tissue microsomes; however, the influx of F6P was much higher in adipose microsomes compared with liver microsomes.

Furthermore, our data revealed that the transport was not inhibited by G6P or by a G6PT inhibitor, suggesting that a transporter other than G6PT is responsible for the microsomal uptake of F6P. The GPT previously described in fibrocytes (Leuzzi et al., 2001) may be responsible for F6P transport into the ER lumen. Using the purified H6PDH enzyme, we showed that F6P cannot be directly dehydrogenated by H6PDH, and we also excluded H6PDH as a phosphohexose isomerase. Therefore, we postulate the existence of an ER-luminal hexose-phosphate isomerase that is distinct from the cytosolic enzyme. We began to characterize this novel luminal hexose-6-phosphate isomerase activity and found slight but reproducible differences in pH preference and effects of known inhibitors. Further, the results suggest that F6P promotes prereceptor glucocorticoid activation in white adipose tissue, which might have a role in the pathophysiology of the metabolic syndrome. Moreover, it is known that glucocorticoid activation has a privotal role during preadipocyte differentiation. Therefore, we investigated the effects of fructose on adipocyte survival and differentiation. We demonstrated that fructose can substitute for glucose and that it is sufficient to maintain energy supply and proper differentiation of preadipocytes into mature adipocytes. There was not difference in the lipid content and in the expression of differentiation markers upon cultivation of cells in medium containing fructose instead of glucose, as the only carbohydrate source. However, under physiological conditions these sugars are both present, with fructose being present at lower concentrations. The observation that fructose can be transported more efficiently into adipocytes and has similar effects on preadipocyte differentiation may provide an explanation for the adverse metabolic effects of excessive fructose consumption. The gene expression pattern in cells differentiated in glucose and fructose containing media is currently under investigation.

The second part of our work focused on the identification of new components of the pyridine nucleotide homeostasis in the ER. Especially, we focused on the identification of the enzyme responsible for the isomerization of F6P to G6P and on the enzyme catalyzing the reduction of 6-phosphogluconate.

To identify these and other potential enzymes that influence the homeostasis of the luminal NADPH pool we used rat and mouse liver microsomes and employed an activity-guided purification strategy. We applied a combination of fractionation, affinity purification, gel-electrophoretic separation and mass spectrometry methods to generate a list of potential candidates.

Additionally, we optimized the method for microsomal preparation. After differential centrifugation the microsomal pellets were washed three times to remove proteins that are attached to the cytoplasmic surface of the vesicles. To partially solubilize the microsomal vesicles we treated the washed microsomes with a buffer containing 20 mM of the detergent octylglucoside (OG). This additional step permeabilized the membrane and released soluble luminal proteins as well as some membrane proteins with a single transmembrane helix. The remaining membranous fraction, containing mostly multi-span membrane proteins, could still be pelleted by further centrifugation.

Using this method we separated total microsomal proteins, OG solubilized proteins and ER membrane pellet fraction. After verification that the enzyme activities of interest appeared in the OG solubilized fraction, we further applied a combination of size and ion exchange chromatography for fractionation and partial purification in order to minimize the number of potential candidates. After these steps the number of candidates for the luminal hexose-6-phophate isomerase decreased to less than 15 proteins (Chapter III. Table 1). The most promising candidate proteins now can be modified by attaching an epitope tag for further functional analysis and for subcellular localization studies. Epitope tagging also facilitates affinity purification of the candidate proteins. The incubation of the total microsomal fraction with OG resulted in a separation of solubilized luminal proteins from the membrane. Using protein identification by mass-spectrometry in collaboration with Dr. Paul Jenö we created a valuable list of proteins followed by sequence analysis for the presence of a "Rossmann-fold" pyridine nucleotide binding motif (Appendix II). This list of proteins potentially contains proteins with their catalytic domain facing the ER lumen. However, further research is needed to confirm their intracellular localization and to investigate their relevance for luminal NADPH. Alternatively, luminal enzymes playing a role in the generation and utilization of NADPH in the ER might be glycosylated. Therefore, the OG fraction of microsomes was subjected to concanavalin A and wheat germ agglutinin affinity columns. The aim of this approach was to isolate glycosylated proteins, since non-glycosylated proteins attached to microsomal vesicles at the cytoplasmic surface and proteins with transmembrane helices but facing the cytoplasm will be excluded. The advantage of this strategy is the separation of glycosylated luminal enzymes from total microsomal proteins and the increased chance to identify noval luminal NAD(P)-binding proteins. We identified 321 proteins that eluted from these columns (glycoproteins) and were separated by gel-electrophoresis separation and analyzed by mass-spectrometry (Appendix IV). This list of glycosylated ER proteins should help to identify luminal enzymes that participate in the utilization or generation of luminal NADPH.

In the third part, we optimized the conditions for the determination of the membrane topology of microsomal enzymes. One approach includes the semi-permeabilization of the plasma membrane using highly pure digitonin to allow the access of antibodies to the cytoplasmic but not the luminal compartment. The semi-permeabilization assay can be combined with electron microscopy or confocal microscopy. Another approach is proteinase K digestion of isolated microsomes, followed by immunodetection. Suitable positive and negative controls must be included in both approaches. Additionally, glycosylation analysis can be performed. This assay reveals whether the examined protein is glycosylated and either is a resident ER protein or it passed the ER compartment before reaching its destination (secretory proteins, plasma membrane proteins). If the targeted enzyme contains transmembrane helices, can be constructed chimeric proteins, where the luminal and cytoplasmic parts are exchanged with a protein of known topology. This approach helps to identify the determinants of the topology.

Recently, a functional coupling between 17β-HSD3 and 11β-HSD1 was proposed as a possible mechanism by which glucocorticoids might interfere with testosterone production in Leydig cells (Hu et al., 2008; Latif et al., 2011). According to this hypothesis, both enzymes are dependent on the luminal NADPH/NADP$^+$ pool, and it implies that 11β-HSD1 and 17β-HSD3 are both localized within the ER. Mindnich et al. assigned the intracellular localization of 17β-HSD3 to the ER membrane (Mindnich et al., 2005); however the membrane topology was not solved. Therefore, we investigated a potential functional coupling between 17β-HSD3 and 11β-HSD1 by using the mouse MA-10 Leydig cell line, expressing endogenous levels of the two enzymes, as well as transfected HEK-293 cells. We studied the dependence of the two enzymes on luminal and cytoplasmic NADPH. Using our established methods we determined the membrane topology of 17β-HSD3. We did not observe any functional coupling between 17β-HSD3 and 11β-HSD1. 17β-HSD3-dependent reduction of AD was neither affected by coexpression with 11β-HSD1 nor by overexpression or knock-down of the luminal NADPH generating H6PDH. In contrast, it was decreased by knock-down of the cytoplasmic NADPH generating enzyme G6PDH, suggesting cytoplasmic orientation of 17β-HSD3. Using selective permeabilization of the plasma membrane by digitonin, proteinase K digestion and analysis of glycosylation patterns of wild-type and chimeric enzymes, where the N-terminal anchor sequences between 17β-HSD3 and 11β-HSD1 were exchanged, we demonstrated a cytoplasmic orientation of 17β-HSD3. Importantly, we could show that the N-terminal membrane anchor sequences of 17β-HSD3 and 11β-HSD1 are sufficient to determine their cytoplasmic and luminal orientation, respectively. In conclusion, the results demonstrated a cytoplasmic orientation of 17β-HSD3 and dependence on G6PDH-generated NADPH, explaining the lack of a direct functional coupling with the luminal 11β-HSD1-mediated glucocorticoid metabolism.

5.2 Outlook

Although the SDR superfamily is one of the largest and most heterogenous enzyme family with more than 47.000 members listed in sequence databases and found in all life forms, only 14 members of human SDRs have been well characterized to date. The function of most of the human SDR enzymes remains unknown and the knowledge on the subcelullar localization and membrane topology is scarce (Bray et al., 2009; Persson et al., 2009; Kallberg et al., 2010). Enzymes belonging to the cluster C2 and C3 are membrane-associated proteins that typically catalyze reactions using retinoids, fatty acids and steroids as substrates (Bray et al., 2009). Some of them prefer NADPH as a cofactor, predicted by sequence analysis. Our future goal is to identify luminal SDRs, mainly those utilizing NADPH. Therefore, to begin to characterize such enzymes, we will determine their subcellular localization and initiate a screen for identification of substrates.

Based on our preliminary results on potentially glycosylated proteins 17β-HSD11 and 17β-HSD13 that were predicted to be oxidative NAD$^+$-dependent enzymes and 17β-HSD12 that prefers NADP$^+$ as a cofactor (Lukacik et al., 2006; Moeller and Adamski, 2009) are of specific interest: 17β-HSD11 and 17β-HSD13 share 78% sequence similarity. They have an interesting localization, being bound to the ER or to lipid droplets, depending on the physiological conditions (Yokoi et al., 2007; Horiguchi et al., 2008). The activity of both enzymes toward steroids or other substrates has not been clarified, thus, it is not known at present whether they catalyze oxidative or reductive reactions. Furthermore, the information on the membrane topology of these enzymes is missing. 17β-HSD12 shares highest sequence similarity with 17β-HSD3, but its properties and tissue distribution rather resemble those of 17β-HSD7, which reduces estrone to estradiol and dihydrotestosterone to 3β-adiol (Törn et al., 2003). Similarly, 17β-HSD12 is a NADPH-dependent microsomal enzyme that has been identified as 3-ketoacyl-CoA reductase (KAR) participating in the elongation of long-chain fatty acids (Moon and Horton, 2003), but it was also found to have estrone reductase activity and play an important role in estrogen activation in the mammary gland (Luu-The et al., 2006). Even if the orientation of this enzyme has not yet been determined, its wide distribution and preference for NADPH and together with the preliminary evidence for glycosylation from the present work makes this enzyme a promising candidate for further studies.

Another subgroup of interest includes DHRS1, DHRS3, DHRS7, DHRS7b and DHRS7c. Based on sequence analysis, they are suggested to use NADPH, but both subcellular localization and substrate specificity have not been defined so far. These enzymes belong to the C3 cluster, and little information is available. Thus, we aim to obtain more information on these enzymes by cloning the cDNA and constructing epitope-tagged version of these enzymes in order to determine their membrane topology and for facilitated purification. Using LC-MS based methods, we further aim to define the substrate specificity of these enzymes in future experiments.

Despite the increasing recognition of the importance of ER redox regulation and ER stress regarding the development of diabetes, cardiovascular disease and other metabolic disorders, and despite of the recent evidence for the importance of luminal NADPH for oxidative defense, the regulation of NADPH generation in the ER and the reactions utilizing NADPH in this compartment are insufficiently understood. Our general aim is to identify novel enzymes or mechanisms affecting the pyridine nucleotide balance in the ER. The proposed research contributes to the understanding of how luminal NADPH is regenerated and should enhance the current knowledge on disturbances of luminal NADPH homeostasis regarding the development of metabolic diseases. Discovering enzymes generating or utilizing luminal NADPH should provide novel insight into the role of luminal NADPH in pathophysiological redox processes and mechanisms of the antioxidant defense system in the ER. The expected findings could be relevant to understand the coupling between the cellular energy state, hormonal regulation and ER redox regulation.

Reference list

Agius L (1998) The physiological role of glucokinase binding and translocation in hepatocytes. *Adv Enzyme Regul* 38:303–331

Andersson S, Geissler WM, Wu L, Davis DL, Grumbach MM, New MI, Schwarz HP, Blethen SL, Mendonca BB, Bloise W, Witchel SF, Cutler GB, Jr., Griffin JE, Wilson JD, Russel DW (1996) Molecular genetics and pathophysiology of 17 beta-hydroxysteroid dehydrogenase 3 deficiency. *J Clin Endocrinol Metab* 81:130-136

Appenzeller-Herzog C, Riemer J, Christensen B, Sorensen ES, Ellgaard L (2008) A novel disulphide switch mechanism in Ero1alpha balances ER oxidation in human cells. *EMBO J* 27: 2977–2987

Appenzeller-Herzog C, Riemer J, Zito E, Chin KT, Ron D, Spiess M, Ellgaard L (2010) Disulphide production by Ero1a-PDI relay is rapid and effectively regulated. *EMBO J* 29:3318–3329

Arion WJ, Canfield WK, Ramos FC, Su ML, Burger HJ, Hemmerle H, Schubert G, Below P, Herling AW (1998) Chlorogenic acid analogue S 3483: a potent competitive inhibitor of the hepatic and renal glucose-6-phosphatase systems. *Arch Biochem Biophys* 351:279–285

Ascoli M (1981) Regulation of gonadotropin receptors and gonadotropin responses in a clonal strain of Leydig tumor cells by epidermal growth factor. *J Biol Chem* 256:179-183

Atanasov AG, Nashev LG, Gelman L, Legeza B, Sack R, Portmann R, Odermatt A (2008) Direct protein-protein interaction of 11beta-hydroxysteroid dehydrogenase type 1 and hexose-6-phosphate dehydrogenase in the endoplasmic reticulum lumen. *Biochim Biophys Acta* 1783:1536–1543

Atanasov AG, Nashev LG, Schweizer RA, Frick C, Odermatt A (2004) Hexose-6-phosphate dehydrogenase determines the reaction direction of 11β-hydroxysteroid dehydrogenase type 1 as an oxoreductase. *FEBS Letters* 571 129–133

Balázs Z, Nashev LG, Chandsawangbhuwana C, Baker ME and Odermatt A (2009) Hexose-6-phosphate dehydrogenase modulates the effect of inhibitors and alternative substrates of 11beta-hydroxysteroid dehydrogenase 1. *Mol Cell Endocrinol* 301:117-122

Bánhegyi G, Benedetti A, Fulceri R, Senesi S (2004) Cooperativity between 11beta-hydroxysteroid dehydrogenase type 1 and hexose-6-phosphate dehydrogenase in the lumen of the endoplasmic reticulum. *J Biol Chem* 279:27017–27021

Bánhegyi G, Braun L, Marcolongo P, Csala M, Fulceri R, Mandl J, Benedetti A (1996) Evidence for an UDP-glucuronic acid/phenol glucuronide antiport in rat liver microsomal vesicles. *Biochem J* 315:171–176

Bánhegyi G, Csala M, Nagy G, Sorrentino V, Fulceri R, Benedetti A (2003) Evidence for the transport of glutathione through ryanodine receptor channel type 1. *Biochem J* 376:807–812

Bánhegyi G, Lusini L, Puskás F, Rossi R, Fulceri R, Braun L, Mile V, di Simplicio P, Mandl J, Benedetti A (1999). Preferential transport of glutathione versus glutathione disulfide in rat liver microsomal vesicles. *J Biol Chem* 274:12213–12216

Bánhegyi G, Marcolongo P, Fulceri R, Hinds C, Burchell A, Benedetti A (1997) Demonstration of a metabolically active glucose-6-phosphate pool in the lumen of liver microsomal vesicles. *J Biol Chem* 272:13584–13590

Bánhegyi G, Margittai E, Szarka A, Mandl J, Csala M (2012) Crosstalk and barriers between the electron carriers of the endoplasmic reticulum. *Antioxid Redox Signal* 16(8):772-80

Bass R, Ruddock LW, Klappa P, Freedman RB (2004) A major fraction of endoplasmic reticulum-located glutathione is present as mixed disulfides with protein. *J Biol Chem* 279:5257–5262

Basu R, Singh R, Basu A, Johnson CM, Rizza RA (2006) Effect of nutrient ingestion on total-body and splanchnic cortisol production in humans. *Diabetes* 55:667–674

Beutler E, Morrison M (1967) Localization and characteristics of hexose 6-phosphate dehydrogenase (glucose dehydrogenase) *J. Biol. Chem* 242:5289–5293

Branden,C., Jörnvall, H., Eklund, H. and Furugren, B (1975) Alcohol dehydrogenase. Boyer, P. D. (Ed.) In: The Enzymes, 3rd edn., vol. 11, pp. 103–190, Academic Press, New York.

Bray JE, Marsden BD, Oppermann U (2009) The human short-chain dehydrogenase/reductase (SDR) superfamily: a bioinformatics summary *Chem Biol Interact* 178(1-3):99-109

Brown CM, Dulloo AG, Montani JP (2008) Sugary drinks in the pathogenesis of obesity and cardiovascular diseases. *Int J Obes* (Lond) 32, Suppl 6: S28–S34

Bublitz C, Lawler CA, Steavenson S (1987) The topology of phosphogluconate dehydrogenases in rat liver microsomes. *Arch Biochem Biophys* 259(1):22-8

Bublitz C, Steavenson S (1988) The pentose phosphate pathway in the endoplasmic reticulum. *J Biol Chem* 263(26):12849-53

Bujalska IJ, Gathercole LL, Tomlinson JW, Darimont C, Ermolieff J, Fanjul AN, Rejto PA, Stewart PM (2008a) A novel selective 11beta-hydroxysteroid dehydrogenase type 1 inhibitor prevents human adipogenesis. *J Endocrinol* 197(2):297-307

Bujalska IJ, Hewitt KN, Hauton D, Lavery GG, Tomlinson JW, Walker EA, Stewart PM (2008b) Lack of hexose-6-phosphate dehydrogenase impairs lipid mobilization from mouse adipose tissue. *Endocrinology* 149:2584–2591

Bujalska IJ, Kumar S, Hewison M, Stewart PM (1999) Differentiation of adipose stromal cells: the roles of glucocorticoids and 11β-hydroxysteroid dehydrogenase *Endocrinology* 140:3188–3196

Cabibbo A, Pagani M, Fabbri M, Rocchi M, Farmery MR, Bulleid NJ, Sitia R (2000) ERO1-L, a human protein that favors disulfide bond formation in the endoplasmic reticulum. *J Biol Chem* 275: 4827–4833

Chapman KE, Seckl JR (2008) 11beta-HSD1, inflammation, metabolic disease and age-related cognitive (dys)function. *Neurochem Res* 33(4):624-36

Chelikani P, Fita I, Loewen PC (2004) Diversity of structures and properties among catalases. *Cell Mol Life Sci* 61(2):192-208

Chirgwin JM, Parsons TF, Noltmann EA (1975) Mechanistic implications of the pH independence of inhibition of phosphoglucose isomerase by neutral sugar phosphates. *J Biol Chem* 250:7277–7279

Clarke JL, Mason PJ (2003) Murine hexose-6-phosphate dehydrogenase: a bifunctional enzyme with broad substrate specificity and 6-phosphogluconolactonase activity. *Arch Biochem Biophys* 415:229–234

Csala M, Bánhegyi G, Benedetti A (2006) Endoplasmic reticulum: A metabolic compartment. *FEBS Lett* 580: 2160–2165

Csala M, Margittai E, Bánhegyi G (2010) Redox control of endoplasmic reticulum function. *Antioxid Redox Signal* 13(1):77-108

Cuozzo JW, Kaiser CA (1999) Competition between glutathione and protein thiols for disulphide-bond formation. *Nat. Cell Biol* 1, 130-135

Darakhshan F, Hajduch E, Kristiansen S, Richter EA, Hundal HS (1998) Biochemical and functional characterization of the GLUT5 fructose transporter in rat skeletal muscle. *Biochem J* 336:361–366

Del Bello B, Maellaro E, Sugherini L, Santucci A, Comporti M, Casini AF (1994) Purification of NADPH-dependent dehydroascorbate reductase from rat liver and its identification with 3α-hydroxysteroid dehydrogenase. *Biochem J* 304: 385–390

Depuydt M, Messens J, Collet JF (2011) How proteins form disulfide bonds. *Antioxid Redox Signal* 15: 49–66

Dixon BM, Heath SH, Kim R, Suh JH, Hagen TM (2008) Assessment of endoplasmic reticulum glutathione redox status is confounded by extensive ex vivo oxidation. *Antioxid Redox Signal* 10: 963–972

Draper N, Walker EA, Bujalska IJ, Tomlinson JW, Chalder SM, Arlt W, Lavery GG, Bedendo O, Ray DW, Laing I, Malunowicz E, White PC, Hewison M, Mason PJ, Connell JM, Shackleton CH, Stewart PM (2003) Mutations in the genes encoding 11β-hydroxysteroid dehydrogenase type 1 and hexose-6-phosphate dehydrogenase interact to cause cortisone reductase deficiency. *Nat Genet* 34:434-439

Dzyakanchuk AA, Balázs Z, Nashev LG, Amrein KE, Odermatt A (2009) 11beta-Hydroxysteroid dehydrogenase 1 reductase activity is dependent on a high ratio of NADPH/NADP(+) and is stimulated by extracellular glucose. *Mol Cell Endocrinol* 301(1-2):137-41

Ellgaard L, Ruddock LW (2005) The human protein disulfide isomerase family: Substrate interactions and functional properties. *EMBO Rep* 6: 28–32

Elliott SS, Keim NL, Stern JS, Teff K, Havel PJ (2002) Fructose, weight gain, and the insulin resistance syndrome. *Am J Clin Nutr* 76:911–922

Fairbank M, St-Pierre P, Nabi IR (2009) The complex biology of autocrine motility factor/phosphoglucose isomerase (AMF/PGI) and its receptor, the gp78/AMFR E3 ubiquitin ligase. *Mol Biosyst* 5:793–801

Fenster L, Katz DF, Wyrobek AJ, Pieper C, Rempel DM, Oman D, Swan SH (1997) Effects of psychological stress on human semen quality. *J Androl* 18:194-202

Ferguson SE, Pallikaros Z, Michael AE, Cooke BA (1999) The effects of different culture media, glucose, pyridine nucleotides and adenosine on the activity of 11beta-hydroxysteroid dehydrogenase in rat Leydig cells. *Mol Cell Endocrinol* 158:37-44

Frand AR, Kaiser CA (1998) The ERO1 gene of yeast is required for oxidation of protein dithiols in the endoplasmic reticulum. *Mol Cell* 1: 161–170

Frick C, Atanasov AG, Arnold P, Ozols J, Odermatt A (2004) Appropriate function of 11beta-hydroxysteroid dehydrogenase type 1 in the endoplasmic reticulum lumen is dependent on its N-terminal region sharing similar topological determinants with 50-kDa esterase. *J Biol Chem* 279:31131-31138

Froesch ER, Ginsberg JL (1962) Fructose metabolism of adipose tissue. I. Comparison of fructose and glucose metabolism in epididymal adipose tissue of normal rats. *J Biol Chem* 237:3317–3324

Frost SC, Lane MD (1985) Evidence for the involvement of vicinal sulfhydryl groups in insulin-activated hexose transport by 3T3-L1 adipocytes *J Biol Chem* 260:2646–2652

Fulceri R, Bánhegyi G, Gamberucci A, Giunti R, Mandl J, Benedetti A (1994) Evidence for the intraluminal positioning of p-nitrophenol UDP-glucuronosyltransferase activity in rat liver microsomal vesicles. *Arch Biochem Biophys* 309:43–46

Fullam E, Pojer F, Bergfors T, Jones TA, Cole ST (2012) Structure and function of the transketolase from Mycobacterium tuberculosis and comparison with the human enzyme. *Open Biol* 2(1):110026

Gao HB, Tong MH, Hu YQ, Guo QS, Ge R, Hardy MP (2002) Glucocorticoid induces apoptosis in rat leydig cells. *Endocrinology* 143:130-138

Gao HB, Tong MH, Hu YQ, You HY, Guo QS, Ge RS, Hardy MP (2003) Mechanisms of glucocorticoid-induced Leydig cell apoptosis. *Mol Cell Endocrinol* 199:153-163

Gao X, Qi L, Qiao N, Choi HK, Curhan G, Tucker KL, Ascherio A (2007) Intake of added sugar and sugar-sweetened drink and serum uric acid concentration in US men and women. *Hypertension* 50:306–312

Ge RS, Hardy MP (2000) Initial predominance of the oxidative activity of type I 11beta-hydroxysteroid dehydrogenase in primary rat Leydig cells and transfected cell lines. *J Androl* 21:303-310

Geissler WM, Davis DL, Wu L, Bradshaw KD, Patel S, Mendonca BB, Elliston KO, Wilson JD, Russell DW, Andersson S (1994) Male pseudohermaphroditism caused by mutations of testicular 17 beta-hydroxysteroid dehydrogenase 3. *Nat Genet* 7:34-39

Gerin I, Van Schaftingen E (2002) Evidence for glucose-6-phosphate transport in rat liver microsomes. *FEBS Lett* 517:257–260

Gerin I, Veiga-da-Cunha M, Achouri Y, Collet JF, Van Schaftingen E (1997) Sequence of a putative glucose 6-phosphate translocase, mutated in glycogen storage disease type Ib. *FEBS Lett* 419:235–238

Gomez-Sanchez EP, Romero DG, de Rodriguez AF, Warden MP, Krozowski Z, Gomez-Sanchez CE (2008) Hexose-6-phosphate dehydrogenase and 11β hydroxysteroid dehydrogenase-1 tissue distribution in the rat *Endocrinology* 149:525–533

Hajduch E, Darakhshan F, Hundal HS (1998) Fructose uptake in rat adipocytes: GLUT5 expression and the effects of streptozotocin-induced diabetes. *Diabetologia* 41:821–828

Hales DB, Payne AH (1989) Glucocorticoid-mediated repression of P450scc mRNA and de novo synthesis in cultured Leydig cells. *Endocrinology* 124:2099-2104

Hardy MP, Sottas CM, Ge R, McKittrick CR, Tamashiro KL, McEwen BS, Haider SG, Markham CM, Blanchard RJ, Blanchard DC, Sakai RR (2002) Trends of reproductive hormones in male rats during psychosocial stress: role of glucocorticoid metabolism in behavioral dominance. *Biol Reprod* 67:1750-1755

Hauner H, Entenmann G, Wabitsch M, Gaillard D, Ailhaud G, Negrel R, Pfeiffer EF (1989) Promoting effect of glucocorticoids on the differentiation of human adipocyte precursor cells cultured in a chemically defined medium. *Journal of Clinical Investigation* 84:1663–1670

Havel PJ (2005) Dietary fructose: implications for dysregulation of energy homeostasis and lipid/carbohydrate metabolism. *Nutr Rev* 63:133–157

Hems DA, Brosnan JT (1970) Effects of ischaemia on content of metabolites in rat liver and kidney in vivo. *Biochem J* 120:105–111

Heritage D, Wonderlin WF (2001) Translocon pores in the endoplasmic reticulum are permeable to a neutral, polar molecule. *J Biol Chem* 276:22655–22662

Hermanowski-Vosatka A, Balkovec JM, Cheng K, Chen HY, Hernandez M, Koo GC, Le Grand CB, Li Z, Metzger JM, Mundt SS, Noonan H, Nunes CN, Olson SH, Pikounis B, Ren N, Robertson N, Schaeffer JM, Shah K, Springer MS, Strack AM, Strowski M, Wu K, Wu T, Xiao J, Zhang BB, Wright SD, Thieringer R (2005) 11beta-HSD1 inhibition ameliorates metabolic syndrome and prevents progression of atherosclerosis in mice. *J Exp Med* 202:517–527

Hewitt KN, Walker EA, Stewart PM (2005) Minireview: hexose-6-phosphate dehydrogenase and redox control of 11{beta}-hydroxysteroid dehydrogenase type 1 activity. *Endocrinology* 146:2539–2543

Horiguchi Y, Araki M, Motojima K (2008) 17beta-Hydroxysteroid dehydrogenase type 13 is a liver-specific lipid droplet-associated protein. *Biochem Biophys Res Commun* 370(2):235-8

Hu GX, Lian QQ, Lin H, Latif SA, Morris DJ, Hardy MP, Ge RS (2008) Rapid mechanisms of glucocorticoid signaling in the Leydig cell. *Steroids* 73(9-10):1018-24

Hult M, Elleby B, Shafqat N, Svensson S, Rane A, Jörnvall H, Abrahmsen L, Oppermann U (2004) Human and rodent type 1 11beta-hydroxysteroid dehydrogenases are 7beta-hydroxycholesterol dehydrogenases involved in oxysterol metabolism. *Cell Mol Life Sci* 61(7-8):992-9

Hwang C, Sinskey AJ, and Lodish HF (1992) Oxidized redox state of glutathione in the endoplasmic reticulum. *Science* 257:1496–1502

Jamieson PM, Chapman KE, Edwards CR and Seckl JR (1995) 11 beta-hydroxysteroid dehydrogenase is an exclusive 11 beta- reductase in primary cultures of rat hepatocytes: effect of physicochemical and hormonal manipulations. *Endocrinology* 136:4754-4761

Johnson RJ, Perez-Pozo SE, Sautin YY, Manitius J, Sanchez-Lozada LG, Feig DI, Shafiu M, Segal M, Glassock RJ, Shimada M, Roncal C, Nakagawa T (2009) Hypothesis: could excessive fructose intake and uric acid cause type 2 diabetes? *Endocr Rev* 30:96–116

Jörnvall H, Persson B, Krook M, Atrian S, Gonzalez-Duarte R, Jeffery J, Ghosh D (1995) Short-chain dehydrogenases/reductases (SDR). *Biochemistry* 34, 6003–6013

Kallberg Y, Oppermann U, Jörnvall H, Persson B (2002) Short-chain dehydrogenases/reductases (SDRs). *Eur J Biochem* 269(18):4409-17

Kallberg Y, Oppermann U, Persson B (2010) Classification of the short-chain dehydrogenase/reductase superfamily using hidden Markov models. *FEBS J* 277(10):2375-86

Karala AR, Lappi AK, Saaranen M, and Ruddock LW (2009) Efficient peroxide mediated oxidative refolding of a protein at physiological pH and implications for oxidative folding in the endoplasmic reticulum. *Antioxid Redox Signal* 11: 963–970

Kavanagh KL, Jörnvall H, Persson B, Oppermann U (2008) Medium- and short-chain dehydrogenase/reductase gene and protein families : the SDR superfamily: functional and structural diversity within a family of metabolic and regulatory enzymes. *Cell Mol Life Sci* 65(24):3895-906

Kereszturi É, Kálmán FS, Kardon T, Csala M, Bánhegyi G (2010) Decreased prereceptorial glucocorticoid activating capacity in starvation due to an oxidative shift of pyridine nucleotides in the endoplasmic reticulum. *FEBS Lett* 584(22):4703-8

Kochetov GA (1982) Transketolase from yeast, rat liver, and pig liver. *Methods Enzymol* 90, 209–223

Kotelevtsev Y, Holmes MC, Burchell A, Houston PM, Schmoll D, Jamieson P, Best R, Brown R, Edwards CR, Seckl JR, John J. Mullins (1997) 11β-Hydroxysteroid dehydrogenase type 1 knockout mice show attenuated glucocorticoid-inducible responses and resist hyperglycemia on obesity or stress. *PNAS* 94:14924–14929

Kozak M (1987) At least six nucleotides preceding the AUG initiator codon enhance translation in mammalian cells. *J Mol Biol* 196:947-950

Larade K, Jiang Z, Zhang Y, Wang W, Bonner-Weir S, Zhu H, Bunn HF (2008) Loss of Ncb5or results in impaired fatty acid desaturation, lipoatrophy, and diabetes. *J Biol Chem* 283:29285–29291

Lamb HK, Mee C, Xu W, Liu L, Blond S, Cooper A, Charles IG, Hawkins AR (2006) The affinity of a major Ca2+ binding site on GRP78 is differentially enhanced by ADP and ATP. *J Biol Chem* 281:8796–8805

Latif SA, Shen M, Ge RS, Sottas CM, Hardy MP, Morris DJ (2011) Role of 11beta-OH-C(19) and C(21) steroids in the coupling of 11beta-HSD1 and 17beta-HSD3 in regulation of testosterone biosynthesis in rat Leydig cells. *Steroids* 76:682-689.

Lavery GG, Hauton D, Hewitt KN, Brice SM, Sherlock M, Walker EA, Stewart PM (2007) Hypoglycemia with enhanced hepatic glycogen synthesis in recombinant mice lacking hexose-6-phosphate dehydrogenase. *Endocrinology* 148:6100–6106

Lavery GG, Walker EA, Draper N, Jeyasuria P, Marcos J, Shackleton CH, Parker KL, White PC, Stewart PM (2006) Hexose-6-phosphate dehydrogenase knock-out mice lack 11 beta-hydroxysteroid dehydrogenase type 1-mediated glucocorticoid generation. *J Biol Chem* 281:6546–6551

Lavery GG, Walker EA, Turan N, Rogoff D, Ryder JW, Shelton JM, Richardson JA, Falciani F, White PC, Stewart PM, Parker KL, McMillan DR (2008) Deletion of hexose-6-phosphate dehydrogenase activates the unfolded protein response pathway and induces skeletal myopathy. *J Biol Chem* 283(13):8453-61

Leckie CM, Welberg LA, Seckl JR (1998) 11beta-hydroxysteroid dehydrogenase is a predominant reductase in intact rat Leydig cells. *J Endocrinol* 159:233-238

Lesk AM (1995) NAD-binding domains of dehydrogenases. *Curr. Opin. Struct. Biol* 5, 775–783

Leuzzi R, Fulceri R, Marcolongo P, Bánhegyi G, Zammarchi E, Stafford K, Burchell A, Benedetti A (2001) Glucose-6-phosphate transport in fibroblast microsomes from glycogen storage disease type 1b patients: evidence for multiple glucose-6-phosphate transport sytems. *Biochem J* 357:557–562

Liu Y, Park F, Pietrusz JL, Jia G, R.J, Singh RJ, B.C. Netzel BC, Liang M (2008) Suppression of 11β-hydroxysteroid dehydrogenase type 1 with RNA interference substantially attenuates 3T3-L1 adipogenesis *Physiol Genomics* 32:343–351

Lizák B, Csala M, Benedetti A, Bánhegyi G (2008) The translocon and the non-specific transport of small molecules in the endoplasmic reticulum. *Mol Membr Biol* 25: 95–101

Lo S, Allera A, Albers P, Heimbrecht J, Jantzen E, Klingmuller D, Steckelbroeck S (2003) Dithioerythritol (DTE) prevents inhibitory effects of triphenyltin (TPT) on the key enzymes of the human sex steroid hormone metabolism. *J Steroid Biochem Mol Biol* 84:569-576

Lukacik P, Kavanagh KL, Oppermann U (2006) Structure and function of human 17beta-hydroxysteroid dehydrogenases. *Mol Cell Endocrinol* 248(1-2):61-71

Luu-The V, Tremblay P, Labrie F (2006) Characterization of type 12 17beta-hydroxysteroid dehydrogenase, an isoform of type 3 17beta-hydroxysteroid dehydrogenase responsible for estradiol formation in women. *Mol Endocrinol* 20(2):437-43

Mandl J, Mészáros T, Bánhegyi G, Hunyady L, Csala M (2009) Endoplasmic reticulum: nutrient sensor in physiology and pathology. *Trends Endocrinol Metab* 20(4):194-201

Marcolongo P, Piccirella S, Senesi S, Wunderlich L, Gerin I, Mandl J, Fulceri R, Bánhegyi G, Benedetti A (2007) The glucose-6-phosphate transporter-hexose-6-phosphate dehydrogenase-11β-hydroxysteroid dehydrogenase type 1 system of the adipose tissue. *Endocrinology* 148:2487–2495

Marcolongo P, Senesi S, Gava B, Fulceri R, Sorrentino V, Margittai E, Lizák B, Csala M, Bánhegyi G, Benedetti A (2008) Metyrapone prevents cortisone-induced preadipocyte differentiation by depleting luminal NADPH of the endoplasmic reticulum. *Biochem Pharmacol* 76(3):382-90

Marcolongo P, Senesi S, Giunti R, Csala M, Fulceri R, Bánhegyi G, Benedetti A (2011) Expression of hexose-6-phosphate dehydrogenase in rat tissues. *J Steroid Biochem Mol Biol* 126(3-5):57-64

Margittai E, Bánhegyi G (2008) Isocitrate dehydrogenase: A NADPH-generating enzyme in the lumen of the endoplasmic reticulum. *Arch Biochem Biophys* 471(2):184-90

Marquardt T, Hebert DN, Helenius A (1993) Posttranslational folding of influenza hemagglutinin in isolated endoplasmic reticulum-derived microsomes. *J Biol Chem* 268: 19618–19625

Masuzaki H, Paterson J, Shinyama H, Morton NM, Mullins JJ, Seckl JR, Flier JS (2001) A transgenic model of visceral obesity and the metabolic syndrome. *Science* 294:2166–2170

Mathias RA, Chen YS, Kapp EA, Greening DW, Mathivanan S, Simpson RJ (2011) Triton X-114 phase separation in the isolation and purification of mouse liver microsomal membrane proteins. *Methods* 54(4):396-406

May JM, Qu ZC, Whitesell RR, Cobb CE (1996) Ascorbate recycling in human erythrocytes: role of GSH in reducing dehydroascorbate. *Free Radic Biol Med* 20:543–551

McCormick KL, Wang X, Mick GJ (2008) Modification of microsomal 11beta-HSD1 activity by cytosolic compounds: glutathione and hexose phosphoesters. *J Steroid Biochem Mol Biol* 111(1-2):18-23

Merksamer PI, Trusina A, Papa FR (2008) Real-time redox measurements during endoplasmic reticulum stress reveal interlinked protein folding functions. *Cell* 135: 933–947

Mindnich R, Haller F, Halbach F, Moeller G, Hrabe de Angelis M, Adamski J (2005) Androgen metabolism via 17beta-hydroxysteroid dehydrogenase type 3 in mammalian and non-mammalian vertebrates: comparison of the human and the zebrafish enzyme. *J Mol Endocrinol* 35:305-316

Moeller G, Adamski J (2009) Integrated view on 17beta-hydroxysteroid dehydrogenases. *Mol Cell Endocrinol* 301(1-2):7-19

Molteni SN, Fassio A, Ciriolo MR, Filomeni G, Pasqualetto E, Fagioli C, Sitia R (2004) Glutathione limits Ero1-dependent oxidation in the endoplasmic reticulum. *J Biol Chem* 279: 32667–32673

Monder C, Sakai RR, Miroff Y, Blanchard DC, Blanchard RJ (1994) Reciprocal changes in plasma corticosterone and testosterone in stressed male rats maintained in a visible burrow system: evidence for a mediating role of testicular 11 beta-hydroxysteroid dehydrogenase. *Endocrinology* 134:1193-1198

Montonen J, Järvinen R, Knekt P, Heliövaara M, Reunanen A (2007) Consumption of sweetened beverages and intakes of fructose and glucose predict type 2 diabetes occurrence. *J Nutr* 137:1447–1454

Moon YA, Horton JD (2003) Identification of two mammalian reductases involved in the two-carbon fatty acyl elongation cascade. *J Biol Chem* 278(9):7335-43

Muller C, Pompon D, Urban P, Morfin R (2006) Inter-conversion of 7alpha- and 7beta-hydroxy-dehydroepiandrosterone by the human 11beta-hydroxysteroid dehydrogenase type 1. *J Steroid Biochem Mol Biol* 99(4-5):215-22

Mustonen MV, Poutanen MH, Isomaa VV, Vihko PT, Vihko RK (1997) Cloning of mouse 17beta-hydroxysteroid dehydrogenase type 2, and analysing expression of the mRNAs for types 1, 2, 3, 4 and 5 in mouse embryos and adult tissues. *Biochem J* 325:199-205

Mziaut H, Korza G, Hand AR, Gerard C, Ozols J (1999) Targeting proteins to the lumen of endoplasmic reticulum using N-terminal domains of 11beta-hydroxysteroid dehydrogenase and the 50-kDa esterase. *J Biol Chem* 274(20):14122-9

Nakashima A, Koshiyama K, Uozumi T, Monden Y, Hamanaka Y (1975) Effects of general anaesthesia and severity of surgical stress on serum LH and testosterone in males. *Acta Endocrinol* (Copenh) 78:258-269

Nardai G, Braun L, Csala M, Mile V, Csermely P, Benedetti A, Mandl J, Bánhegyi G (2001) Protein-disulfide isomeraseand protein thiol-dependent dehydroascorbate reduction and ascorbate accumulation in the lumen of the endoplasmic reticulum. *J Biol Chem* 276: 8825–8828

Nashev LG, Chandsawangbhuwana C, Balazs Z, Atanasov AG, Dick B, Frey FJ, Baker ME, Odermatt A (2007) Hexose-6-phosphate dehydrogenase modulates 11beta-hydroxysteroid dehydrogenase type 1-dependent metabolism of 7-keto- and 7beta-hydroxy-neurosteroids.*PLoS One* 2(6):e561

Nashev LG, Schuster D, Laggner C, Sodha S, Langer T, Wolber G, Odermatt A (2010) The UV-filter benzophenone-1 inhibits 17beta-hydroxysteroid dehydrogenase type 3: Virtual screening as a strategy to identify potential endocrine disrupting chemicals. *Biochem Pharmacol* 79:1189-1199

Nguyen S, Choi HK, Lustig RH, Hsu CY (2009) Sugar-sweetened beverages, serum uric acid, and blood pressure in adolescents. *J Pediatr* 154: 807–813

Nikiforov A, Dolle C, Niere M, Ziegler M (2011) Pathways and subcellular compartmentation of NAD biosynthesis in human cells: from entry of extracellular precursors to mitochondrial NAD generation. *J Biol Chem* 286: 21767–21778

Odermatt A, Arnold P, Stauffer A, Frey BM, Frey FJ (1999) The N-terminal anchor sequences of 11β-hydroxysteroid dehydrogenases determine their orientation in the endoplasmic reticulum membrane. *J Biol Chem* 274:28762–28770

Odermatt A, Da Cunha T, Penno CA, Chandsawangbhuwana C, Reichert C, Wolf A, Dong M, Baker ME (2011) Hepatic reduction of the secondary bile acid 7-oxolithocholic acid is mediated by 11β-hydroxysteroid dehydrogenase 1. *Biochem J* 436(3):621-9

Odermatt A, Nashev LG (2010) The glucocorticoid-activating enzyme 11beta-hydroxysteroid dehydrogenase type 1 has broad substrate specificity: Physiological and toxicological considerations. *J Steroid Biochem Mol Biol*
119 (1-2):1-13

Ohno S, Nakajima Y, Nakajin S (2005) Triphenyltin and Tributyltin inhibit pig testicular 17beta-hydroxysteroid dehydrogenase activity and suppress testicular testosterone biosynthesis. *Steroids* 70:645-651.

Orr TE, Mann DR (1990) Effects of restraint stress on plasma LH and testosterone concentrations, Leydig cell LH/hCG receptors, and in vitro testicular steroidogenesis in adult rats. *Horm Behav* 24:324-341

Orr TE, Mann DR (1992) Role of glucocorticoids in the stress-induced suppression of testicular steroidogenesis in adult male rats. *Horm Behav* 26:350-363

Orr TE, Taylor MF, Bhattacharyya AK, Collins DC, Mann DR (1994) Acute immobilization stress disrupts testicular steroidogenesis in adult male rats by inhibiting the activities of 17 alpha-hydroxylase and 17,20-lyase without affecting the binding of LH/hCG receptors. *J Androl* 15:302-308

Ozols J (1995) Lumenal orientation and post-translational modifications of the liver microsomal 11b-hydroxysteroid dehydrogenase. *J Biol Chem* 270:10360

Persson B, Kallberg Y, Bray JE, Bruford E, Dellaporta SL, Favia AD, Duarte RG, Jörnvall H, Kavanagh KL, Kedishvili N, Kisiela M, Maser E, Mindnich R, Orchard S, Penning TM, Thornton JM, Adamski J, Oppermann U (2009) The SDR (short-chain dehydrogenase/reductase and related enzymes) nomenclature initiative. *Chem Biol Interact* 178(1-3):94-8

Piccirella S, Czegle I, Lizák B, Margittai E , Senesi S, Papp E, Csala M, Fulceri R, Csermely P, Mandl J, Benedetti A, Bánhegyi G (2006) Uncoupled redox systems in the lumen of the endoplasmic reticulum. Pyridine nucleotides stay reduced in an oxidative environment. *J Biol Chem* 281: 4671–4677

Pollak N, Dolle C, Ziegler M (2007) The power to reduce: Pyridine nucleotides–small molecules with a multitude of functions. *Biochem J* 402: 205–218

Pollard MG, Travers KJ, Weissman JS (1998) Ero1p: A novel and ubiquitous protein with an essential role in oxidative protein folding in the endoplasmic reticulum. *Mol Cell* 1: 171–182

Prieto PG, Cancelas J, Villanueva-Peñacarrillo ML, Valverde I, Malaisse WJ (2004) Plasma d-glucose, d-fructose and insulin responses after oral administration of d-glucose, d-fructose and sucrose to normal rats. *J Am Coll Nutr* 23:414–419

Ramming T, Appenzeller-Herzog C (2012) The physiological functions of mammalian endoplasmic oxidoreductin 1: on disulfides and more. *Antioxid Redox Signal* 16(10):1109-18

Riemer J, Appenzeller-Herzog C, Johansson L, Bodenmiller B, Hartmann-Petersen R, Ellgaard L (2009) A luminal flavoprotein in endoplasmic reticulum-associated degradation. *Proc Natl Acad Sci U S A* 106(35):14831-6

Rogoff D, Black K, McMillan DR, White PC (2010) Contribution of hexose-6-phosphate dehydrogenase to NADPH content and redox environment in the endoplasmic reticulum. *Redox Rep* 15(2):64-70

Rogoff D, Ryder JW, Black K, Yan Z, Burgess SC, McMillan DR, White PC (2007) Abnormalities of glucose homeostasis and the hypothalamic-pituitary-adrenal axis in mice lacking hexose-6-phosphate dehydrogenase. *Endocrinology* 148:5072–5080

Schweizer RA, Zürcher M, Balazs Z, Dick B, Odermatt A (2004) Rapid hepatic metabolism of 7-ketocholesterol by 11beta-hydroxysteroid dehydrogenase type 1: species-specific differences between the rat, human, and hamster enzyme. *J Biol Chem* 279(18):18415-24

Semjonous NM, Sherlock M, Jeyasuria P, Parker KL, Walker EA, Stewart PM, Lavery GG (2011) Hexose-6-phosphate dehydrogenase contributes to skeletal muscle homeostasis independent of 11β-hydroxysteroid dehydrogenase type 1. *Endocrinology* 152(1):93-102

Senesi S, Legeza B, Balázs Z, Csala M, Marcolongo P, Kereszturi E, Szelényi P, Egger C, Fulceri R, Mandl J, Giunti R, Odermatt A, Bánhegyi G, Benedetti A (2010) Contribution of fructose-6-phosphate to glucocorticoid activation in the endoplasmic reticulum: possible implication in the metabolic syndrome. *Endocrinology* 151(10):4830-9

Sha JA, Dudley K, Rajapaksha WR, O'Shaughnessy PJ (1997) Sequence of mouse 17beta-hydroxysteroid dehydrogenase type 3 cDNA and tissue distribution of the type 1 and type 3 isoform mRNAs. *J Steroid Biochem Mol Biol* 60:19-24

Shtivelman E (1997) A link between metastasis and resistance to apoptosis of variant small cell lung carcinoma. *Oncogene* 14, 2167–2173

Simpson IA, Yver DR, Hissin PJ, Wardzala LJ, Karnieli E, Salans LB, Cushman SW (1983) Insulin-stimulated translocation of glucose transporters in the isolated rat adipose cells: characterization of subcellular fractions. *Biochim Biophys Acta* 763:393–407

Skarydova L, Wsol V (2012) Human microsomal carbonyl reducing enzymes in the metabolism of xenobiotics: well-known and promising members of the SDR superfamily. *Drug Metab Rev* 44:173-191

Smals AG, Kloppenborg PW, Benraad TJ (1977) Plasma testosterone profiles in Cushing's syndrome. *J Clin Endocrinol Metab* 45:240-245

Stanhope KL, Havel PJ (2008) Fructose consumption: potential mechanisms for its effects to increase visceral adiposity and induce dyslipidemia and insulin resistance. *Curr Opin Lipidol* 19:16–24

Stanhope KL, Havel PJ (2009a) Fructose consumption: considerations for future research on its effects on adipose distribution, lipid metabolism, and insulin sensitivity in humans. *J Nutr* 139:1236S–1241

Stanhope KL, Schwarz JM, Keim NL, Griffen SC, Bremer AA, Graham JL, Hatcher B, Cox CL, Dyachenko A, Zhang W, McGahan JP, Seibert A, Krauss RM, Chiu S, Schaefer EJ, Ai M, Otokozawa S, Nakajima K, Nakano T, Beysen C, Hellerstein MK, Berglund L, Havel PJ (2009b) Consuming fructose-sweetened, not glucose-sweetened, beverages increases visceral adiposity and lipids and decreases insulin sensitivity in overweight/obese humans. *J Clin Invest* 119:1322–1334

Stimson RH, Lobley GE, Maraki I, Morton NM, Andrew R, Walker BR (2010) Effects of proportions of dietary macronutrients on glucocorticoid metabolism in diet-induced obesity in rats. *PLoS One* 5:e8779

Száraz P, Bánhegyi G, Benedetti A (2010) Altered redox state of luminal pyridine nucleotides facilitates the sensitivity towards oxidative injury and leads to endoplasmic reticulum stress dependent autophagy in HepG2 cells. *Int J Biochem Cell Biol* 42(1):157-66

Tappy L, Lê KA (2010) Metabolic effects of fructose and the worldwide increase in obesity. *Physiol Rev* 90:23–46

Thieringer R, Le Grand CB, Carbin L, Cai TQ, Wong B, Wright SD, Hermanowski-Vosatka A (2001) 11 Beta-hydroxysteroid dehydrogenase type 1 is induced in human monocytes upon differentiation to macrophages. *J Immunol* 167:30-35

Tomlinson JW, Finney J, Gay C, Hughes BA, Hughes SV, Stewart PM (2008) Impaired glucose tolerance and insulin resistance are associated with increased adipose 11β-hydroxysteroid dehydrogenase type 1 expression and elevated hepatic 5α-reductase activity. *Diabetes* 57:2652–2660

Tomlinson JW, Sinha B, Bujalska I, Hewison M, Stewart PM (2002) Expression of 11β-hydroxysteroid dehydrogenase type 1 in adipose tissue is not increased in human obesity. *Journal of Clinical Endocrinology and Metabolism* 87:5630–5635.

Tomlinson JW, Walker EA, Bujalska IJ, Draper N, Lavery GG, Cooper MS, Hewison M, Stewart PM (2004) 11beta-hydroxysteroid dehydrogenase type 1: a tissue-specific regulator of glucocorticoid response. *Endocr Rev* 25(5):831-66

Törn S, Nokelainen P, Kurkela R, Pulkka A, Menjivar M, Ghosh S, Coca-Prados M, Peltoketo H, Isomaa V, Vihko P (2003) Production, purification, and functional analysis of recombinant human and mouse 17beta-hydroxysteroid dehydrogenase type 7. *Biochem Biophys Res Commun* 305(1):37-45

Vandesompele J, De Preter K, Pattyn F, Poppe B, Van Roy N, De Paepe A, Speleman F (2002) Accurate normalization of real-time quantitative RT-PCR data by geometric averaging of multiple internal control genes. *Genome Biol* 3(7):RESEARCH0034

Van Schaftingen E, Detheux M, Veiga da Cunha M (1994) Short-term control of glucokinase activity: role of a regulatory protein. *FASEB J* 8:414–419

Van Schaftingen E, Gerin I (2002) The glucose-6-phosphatase system *Biochem. J* 362:513–532

Wang X, Mick GJ, Maser E, McCormick K (2011) Manifold effects of palmitoylcarnitine on endoplasmic reticulum metabolism: 11β-hydroxysteroid dehydrogenase 1, flux through hexose-6-phosphate dehydrogenase and NADPH concentration. *Biochem J* 437(1):109-15

Wang X, Walsh LP, Reinhart AJ, Stocco DM (2000) The role of arachidonic acid in steroidogenesis and steroidogenic acute regulatory (StAR) gene and protein expression. *J Biol Chem* 275:20204-20209

Wells WW, Xu DP, Yang YF, Rocque PA (1990) Mammalian thioltransferase (glutaredoxin) and protein disulfide isomerase have dehydroascorbate reductase activity. *J Biol Chem* 265:15361–15364

Yokoi Y, Horiguchi Y, Araki M, Motojima K (2007) Regulated expression by PPARalpha and unique localization of 17beta-hydroxysteroid dehydrogenase type 11 protein in mouse intestine and liver. *FEBS J* 274(18):4837-47

Yuan K, Zhao B, Li XW, Hu GX, Su Y, Chu Y, Akingbemi BT, Lian QQ, Ge RS (2012) Effects of phthalates on 3beta-hydroxysteroid dehydrogenase and 17beta-hydroxysteroid dehydrogenase 3 activities in human and rat testes. *Chem Biol Interact* 195:180-188

Zhang M, Hu P, Napoli JL (2004) Elements in the N-terminal signaling sequence that determine cytosolic topology of short-chain dehydrogenases/reductases: Studies with retinol dehydrogenase type 1 and cis-retinol/androgen dehydrogenase type 1. *J Biol Chem* 279(49):51482-9

Zhang YL, Zhong X, Gjoka Z, Li Y, Stochaj W, Stahl M, Kriz R, Tobin JF, Erbe D, Suri V (2009) H6PDH interacts directly with 11beta-HSD1: implications for determining the directionality of glucocorticoid catalysis. *Arch Biochem Biophys* 483(1):45-54

Zhu H, Larade K, Jackson TA, Xie J, Ladoux A, Acker H, Berchner-Pfannschmidt U, Fandrey J, Cross AR, Lukat–Rodgers GS, Rodgers KR, Bunn HF (2004) NCB5OR is a novel soluble NAD(P)H reductase localized in the endoplasmic reticulum. *J Biol Chem* 279: 30316–30325

Zito E, Chin KT, Blais J, Harding HP, Ron D (2010a) ERO1-beta, a pancreas-specific disulfide oxidase, promotes insulin biogenesis and glucose homeostasis. *J Cell Biol* 188: 821–832

Zito E, Melo EP, Yang Y, Wahlander Å, Neubert TA, Ron D (2010b) Oxidative protein folding by an endoplasmic reticulum-localized peroxiredoxin. *Mol Cell* 40(5):787-97.

List of abbreviations

6PGDH	6-phosphogluconate dehydrogenase
11β-HSD1	11β-hydroxysteroid dehydrogenase type 1
11β-HSD2	11β-hydroxysteroid dehydrogenase type 2
17β-HSD3	17β-hydroxysteroid dehydrogenase type 3
AD	4-androstene-3,17-dione
BP1	benzophenone-1
ConA	concanavalin A
DHA	dehydroascorbate
DHRS	dehydrogenase/reductase SDR family member
ER	endoplasmic reticulum
ERAD	ER-associated degradation
Ero1-α	ER oxidoreductin 1-α
F6P	fructose-6-phosphate
FABP4	fatty acid binding protein 4
G6P	glucose-6-phosphate
G6PDH	glucose-6-phosphate dehydrogenase
G6PT	glucose-6-phosphate transporter
GAPDH	glyceraldehyde-3-phosphate dehydrogenase
GR	glucocorticoid receptor
GSH	glutathione
H6PDH	hexose-6-phosphate dehydrogenase
MR	mineralocorticoid receptors
MS	microsomal fraction
NAD	nicotinamide adenine dinucleotide
NADPH	reduced nicotinamide adenine dinucleotide phosphate
NCB5OR	NADPH cytochrome b5 oxidoreductase
OG	octylglucoside
PDI	protein disulfide isomerase
PGI	phosphoglucose isomerase
PPARγ	peroxisome proliferator-activated receptor gamma
SDR	short chain dehydrogenase/reductase
siRNA	small interfering ribonucleic acid
UPR	unfolded protein response
WGA	wheat germ agglutinin

List of proteins identified by mass-spectrometry after octylglucoside treatment

The total microsomal fraction:

LRP1_MOUSE	Prolow-density lipoprotein receptor-related protein 1
FRIL1_RAT	Ferritin light chain 1
Q7TP91_RAT	Ab1-205
CLH_RAT	Clathrin heavy chain 1
MYH9_RAT	Myosin-9
APOB_RAT	Apolipoprotein B-100
FAS_RAT	Fatty acid synthase
A1I3_RAT	Alpha-1-inhibitor 3
UGGG1_RAT	UDP-glucose:glycoprotein glucosyltransferase 1
B5DFK1_RAT	Copa protein
CO3_RAT	Complement C3
A1M_RAT	Alpha-1-macroglobulin
Q3KRF2_RAT	High density lipoprotein binding protein
Q6P136_RAT	Hyou1 protein
SC31A_RAT	Protein transport protein Sec31A
AT2A2_RAT	Sarcoplasmic/endoplasmic reticulum calcium ATPase 2
AT1A1_RAT	Sodium/potassium-transporting ATPase subunit alpha-1
TPP2_RAT	Tripeptidyl-peptidase 2
CPSM_RAT	Carbamoyl-phosphate synthase [ammonia], mitochondrial
ACLY_RAT	ATP-citrate synthase
A2AMV0_MOUSE	Novel DUF1620 domain containing protein
DPP4_RAT	Dipeptidyl peptidase 4
LDLR_RAT	Low-density lipoprotein receptor
STRUM_MOUSE	Strumpellin
Q9JL97_RAT	GPI-anchored ceruloplasmin
DDB1_RAT	DNA damage-binding protein 1
MYO1B_RAT	Myosin-Ib
SC24A_MOUSE	Protein transport protein Sec24A
B5DEG8_RAT	LOC685144 protein (RCG41932)
VPP1_RAT	V-type proton ATPase 116 kDa subunit a isoform 1
MYO1C_RAT	Myosin-Ic
ENPP1_RAT	Ectonucleotide pyrophosphatase/phosphodiesterase family member 1
ENPL_RAT	Endoplasmin
SND1_RAT	Staphylococcal nuclease domain-containing protein 1
Q5EBC3_RAT	Methylenetetrahydrofolate dehydrogenase (NADP+ dependent),
GANAB_MOUSE	Neutral alpha-glucosidase AB
AP2B1_RAT	AP-2 complex subunit beta-1
MVP_RAT	Major vault protein
COPB_RAT	Coatomer subunit beta
EIF3B_RAT	Eukaryotic translation initiation factor 3 subunit B
PIGR_RAT	Polymeric immunoglobulin receptor
ERAP1_RAT	Endoplasmic reticulum aminopeptidase 1
TERA_RAT	Transitional endoplasmic reticulum ATPase
Q91X33_MOUSE	Microsomal triglyceride transfer protein
C1TC_RAT	C-1-tetrahydrofolate synthase, cytoplasmic
Q7M079_RAT	Calcium-binding protein 4 (Fragment)
COPG_RAT	Coatomer subunit gamma
COPB2_RAT	Coatomer subunit beta
Q5U302_RAT	Catenin (Cadherin associated protein), alpha 1
FTHFD_RAT	10-formyltetrahydrofolate dehydrogenase
EF2_RAT	Elongation factor 2
AP2A2_RAT	AP-2 complex subunit alpha-2
CALX_RAT	Calnexin

B5DFC3_RAT	SEC23A (S. cerevisiae) (Predicted)
HS90B_RAT	Heat shock protein HSP 90-beta
DDX1_RAT	ATP-dependent RNA helicase DDX1
PLMN_RAT	Plasminogen
B3DMA2_RAT	Acyl-Coenzyme A dehydrogenase family, member 11
GCS1_RAT	Mannosyl-oligosaccharide glucosidase
G6PE_MOUSE	GDH/6PGL endoplasmic bifunctional protein
PDIA4_RAT	Protein disulfide-isomerase A4
NCPR_RAT	NADPH--cytochrome P450 reductase
ACSL1_RAT	Long-chain-fatty-acid--CoA ligase 1
DHB4_RAT	Peroxisomal multifunctional enzyme type 2
ECHP_RAT	Peroxisomal bifunctional enzyme
B1WC34_RAT	Protein kinase C substrate 80K-H
ECHA_RAT	Trifunctional enzyme subunit alpha, mitochondrial
TRFE_RAT	Serotransferrin
K6PL_RAT	6-phosphofructokinase, liver type
ACOX2_RAT	Peroxisomal acyl-coenzyme A oxidase 2
Q5WQV5_RAT	Radixin
Q6P6R6_RAT	Transglutaminase 2, C polypeptide
ALBU_RAT	Serum albumin
GRP78_RAT	78 kDa glucose-regulated protein
HSP7C_RAT	Heat shock cognate 71 kDa protein
S27A5_RAT	Bile acyl-CoA synthetase
ANXA6_RAT	Annexin A6
S27A2_RAT	Very long-chain acyl-CoA synthetase
RPN2_RAT	Dolichyl-diphosphooligosaccharide--protein glycosyltransferase subunit 2
Q6P7A7_RAT	Ribophorin I
CMC2_MOUSE	Calcium-binding mitochondrial carrier protein Aralar2
Q3KR94_RAT	Vitronectin
RETST_RAT	All-trans-retinol 13,14-reductase
HNRPQ_RAT	Heterogeneous nuclear ribonucleoprotein Q
SPA3K_RAT	Serine protease inhibitor A3K
EST2_RAT	Liver carboxylesterase 1
DHSA_RAT	Succinate dehydrogenase [ubiquinone] flavoprotein subunit, mitochondrial
ETFD_RAT	Electron transfer flavoprotein-ubiquinone oxidoreductase, mitochondrial
EST4_RAT	Liver carboxylesterase 4
FAAH1_RAT	Fatty-acid amide hydrolase 1
TCPE_RAT	T-complex protein 1 subunit epsilon
AOFB_RAT	Amine oxidase [flavin-containing] B
TCPG_RAT	T-complex protein 1 subunit gamma
PDIA1_RAT	Protein disulfide-isomerase
SAC1_RAT	Phosphatidylinositide phosphatase SAC1
CATA_RAT	Catalase
EHD3_RAT	EH domain-containing protein 3
PDIA3_RAT	Protein disulfide-isomerase A3
CES3_RAT	Carboxylesterase 3
CALR_RAT	Calreticulin
LMAN1_RAT	Protein ERGIC-53
UD11_RAT	UDP-glucuronosyltransferase 1-1
EST3_RAT	Liver carboxylesterase 3
FMO5_RAT	Dimethylaniline monooxygenase [N-oxide-forming] 5
NUCL_RAT	Nucleolin
ATPA_RAT	ATP synthase subunit alpha, mitochondrial
DHE3_RAT	Glutamate dehydrogenase 1, mitochondrial
CP4A2_RAT	Cytochrome P450 4A2
UD2B5_RAT	UDP-glucuronosyltransferase 2B5
TCPB_RAT	T-complex protein 1 subunit beta
FMO1_RAT	Dimethylaniline monooxygenase [N-oxide-forming] 1
ATLA3_RAT	Atlastin-3
Q4V8I9_RAT	UDP-glucose pyrophosphorylase 2
FMO3_RAT	Dimethylaniline monooxygenase [N-oxide-forming] 3

PRRC1_RAT	Protein PPRC1
CP2D1_RAT	Cytochrome P450 2D1
A1AT_RAT	Alpha-1-antiproteinase
CP2B3_RAT	Cytochrome P450 2B3
ATPB_RAT	ATP synthase subunit beta, mitochondrial
CP4F4_RAT	Cytochrome P450 4F4
TBB2A_RAT	Tubulin beta-2A chain
AL3A2_RAT	Fatty aldehyde dehydrogenase
CP3A2_RAT	Cytochrome P450 3A2
UD2B4_RAT	UDP-glucuronosyltransferase 2B4
CP2CN_RAT	Cytochrome P450 2C23
CP4AE_RAT	Cytochrome P450 4A14
UD2B3_RAT	UDP-glucuronosyltransferase 2B3
CP2CB_RAT	Cytochrome P450 2C11
CP51A_RAT	Cytochrome P450 51A1
CP1A2_RAT	Cytochrome P450 1A2
CP2E1_RAT	Cytochrome P450 2E1
CP4F1_RAT	Cytochrome P450 4F1
CP2J3_RAT	Cytochrome P450 2J3
CP2DQ_RAT	Cytochrome P450 2D26
CP2CD_RAT	Cytochrome P450 2C13, male-specific
CP2C7_RAT	Cytochrome P450 2C7
CP3AI_RAT	Cytochrome P450 3A18
CP2A2_RAT	Cytochrome P450 2A2
PDIA6_RAT	Protein disulfide-isomerase A6
RL4_RAT	60S ribosomal protein L4
Q63125_RAT	Rat cytochrome P-450b type b (Fragment)
AAAD_RAT	Arylacetamide deacetylase
Q9WTN7_RAT	Sterol 12-alpha hydroxylase
HYEP_RAT	Epoxide hydrolase 1
Q4QQW7_RAT	Cytochrome P450, family 2, subfamily c, polypeptide 7
EF1A1_RAT	Elongation factor 1-alpha 1
RL3_RAT	60S ribosomal protein L3
CP2A1_RAT	Cytochrome P450 2A1
NTCP_RAT	Sodium/bile acid cotransporter
CP270_RAT	Cytochrome P450 2C70
BHMT1_RAT	Betaine--homocysteine S-methyltransferase 1
Q6AYD3_RAT	Proliferation-associated 2G4
GGLO_RAT	L-gulonolactone oxidase
IF4A2_RAT	Eukaryotic initiation factor 4A-II
Q6P6S9_RAT	Ectonucleoside triphosphate diphosphohydrolase 5
OST48_RAT	Dolichyl-diphosphooligosaccharide--protein glycosyltransferase 48 kDa subunit
ASGR1_RAT	Asialoglycoprotein receptor 1
ASSY_RAT	Argininosuccinate synthase
BASI_RAT	Basigin
A2IBE0_RAT	Membrane-bound carbonic anhydrase 14
METK1_RAT	S-adenosylmethionine synthetase isoform type-1
CGL_RAT	Cystathionine gamma-lyase
SCPDH_RAT	Probable saccharopine dehydrogenase
ACTB_RAT	Actin, cytoplasmic 1
Q5BJN6_RAT	Paraoxonase 1
RSSA_RAT	40S ribosomal protein SA
PON3_RAT	Serum paraoxonase/lactonase 3
Q7TP48_RAT	Ab2-305
FAAA_RAT	Fumarylacetoacetase
DJB11_RAT	DnaJ homolog subfamily B member 11
E2AK1_RAT	Eukaryotic translation initiation factor 2-alpha kinase 1
HPPD_RAT	4-hydroxyphenylpyruvate dioxygenase
PON2_RAT	Serum paraoxonase/arylesterase 2
ALDOB_RAT	Fructose-bisphosphate aldolase B
3BHS5_RAT	3 beta-hydroxysteroid dehydrogenase type 5

PON1_RAT	Serum paraoxonase/arylesterase 1
Q5I0F0_RAT	Developmentally regulated GTP binding protein 1
F16P1_RAT	Fructose-1,6-bisphosphatase 1
DHCR7_RAT	7-dehydrocholesterol reductase
NSDHL_RAT	Sterol-4-alpha-carboxylate 3-dehydrogenase, decarboxylating
ARGI1_RAT	Arginase-1
ANXA1_RAT	Annexin A1
HNRPC_RAT	Heterogeneous nuclear ribonucleoprotein C (Fragment)
S61A1_RAT	Protein transport protein Sec61 subunit alpha isoform 1
RL6_MOUSE	60S ribosomal protein L6
Q9QX80_RAT	CArG-binding factor A
Q5BK21_RAT	Transmembrane 7 superfamily member 2
IF2A_RAT	Eukaryotic translation initiation factor 2 subunit 1
RLA0_RAT	60S acidic ribosomal protein P0
RL6_RAT	60S ribosomal protein L6
ADH1_RAT	Alcohol dehydrogenase 1
B2RYX0_RAT	Naca protein
EIF3I_RAT	Eukaryotic translation initiation factor 3 subunit I
G3P_RAT	Glyceraldehyde-3-phosphate dehydrogenase
Q68G38_RAT	Dystonia 1
SSRA_RAT	Translocon-associated protein subunit alpha
Q6I7R1_RAT	Dehydrogenase/reductase (SDR family) member 7
RGN_RAT	Regucalcin
DHI1_RAT	Corticosteroid 11-beta-dehydrogenase isozyme 1
B0BNG3_RAT	Lman2 protein
RL5_RAT	60S ribosomal protein L5
URIC_RAT	Uricase
DIDH_RAT	3-alpha-hydroxysteroid dehydrogenase
HPT_RAT	Haptoglobin
PECR_RAT	Peroxisomal trans-2-enoyl-CoA reductase
LDHA_RAT	L-lactate dehydrogenase A chain
LRC59_RAT	Leucine-rich repeat-containing protein 59
VDAC1_RAT	Voltage-dependent anion-selective channel protein 1
PHB2_RAT	Prohibitin-2
GBLP_RAT	Guanine nucleotide-binding protein subunit beta-2-like 1
MDHC_RAT	Malate dehydrogenase, cytoplasmic
APOE_RAT	Apolipoprotein E
NB5R3_RAT	NADH-cytochrome b5 reductase 3
RS3_RAT	40S ribosomal protein S3
ANXA5_RAT	Annexin A5
RL7_RAT	60S ribosomal protein L7
MLEC_RAT	Malectin
DHB11_RAT	Estradiol 17-beta-dehydrogenase 11
SNAA_RAT	Alpha-soluble NSF attachment protein
RS2_RAT	40S ribosomal protein S2
DHB2_RAT	Estradiol 17-beta-dehydrogenase 2
DHB13_RAT	17-beta hydroxysteroid dehydrogenase 13
B0BN52_RAT	Mitochondrial carrier homolog 2 (C. elegans)
RS3A_RAT	40S ribosomal protein S3a
B0K031_RAT	RCG30479, isoform CRA_b
RDH2_RAT	Retinol dehydrogenase 2
RDH3_RAT	Retinol dehydrogenase 3
RS6_RAT	40S ribosomal protein S6
RL7A_HUMAN	60S ribosomal protein L7a
H17B6_RAT	Hydroxysteroid 17-beta dehydrogenase 6
RL8_RAT	60S ribosomal protein L8
RDH7_RAT	Retinol dehydrogenase 7
RS4X_RAT	40S ribosomal protein S4, X isoform
ADT2_RAT	ADP/ATP translocase 2
RL7A_RAT	60S ribosomal protein L7a
GPSN2_RAT	Synaptic glycoprotein SC2

DHB12_RAT	Estradiol 17-beta-dehydrogenase 12
RS15A_RAT	40S ribosomal protein S15a
CAH3_RAT	Carbonic anhydrase 3
PSA4_RAT	Proteasome subunit alpha type-4
CRP_RAT	C-reactive protein
O89035_RAT	Mitochondrial dicarboxylate carrier
ERP29_RAT	Endoplasmic reticulum protein ERp29
RS8_RAT	40S ribosomal protein S8
RL13_RAT	60S ribosomal protein L13
RL10A_RAT	60S ribosomal protein L10a
PRDX1_RAT	Peroxiredoxin-1
PGRC1_RAT	Membrane-associated progesterone receptor component 1
Q9Z0V5_RAT	PRx IV
MET7B_RAT	Methyltransferase-like protein 7B
B0BNK1_RAT	RCG32615, isoform CRA_a
RL14_RAT	60S ribosomal protein L14
RL19_RAT	60S ribosomal protein L19
GSTA3_RAT	Glutathione S-transferase alpha-3
GSTM1_RAT	Glutathione S-transferase Mu 1
RS8_BOVIN	40S ribosomal protein S8
SC22B_RAT	Vesicle-trafficking protein SEC22b
RL9_RAT	60S ribosomal protein L9
RL15_RAT	60S ribosomal protein L15
RAB7A_RAT	Ras-related protein Rab-7a
GSTA1_RAT	Glutathione S-transferase alpha-1
RL13A_RAT	60S ribosomal protein L13a
RL18_RAT	60S ribosomal protein L18
RL10_RAT	60S ribosomal protein L10
RS9_RAT	40S ribosomal protein S9
RAB8B_RAT	Ras-related protein Rab-8B
RS7_RAT	40S ribosomal protein S7
RL21_RAT	60S ribosomal protein L21
RET4_RAT	Retinol-binding protein 4
GBRT_HUMAN	Gamma-aminobutyric acid receptor subunit theta
TMED2_RAT	Transmembrane emp24 domain-containing protein 2
Q6PDW2_RAT	Ribosomal protein L21
RER1_RAT	Protein RER1
RL31_RAT	60S ribosomal protein L31
PPIB_RAT	Peptidyl-prolyl cis-trans isomerase B
RL29_RAT	60S ribosomal protein L29
FRIH_RAT	Ferritin heavy chain
AP1B1_RAT	AP-1 complex subunit beta-1
HS90A_RAT	Heat shock protein HSP 90-alpha
VPS35_MOUSE	Vacuolar protein sorting-associated protein 35
Q99PS8_RAT	Histidine-rich glycoprotein
Q6IMZ3_RAT	Anxa6 protein
RPN1_RAT	Dolichyl-diphosphooligosaccharide--protein glycosyltransferase subunit 1
PABP1_RAT	Polyadenylate-binding protein 1
SPA3L_RAT	Serine protease inhibitor A3L
ATPB_HUMAN	ATP synthase subunit beta, mitochondrial
Q3MIE4_RAT	Vesicle amine transport protein 1 homolog (T californica)
NUCB2_RAT	Nucleobindin-2
Q6P3V8_RAT	Eukaryotic translation initiation factor 4A1
CP2CC_RAT	Cytochrome P450 2C12, female-specific
MPRD_RAT	Cation-dependent mannose-6-phosphate receptor
APOA4_RAT	Apolipoprotein A-IV
DHSO_RAT	Sorbitol dehydrogenase
QOR_RAT	Quinone oxidoreductase
BDH_RAT	D-beta-hydroxybutyrate dehydrogenase, mitochondrial
PSA7_RAT	Proteasome subunit alpha type-7
GSTM2_RAT	Glutathione S-transferase Mu 2

MUG1_RAT	Murinoglobulin-1
CERU_RAT	Ceruloplasmin
EZRI_RAT	Ezrin
P70540_RAT	Peroxisomal multifunctional enzyme type II
TKT_RAT	Transketolase
B5DF80_RAT	Poly(A) binding protein, cytoplasmic 3 (Similar to RIKEN cDNA 4932702K14)
B5DF18_RAT	Activating transcription factor 6
DHAK_RAT	Bifunctional ATP-dependent dihydroxyacetone kinase/FAD-AMP lyase (cyclizing)
COPD_RAT	Coatomer subunit delta
SPA3N_RAT	Serine protease inhibitor A3N
AL9A1_RAT	4-trimethylaminobutyraldehyde dehydrogenase
ACOX1_RAT	Peroxisomal acyl-coenzyme A oxidase 1
CSAD_RAT	Cysteine sulfinic acid decarboxylase
FETUB_RAT	Fetuin-B
ENOA_RAT	Alpha-enolase
METK2_RAT	S-adenosylmethionine synthetase isoform type-2
BAAT_RAT	Bile acid-CoA:amino acid N-acyltransferase
HNRPK_RAT	Heterogeneous nuclear ribonucleoprotein K
LICH_RAT	Lysosomal acid lipase/cholesteryl ester hydrolase
SAHH_RAT	Adenosylhomocysteinase
IDHC_RAT	Isocitrate dehydrogenase [NADP] cytoplasmic
VP26A_RAT	Vacuolar protein sorting-associated protein 26A
HAOX1_MOUSE	Hydroxyacid oxidase 1
CHID1_RAT	Chitinase domain-containing protein 1
CS066_RAT	UPF0515 protein C19orf66 homolog
HNRPD_RAT	Heterogeneous nuclear ribonucleoprotein D0
AK1D1_RAT	3-oxo-5-beta-steroid 4-dehydrogenase
HAOX2_RAT	Hydroxyacid oxidase 2
B0BN46_RAT	Grhpr protein
PAHX_RAT	Phytanoyl-CoA dioxygenase, peroxisomal
B2RYF8_RAT	Cnpy3 protein
B5DF91_RAT	ELAV (Embryonic lethal, abnormal vision, Drosophila)-like 1 (Hu antigen R)
ST1E1_RAT	Estrogen sulfotransferase, isoform 1
Q2MHD9_RAT	17beta-hydroxysteroid dehydrogenase
Q5BK78_RAT	Sumf2 protein
ASPD_RAT	Putative L-aspartate dehydrogenase
KHK_RAT	Ketohexokinase
MBL1_RAT	Mannose-binding protein A
MBL2_RAT	Mannose-binding protein C
HAP28_RAT	28 kDa heat- and acid-stable phosphoprotein
GSTA5_RAT	Glutathione S-transferase alpha-5
PEBP1_RAT	Phosphatidylethanolamine-binding protein 1
GSTP1_RAT	Glutathione S-transferase P
HBB1_RAT	Hemoglobin subunit beta-1
MUP_RAT	Major urinary protein
HBA_RAT	Hemoglobin subunit alpha-1/2
SODC_RAT	Superoxide dismutase [Cu-Zn]
CNPY2_MOUSE	Protein canopy homolog 2
PPIA_RAT	Peptidyl-prolyl cis-trans isomerase A
TTHY_RAT	Transthyretin
ARMET_RAT	Protein ARMET
REEP6_RAT	Receptor expression-enhancing protein 6
IF5A1_RAT	Eukaryotic translation initiation factor 5A-1
UK114_RAT	Ribonuclease UK114
RLA1_RAT	60S acidic ribosomal protein P1
CYB5_RAT	Cytochrome b5
RRBP1_MOUSE	Ribosome-binding protein 1
HYOU1_RAT	Hypoxia up-regulated protein 1
FINC_RAT	Fibronectin
CO4_RAT	Complement C4
MUG2_RAT	Murinoglobulin-2

UBE4A_RAT	Ubiquitin conjugation factor E4 A
ITIH3_RAT	Inter-alpha-trypsin inhibitor heavy chain H3
Q5EBC0_RAT	Inter alpha-trypsin inhibitor, heavy chain 4
RENT1_MOUSE	Regulator of nonsense transcripts 1
MTP_MOUSE	Microsomal triglyceride transfer protein large subunit
PYGL_RAT	Glycogen phosphorylase, liver form
B2RYN6_RAT	Adaptor-related protein complex 1, gamma 1 subunit, isoform CRA_b
Q5PQK5_RAT	Radixin
Q7TMC7_RAT	Ab2-417
THRB_RAT	Prothrombin
PICA_RAT	Phosphatidylinositol-binding clathrin assembly protein
HSP72_RAT	Heat shock-related 70 kDa protein 2
Q68FT7_RAT	Phenylalanyl-tRNA synthetase, beta subunit
Q7TMB9_RAT	Ab1-021
A1CF_RAT	APOBEC1 complementation factor
AIFM1_RAT	Apoptosis-inducing factor 1, mitochondrial
B5DFH4_RAT	Papss2 protein
Q66WT9_RAT	Clathrin-assembly lymphoid myeloid leukemia protein
TCPA_RAT	T-complex protein 1 subunit alpha
Q8K3R0_RAT	Carboxylesterase isoenzyme
EST5_RAT	Liver carboxylesterase B-1
PCKGC_RAT	Phosphoenolpyruvate carboxykinase, cytosolic [GTP]
STIP1_RAT	Stress-induced-phosphoprotein 1
A1L114_RAT	Fga protein
NUCB1_RAT	Nucleobindin-1
DNJC3_RAT	DnaJ homolog subfamily C member 3
VTDB_RAT	Vitamin D-binding protein
CP2D4_RAT	Cytochrome P450 2D4
AP1M1_RAT	AP-1 complex subunit mu-1
EF1G_RAT	Elongation factor 1-gamma
FIBG_RAT	Fibrinogen gamma chain
ARP3_RAT	Actin-related protein 3
Q5VLR5_RAT	BWK4
NSF1C_RAT	NSFL1 cofactor p47
TXND5_MOUSE	Thioredoxin domain-containing protein 5
PGK1_RAT	Phosphoglycerate kinase 1
PURA_MOUSE	Transcriptional activator protein Pur-alpha
Q3KR93_RAT	Putative uncharacterized protein
PURB_RAT	Transcriptional activator protein Pur-beta
THIKA_RAT	3-ketoacyl-CoA thiolase A, peroxisomal
Q9Z0U8_RAT	Nucleic acid binding factor pRM10
GALM_RAT	Aldose 1-epimerase
SEC13_RAT	Protein SEC13 homolog
CATB_RAT	Cathepsin B
ADH1_MOUSE	Alcohol dehydrogenase 1
Q68FR9_RAT	Eukaryotic translation elongation factor 1 delta (Guanine nucleotide exchange
ARK72_RAT	Aflatoxin B1 aldehyde reductase member 2
HEM2_RAT	Delta-aminolevulinic acid dehydratase
Q5BJN1_RAT	START domain containing 10
MGLL_RAT	Monoglyceride lipase
CLCA_RAT	Clathrin light chain A
ARK73_RAT	Aflatoxin B1 aldehyde reductase member 3
ASPD_MOUSE	Putative L-aspartate dehydrogenase
ROA2_RAT	Heterogeneous nuclear ribonucleoproteins A2/B1
GNMT_RAT	Glycine N-methyltransferase
ST1E3_RAT	Estrogen sulfotransferase, isoform 3
NIT2_RAT	Nitrilase homolog 2
ARPC2_RAT	Actin-related protein 2/3 complex subunit 2
DECR_RAT	2,4-dienoyl-CoA reductase, mitochondrial
VATE1_RAT	V-type proton ATPase subunit E 1
CATZ_RAT	Cathepsin Z

PNPH_RAT	Purine nucleoside phosphorylase
DECR2_RAT	Peroxisomal 2,4-dienoyl-CoA reductase
1433E_RAT	14-3-3 protein epsilon
RSU1_MOUSE	Ras suppressor protein 1
RS3_HUMAN	40S ribosomal protein S3
1433G_RAT	14-3-3 protein gamma
Q6P9V7_RAT	Proteasome (Prosome, macropain) 28 subunit, alpha
PSA1_RAT	Proteasome subunit alpha type-1
DCXR_RAT	L-xylulose reductase
D3D2_RAT	3,2-trans-enoyl-CoA isomerase, mitochondrial
1433Z_RAT	14-3-3 protein zeta/delta
PSA3_RAT	Proteasome subunit alpha type-3
KAD2_RAT	Adenylate kinase 2, mitochondrial
B5DEN5_RAT	Eukaryotic translation elongation factor 1 beta 2 (RCG22471, isoform CRA_b)
SAMP_RAT	Serum amyloid P-component
GDIR1_RAT	Rho GDP-dissociation inhibitor 1
GSTM4_RAT	Glutathione S-transferase Yb-3
PSA6_RAT	Proteasome subunit alpha type-6
DHPR_RAT	Dihydropteridine reductase
PRDX6_RAT	Peroxiredoxin-6
FUBP2_RAT	Far upstream element-binding protein 2
HUTU_MOUSE	Probable urocanate hydratase
AFAM_RAT	Afamin
Q6QI47_RAT	LRRGT00161
HEMO_RAT	Hemopexin
SBP1_RAT	Selenium-binding protein 1
PGCP_RAT	Plasma glutamate carboxypeptidase
AL7A1_MOUSE	Alpha-aminoadipic semialdehyde dehydrogenase
DLDH_RAT	Dihydrolipoyl dehydrogenase, mitochondrial
ANX11_MOUSE	Annexin A11
AL8A1_MOUSE	Aldehyde dehydrogenase family 8 member A1
MMSA_RAT	Methylmalonate-semialdehyde dehydrogenase [acylating], mitochondrial
FETUA_RAT	Alpha-2-HS-glycoprotein
6PGD_RAT	6-phosphogluconate dehydrogenase, decarboxylating
FUMH_RAT	Fumarate hydratase, mitochondrial
PGK1_MOUSE	Phosphoglycerate kinase 1
BUP1_RAT	Beta-ureidopropionase
AATC_RAT	Aspartate aminotransferase, cytoplasmic
THIL_RAT	Acetyl-CoA acetyltransferase, mitochondrial
PLBL1_RAT	Putative phospholipase B-like 1
CATD_RAT	Cathepsin D
BAAT_MOUSE	Bile acid-CoA:amino acid N-acyltransferase
ANXA2_RAT	Annexin A2
AK1A1_RAT	Alcohol dehydrogenase [NADP+]
CATL1_RAT	Cathepsin L1
Q5U362_RAT	Annexin A4
GNMT_HUMAN	Glycine N-methyltransferase

The microsomal pellet after OG treatment (PELLET):

LRP1_MOUSE	Prolow-density lipoprotein receptor-related protein 1
FRIL1_RAT	Ferritin light chain 1
Q7TP91_RAT	Ab1-205
CLH_RAT	Clathrin heavy chain 1
MYH9_RAT	Myosin-9
APOB_RAT	Apolipoprotein B-100
FAS_RAT	Fatty acid synthase
A1I3_RAT	Alpha-1-inhibitor 3
UGGG1_RAT	UDP-glucose:glycoprotein glucosyltransferase 1

B5DFK1_RAT	Copa protein
CO3_RAT	Complement C3
A1M_RAT	Alpha-1-macroglobulin
Q3KRF2_RAT	High density lipoprotein binding protein
Q6P136_RAT	Hyou1 protein
SC31A_RAT	Protein transport protein Sec31A
AT2A2_RAT	Sarcoplasmic/endoplasmic reticulum calcium ATPase 2
AT1A1_RAT	Sodium/potassium-transporting ATPase subunit alpha-1
TPP2_RAT	Tripeptidyl-peptidase 2
CPSM_RAT	Carbamoyl-phosphate synthase [ammonia], mitochondrial
ACLY_RAT	ATP-citrate synthase
A2AMV0_MOUSE	Novel DUF1620 domain containing protein
DPP4_RAT	Dipeptidyl peptidase 4
LDLR_RAT	Low-density lipoprotein receptor
STRUM_MOUSE	Strumpellin
Q9JL97_RAT	GPI-anchored ceruloplasmin
DDB1_RAT	DNA damage-binding protein 1
MYO1B_RAT	Myosin-Ib
SC24A_MOUSE	Protein transport protein Sec24A
B5DEG8_RAT	LOC685144 protein (RCG41932)
VPP1_RAT	V-type proton ATPase 116 kDa subunit a isoform 1
MYO1C_RAT	Myosin-Ic
ENPP1_RAT	Ectonucleotide pyrophosphatase/phosphodiesterase family member 1
ENPL_RAT	Endoplasmin
SND1_RAT	Staphylococcal nuclease domain-containing protein 1
Q5EBC3_RAT	Methylenetetrahydrofolate dehydrogenase (NADP+ dependent), methenyltetrahydrofolate cyclohydrolase, formyltetrahydrofolate synthase
GANAB_MOUSE	Neutral alpha-glucosidase AB
AP2B1_RAT	AP-2 complex subunit beta-1
MVP_RAT	Major vault protein
COPB_RAT	Coatomer subunit beta
EIF3B_RAT	Eukaryotic translation initiation factor 3 subunit B
PIGR_RAT	Polymeric immunoglobulin receptor
ERAP1_RAT	Endoplasmic reticulum aminopeptidase 1
TERA_RAT	Transitional endoplasmic reticulum ATPase
Q91X33_MOUSE	Microsomal triglyceride transfer protein
C1TC_RAT	C-1-tetrahydrofolate synthase, cytoplasmic
Q7M079_RAT	Calcium-binding protein 4 (Fragment)
COPG_RAT	Coatomer subunit gamma
COPB2_RAT	Coatomer subunit beta
Q5U302_RAT	Catenin (Cadherin associated protein), alpha 1
FTHFD_RAT	10-formyltetrahydrofolate dehydrogenase
EF2_RAT	Elongation factor 2
AP2A2_RAT	AP-2 complex subunit alpha-2
CALX_RAT	Calnexin
B5DFC3_RAT	SEC23A (S. cerevisiae) (Predicted)
HS90B_RAT	Heat shock protein HSP 90-beta
DDX1_RAT	ATP-dependent RNA helicase DDX1
PLMN_RAT	Plasminogen
B3DMA2_RAT	Acyl-Coenzyme A dehydrogenase family, member 11
GCS1_RAT	Mannosyl-oligosaccharide glucosidase
G6PE_MOUSE	GDH/6PGL endoplasmic bifunctional protein
PDIA4_RAT	Protein disulfide-isomerase A4
NCPR_RAT	NADPH--cytochrome P450 reductase
ACSL1_RAT	Long-chain-fatty-acid--CoA ligase 1
DHB4_RAT	Peroxisomal multifunctional enzyme type 2
ECHP_RAT	Peroxisomal bifunctional enzyme
B1WC34_RAT	Protein kinase C substrate 80K-H
ECHA_RAT	Trifunctional enzyme subunit alpha, mitochondrial
TRFE_RAT	Serotransferrin
K6PL_RAT	6-phosphofructokinase, liver type

ACOX2_RAT	Peroxisomal acyl-coenzyme A oxidase 2
Q5WQV5_RAT	Radixin
Q6P6R6_RAT	Transglutaminase 2, C polypeptide
ALBU_RAT	Serum albumin
GRP78_RAT	78 kDa glucose-regulated protein
HSP7C_RAT	Heat shock cognate 71 kDa protein
S27A5_RAT	Bile acyl-CoA synthetase
ANXA6_RAT	Annexin A6
S27A2_RAT	Very long-chain acyl-CoA synthetase
RPN2_RAT	Dolichyl-diphosphooligosaccharide--protein glycosyltransferase subunit 2
Q6P7A7_RAT	Ribophorin I
CMC2_MOUSE	Calcium-binding mitochondrial carrier protein Aralar2
Q3KR94_RAT	Vitronectin
RETST_RAT	All-trans-retinol 13,14-reductase
HNRPQ_RAT	Heterogeneous nuclear ribonucleoprotein Q
SPA3K_RAT	Serine protease inhibitor A3K
EST2_RAT	Liver carboxylesterase 1
DHSA_RAT	Succinate dehydrogenase [ubiquinone] flavoprotein subunit, mitochondrial
ETFD_RAT	Electron transfer flavoprotein-ubiquinone oxidoreductase, mitochondrial
EST4_RAT	Liver carboxylesterase 4
FAAH1_RAT	Fatty-acid amide hydrolase 1
TCPE_RAT	T-complex protein 1 subunit epsilon
AOFB_RAT	Amine oxidase [flavin-containing] B
TCPG_RAT	T-complex protein 1 subunit gamma
PDIA1_RAT	Protein disulfide-isomerase
SAC1_RAT	Phosphatidylinositide phosphatase SAC1
CATA_RAT	Catalase
EHD3_RAT	EH domain-containing protein 3
PDIA3_RAT	Protein disulfide-isomerase A3
CES3_RAT	Carboxylesterase 3
CALR_RAT	Calreticulin
LMAN1_RAT	Protein ERGIC-53
UD11_RAT	UDP-glucuronosyltransferase 1-1
EST3_RAT	Liver carboxylesterase 3
FMO5_RAT	Dimethylaniline monooxygenase [N-oxide-forming] 5
NUCL_RAT	Nucleolin
ATPA_RAT	ATP synthase subunit alpha, mitochondrial
DHE3_RAT	Glutamate dehydrogenase 1, mitochondrial
CP4A2_RAT	Cytochrome P450 4A2
UD2B5_RAT	UDP-glucuronosyltransferase 2B5
TCPB_RAT	T-complex protein 1 subunit beta
FMO1_RAT	Dimethylaniline monooxygenase [N-oxide-forming] 1
ATLA3_RAT	Atlastin-3
Q4V8I9_RAT	UDP-glucose pyrophosphorylase 2
FMO3_RAT	Dimethylaniline monooxygenase [N-oxide-forming] 3
PRRC1_RAT	Protein PPRC1
CP2D1_RAT	Cytochrome P450 2D1
A1AT_RAT	Alpha-1-antiproteinase
CP2B3_RAT	Cytochrome P450 2B3
ATPB_RAT	ATP synthase subunit beta, mitochondrial
CP4F4_RAT	Cytochrome P450 4F4
TBB2A_RAT	Tubulin beta-2A chain
AL3A2_RAT	Fatty aldehyde dehydrogenase
CP3A2_RAT	Cytochrome P450 3A2
UD2B4_RAT	UDP-glucuronosyltransferase 2B4
CP2CN_RAT	Cytochrome P450 2C23
CP4AE_RAT	Cytochrome P450 4A14
UD2B3_RAT	UDP-glucuronosyltransferase 2B3
CP2CB_RAT	Cytochrome P450 2C11
CP51A_RAT	Cytochrome P450 51A1
CP1A2_RAT	Cytochrome P450 1A2

CP2E1_RAT	Cytochrome P450 2E1
CP4F1_RAT	Cytochrome P450 4F1
CP2J3_RAT	Cytochrome P450 2J3
CP2DQ_RAT	Cytochrome P450 2D26
CP2CD_RAT	Cytochrome P450 2C13, male-specific
CP2C7_RAT	Cytochrome P450 2C7
CP3AI_RAT	Cytochrome P450 3A18
CP2A2_RAT	Cytochrome P450 2A2
PDIA6_RAT	Protein disulfide-isomerase A6
RL4_RAT	60S ribosomal protein L4
Q63125_RAT	Rat cytochrome P-450b type b (Fragment)
AAAD_RAT	Arylacetamide deacetylase
Q9WTN7_RAT	Sterol 12-alpha hydroxylase
HYEP_RAT	Epoxide hydrolase 1
Q4QQW7_RAT	Cytochrome P450, family 2, subfamily c, polypeptide 7
EF1A1_RAT	Elongation factor 1-alpha 1
RL3_RAT	60S ribosomal protein L3
CP2A1_RAT	Cytochrome P450 2A1
NTCP_RAT	Sodium/bile acid cotransporter
CP270_RAT	Cytochrome P450 2C70
BHMT1_RAT	Betaine--homocysteine S-methyltransferase 1
Q6AYD3_RAT	Proliferation-associated 2G4
GGLO_RAT	L-gulonolactone oxidase
IF4A2_RAT	Eukaryotic initiation factor 4A-II
Q6P6S9_RAT	Ectonucleoside triphosphate diphosphohydrolase 5
OST48_RAT	Dolichyl-diphosphooligosaccharide--protein glycosyltransferase 48 kDa subunit
ASGR1_RAT	Asialoglycoprotein receptor 1
ASSY_RAT	Argininosuccinate synthase
BASI_RAT	Basigin
A2IBE0_RAT	Membrane-bound carbonic anhydrase 14
METK1_RAT	S-adenosylmethionine synthetase isoform type-1
CGL_RAT	Cystathionine gamma-lyase
SCPDH_RAT	Probable saccharopine dehydrogenase
ACTB_RAT	Actin, cytoplasmic 1
Q5BJN6_RAT	Paraoxonase 1
RSSA_RAT	40S ribosomal protein SA
PON3_RAT	Serum paraoxonase/lactonase 3
Q7TP48_RAT	Ab2-305
FAAA_RAT	Fumarylacetoacetase
DJB11_RAT	DnaJ homolog subfamily B member 11
E2AK1_RAT	Eukaryotic translation initiation factor 2-alpha kinase 1
HPPD_RAT	4-hydroxyphenylpyruvate dioxygenase
PON2_RAT	Serum paraoxonase/arylesterase 2
ALDOB_RAT	Fructose-bisphosphate aldolase B
3BHS5_RAT	3 beta-hydroxysteroid dehydrogenase type 5
PON1_RAT	Serum paraoxonase/arylesterase 1
Q5I0F0_RAT	Developmentally regulated GTP binding protein 1
F16P1_RAT	Fructose-1,6-bisphosphatase 1
DHCR7_RAT	7-dehydrocholesterol reductase
NSDHL_RAT	Sterol-4-alpha-carboxylate 3-dehydrogenase, decarboxylating
ARGI1_RAT	Arginase-1
ANXA1_RAT	Annexin A1
HNRPC_RAT	Heterogeneous nuclear ribonucleoprotein C (Fragment)
S61A1_RAT	Protein transport protein Sec61 subunit alpha isoform 1
RL6_MOUSE	60S ribosomal protein L6
Q9QX80_RAT	CArG-binding factor A
Q5BK21_RAT	Transmembrane 7 superfamily member 2
IF2A_RAT	Eukaryotic translation initiation factor 2 subunit 1
RLA0_RAT	60S acidic ribosomal protein P0
RL6_RAT	60S ribosomal protein L6
ADH1_RAT	Alcohol dehydrogenase 1

B2RYX0_RAT	Naca protein
EIF3I_RAT	Eukaryotic translation initiation factor 3 subunit I
G3P_RAT	Glyceraldehyde-3-phosphate dehydrogenase
Q68G38_RAT	Dystonia 1
SSRA_RAT	Translocon-associated protein subunit alpha
Q6I7R1_RAT	Dehydrogenase/reductase (SDR family) member 7
RGN_RAT	Regucalcin
DHI1_RAT	Corticosteroid 11-beta-dehydrogenase isozyme 1
B0BNG3_RAT	Lman2 protein
RL5_RAT	60S ribosomal protein L5
URIC_RAT	Uricase
DIDH_RAT	3-alpha-hydroxysteroid dehydrogenase
HPT_RAT	Haptoglobin
PECR_RAT	Peroxisomal trans-2-enoyl-CoA reductase
LDHA_RAT	L-lactate dehydrogenase A chain
LRC59_RAT	Leucine-rich repeat-containing protein 59
VDAC1_RAT	Voltage-dependent anion-selective channel protein 1
PHB2_RAT	Prohibitin-2
GBLP_RAT	Guanine nucleotide-binding protein subunit beta-2-like 1
MDHC_RAT	Malate dehydrogenase, cytoplasmic
APOE_RAT	Apolipoprotein E
NB5R3_RAT	NADH-cytochrome b5 reductase 3
RS3_RAT	40S ribosomal protein S3
ANXA5_RAT	Annexin A5
RL7_RAT	60S ribosomal protein L7
MLEC_RAT	Malectin
DHB11_RAT	Estradiol 17-beta-dehydrogenase 11
SNAA_RAT	Alpha-soluble NSF attachment protein
RS2_RAT	40S ribosomal protein S2
DHB2_RAT	Estradiol 17-beta-dehydrogenase 2
DHB13_RAT	17-beta hydroxysteroid dehydrogenase 13
B0BN52_RAT	Mitochondrial carrier homolog 2 (C. elegans)
RS3A_RAT	40S ribosomal protein S3a
B0K031_RAT	RCG30479, isoform CRA_b
RDH2_RAT	Retinol dehydrogenase 2
RDH3_RAT	Retinol dehydrogenase 3
RS6_RAT	40S ribosomal protein S6
RL7A_HUMAN	60S ribosomal protein L7a
H17B6_RAT	Hydroxysteroid 17-beta dehydrogenase 6
RL8_RAT	60S ribosomal protein L8
RDH7_RAT	Retinol dehydrogenase 7
RS4X_RAT	40S ribosomal protein S4, X isoform
ADT2_RAT	ADP/ATP translocase 2
RL7A_RAT	60S ribosomal protein L7a
GPSN2_RAT	Synaptic glycoprotein SC2
DHB12_RAT	Estradiol 17-beta-dehydrogenase 12
RS15A_RAT	40S ribosomal protein S15a
CAH3_RAT	Carbonic anhydrase 3
PSA4_RAT	Proteasome subunit alpha type-4
CRP_RAT	C-reactive protein
O89035_RAT	Mitochondrial dicarboxylate carrier
ERP29_RAT	Endoplasmic reticulum protein ERp29
RS8_RAT	40S ribosomal protein S8
RL13_RAT	60S ribosomal protein L13
RL10A_RAT	60S ribosomal protein L10a
PRDX1_RAT	Peroxiredoxin-1
PGRC1_RAT	Membrane-associated progesterone receptor component 1
Q9Z0V5_RAT	PRx IV
MET7B_RAT	Methyltransferase-like protein 7B
B0BNK1_RAT	RCG32615, isoform CRA_a
RL14_RAT	60S ribosomal protein L14

RL19_RAT	60S ribosomal protein L19
GSTA3_RAT	Glutathione S-transferase alpha-3
GSTM1_RAT	Glutathione S-transferase Mu 1
RS8_BOVIN	40S ribosomal protein S8
SC22B_RAT	Vesicle-trafficking protein SEC22b
RL9_RAT	60S ribosomal protein L9
RL15_RAT	60S ribosomal protein L15
RAB7A_RAT	Ras-related protein Rab-7a
GSTA1_RAT	Glutathione S-transferase alpha-1
RL13A_RAT	60S ribosomal protein L13a
RL18_RAT	60S ribosomal protein L18
RL10_RAT	60S ribosomal protein L10
RS9_RAT	40S ribosomal protein S9
RAB8B_RAT	Ras-related protein Rab-8B
RS7_RAT	40S ribosomal protein S7
RL21_RAT	60S ribosomal protein L21
RET4_RAT	Retinol-binding protein 4
GBRT_HUMAN	Gamma-aminobutyric acid receptor subunit theta
TMED2_RAT	Transmembrane emp24 domain-containing protein 2
Q6PDW2_RAT	Ribosomal protein L21
RER1_RAT	Protein RER1
RL31_RAT	60S ribosomal protein L31
PPIB_RAT	Peptidyl-prolyl cis-trans isomerase B
RL29_RAT	60S ribosomal protein L29
FRIH_RAT	Ferritin heavy chain

The OG solubilized fraction (supernatant):

CLH_RAT	Clathrin heavy chain 1
A1I3_RAT	Alpha-1-inhibitor 3
CO3_RAT	Complement C3
A1M_RAT	Alpha-1-macroglobulin
SC31A_RAT	Protein transport protein Sec31A
AT1A1_RAT	Sodium/potassium-transporting ATPase subunit alpha-1
TPP2_RAT	Tripeptidyl-peptidase 2
Q6P136_RAT	Hyou1 protein
B5DEG8_RAT	LOC685144 protein (RCG41932)
ENPL_RAT	Endoplasmin
AP1B1_RAT	AP-1 complex subunit beta-1
SND1_RAT	Staphylococcal nuclease domain-containing protein 1
Q5EBC3_RAT	Methylenetetrahydrofolate dehydrogenase (NADP+ dependent),
Q91X33_MOUSE	Microsomal triglyceride transfer protein
TERA_RAT	Transitional endoplasmic reticulum ATPase
HS90A_RAT	Heat shock protein HSP 90-alpha
CALX_RAT	Calnexin
PLMN_RAT	Plasminogen
G6PE_MOUSE	GDH/6PGL endoplasmic bifunctional protein
B5DFC3_RAT	SEC23A (S. cerevisiae) (Predicted)
B1WC34_RAT	Protein kinase C substrate 80K-H
VPS35_MOUSE	Vacuolar protein sorting-associated protein 35
Q99PS8_RAT	Histidine-rich glycoprotein
ACSL1_RAT	Long-chain-fatty-acid--CoA ligase 1
GRP78_RAT	78 kDa glucose-regulated protein
PDIA4_RAT	Protein disulfide-isomerase A4
TRFE_RAT	Serotransferrin
ALBU_RAT	Serum albumin
HSP7C_RAT	Heat shock cognate 71 kDa protein
Q6IMZ3_RAT	Anxa6 protein
S27A2_RAT	Very long-chain acyl-CoA synthetase

RPN1_RAT	Dolichyl-diphosphooligosaccharide--protein glycosyltransferase subunit 1
PABP1_RAT	Polyadenylate-binding protein 1
SPA3L_RAT	Serine protease inhibitor A3L
RETST_RAT	All-trans-retinol 13,14-reductase
EST2_RAT	Liver carboxylesterase 1
ETFD_RAT	Electron transfer flavoprotein-ubiquinone oxidoreductase, mitochondrial
PDIA1_RAT	Protein disulfide-isomerase
EST4_RAT	Liver carboxylesterase 4
CES3_RAT	Carboxylesterase 3
PDIA3_RAT	Protein disulfide-isomerase A3
CALR_RAT	Calreticulin
EST3_RAT	Liver carboxylesterase 3
ATPA_RAT	ATP synthase subunit alpha, mitochondrial
UD11_RAT	UDP-glucuronosyltransferase 1-1
A1AT_RAT	Alpha-1-antiproteinase
Q4V8I9_RAT	UDP-glucose pyrophosphorylase 2
FMO5_RAT	Dimethylaniline monooxygenase [N-oxide-forming] 5
AL3A2_RAT	Fatty aldehyde dehydrogenase
CP2D1_RAT	Cytochrome P450 2D1
CP3A2_RAT	Cytochrome P450 3A2
UD2B3_RAT	UDP-glucuronosyltransferase 2B3
CP2DQ_RAT	Cytochrome P450 2D26
UD2B4_RAT	UDP-glucuronosyltransferase 2B4
FMO3_RAT	Dimethylaniline monooxygenase [N-oxide-forming] 3
CP2E1_RAT	Cytochrome P450 2E1
FMO1_RAT	Dimethylaniline monooxygenase [N-oxide-forming] 1
CP4F1_RAT	Cytochrome P450 4F1
CP2CN_RAT	Cytochrome P450 2C23
PDIA6_RAT	Protein disulfide-isomerase A6
CP2CB_RAT	Cytochrome P450 2C11
EF1A1_RAT	Elongation factor 1-alpha 1
CP2A2_RAT	Cytochrome P450 2A2
CP2A1_RAT	Cytochrome P450 2A1
AAAD_RAT	Arylacetamide deacetylase
CP3AI_RAT	Cytochrome P450 3A18
Q3MIE4_RAT	Vesicle amine transport protein 1 homolog (T californica)
BHMT1_RAT	Betaine--homocysteine S-methyltransferase 1
GGLO_RAT	L-gulonolactone oxidase
NUCB2_RAT	Nucleobindin-2
CP2B3_RAT	Cytochrome P450 2B3
Q6P3V8_RAT	Eukaryotic translation initiation factor 4A1
Q6P6S9_RAT	Ectonucleoside triphosphate diphosphohydrolase 5
ASGR1_RAT	Asialoglycoprotein receptor 1
METK1_RAT	S-adenosylmethionine synthetase isoform type-1
CP2CC_RAT	Cytochrome P450 2C12, female-specific
CGL_RAT	Cystathionine gamma-lyase
OST48_RAT	Dolichyl-diphosphooligosaccharide--protein glycosyltransferase 48 kDa subunit
MPRD_RAT	Cation-dependent mannose-6-phosphate receptor
ASSY_RAT	Argininosuccinate synthase
ACTB_RAT	Actin, cytoplasmic 1
PON1_RAT	Serum paraoxonase/arylesterase 1
PON3_RAT	Serum paraoxonase/lactonase 3
APOA4_RAT	Apolipoprotein A-IV
ALDOB_RAT	Fructose-bisphosphate aldolase B
F16P1_RAT	Fructose-1,6-bisphosphatase 1
3BHS5_RAT	3 beta-hydroxysteroid dehydrogenase type 5
NSDHL_RAT	Sterol-4-alpha-carboxylate 3-dehydrogenase, decarboxylating
DHSO_RAT	Sorbitol dehydrogenase
ADH1_RAT	Alcohol dehydrogenase 1
ARGI1_RAT	Arginase-1
G3P_RAT	Glyceraldehyde-3-phosphate dehydrogenase

RGN_RAT	Regucalcin
DHI1_RAT	Corticosteroid 11-beta-dehydrogenase isozyme 1
QOR_RAT	Quinone oxidoreductase
HPT_RAT	Haptoglobin
LDHA_RAT	L-lactate dehydrogenase A chain
PECR_RAT	Peroxisomal trans-2-enoyl-CoA reductase
APOE_RAT	Apolipoprotein E
RDH2_RAT	Retinol dehydrogenase 2
BDH_RAT	D-beta-hydroxybutyrate dehydrogenase, mitochondrial
RDH3_RAT	Retinol dehydrogenase 3
RDH7_RAT	Retinol dehydrogenase 7
PSA4_RAT	Proteasome subunit alpha type-4
CAH3_RAT	Carbonic anhydrase 3
ERP29_RAT	Endoplasmic reticulum protein ERp29
PSA7_RAT	Proteasome subunit alpha type-7
Q9Z0V5_RAT	PRx IV
PGRC1_RAT	Membrane-associated progesterone receptor component 1
GSTM2_RAT	Glutathione S-transferase Mu 2
GSTA1_RAT	Glutathione S-transferase alpha-1
GSTA3_RAT	Glutathione S-transferase alpha-3
SC22B_RAT	Vesicle-trafficking protein SEC22b
GSTM1_RAT	Glutathione S-transferase Mu 1
PRDX1_RAT	Peroxiredoxin-1

List of proteins identified by mass-spectrometry after further separation by protein chromatography

Q5EBC3_RAT	Methylenetetrahydrofolate dehydrogenase (NADP+ dependent),
PLMN_RAT	Plasminogen
ENPL_RAT	Endoplasmin
EST4_RAT	Liver carboxylesterase 4
CES3_RAT	Carboxylesterase 3
TRFE_RAT	Serotransferrin
FUBP2_RAT	Far upstream element-binding protein 2
DHB4_RAT	Peroxisomal multifunctional enzyme type 2
HUTU_MOUSE	Probable urocanate hydratase
AFAM_RAT	Afamin
EST5_RAT	Liver carboxylesterase B-1
TKT_RAT	Transketolase
Q6QI47_RAT	LRRGT00161
EST2_RAT	Liver carboxylesterase 1
HEMO_RAT	Hemopexin
CATA_RAT	Catalase
SPA3L_RAT	Serine protease inhibitor A3L
A1AT_RAT	Alpha-1-antiproteinase
SBP1_RAT	Selenium-binding protein 1
SPA3K_RAT	Serine protease inhibitor A3K
PGCP_RAT	Plasma glutamate carboxypeptidase
AL7A1_MOUSE	Alpha-aminoadipic semialdehyde dehydrogenase
DLDH_RAT	Dihydrolipoyl dehydrogenase, mitochondrial
ANX11_MOUSE	Annexin A11
FETUB_RAT	Fetuin-B
CSAD_RAT	Cysteine sulfinic acid decarboxylase
AL8A1_MOUSE	Aldehyde dehydrogenase family 8 member A1
MMSA_RAT	Methylmalonate-semialdehyde dehydrogenase [acylating], mitochondrial
ENOA_RAT	Alpha-enolase
EF1A1_RAT	Elongation factor 1-alpha 1
ACOX1_RAT	Peroxisomal acyl-coenzyme A oxidase 1
FETUA_RAT	Alpha-2-HS-glycoprotein
6PGD_RAT	6-phosphogluconate dehydrogenase, decarboxylating
FUMH_RAT	Fumarate hydratase, mitochondrial
BHMT1_RAT	Betaine--homocysteine S-methyltransferase 1
CGL_RAT	Cystathionine gamma-lyase
BAAT_RAT	Bile acid-CoA:amino acid N-acyltransferase
SAHH_RAT	Adenosylhomocysteinase
ASSY_RAT	Argininosuccinate synthase
PGK1_MOUSE	Phosphoglycerate kinase 1
FAAA_RAT	Fumarylacetoacetase
HPPD_RAT	4-hydroxyphenylpyruvate dioxygenase
BUP1_RAT	Beta-ureidopropionase
IDHC_RAT	Isocitrate dehydrogenase [NADP] cytoplasmic
PGK1_RAT	Phosphoglycerate kinase 1
ALDOB_RAT	Fructose-bisphosphate aldolase B
AATC_RAT	Aspartate aminotransferase, cytoplasmic
THIL_RAT	Acetyl-CoA acetyltransferase, mitochondrial
PLBL1_RAT	Putative phospholipase B-like 1
ARGI1_RAT	Arginase-1
CATD_RAT	Cathepsin D
BAAT_MOUSE	Bile acid-CoA:amino acid N-acyltransferase
DHSO_RAT	Sorbitol dehydrogenase
G3P_RAT	Glyceraldehyde-3-phosphate dehydrogenase
AK1D1_RAT	3-oxo-5-beta-steroid 4-dehydrogenase
ANXA2_RAT	Annexin A2

AK1A1_RAT	Alcohol dehydrogenase [NADP+]
RGN_RAT	Regucalcin
DIDH_RAT	3-alpha-hydroxysteroid dehydrogenase
ADH1_RAT	Alcohol dehydrogenase 1
Q5BJN1_RAT	START domain containing 10
B0BN46_RAT	Grhpr protein
CATL1_RAT	Cathepsin L1
PECR_RAT	Peroxisomal trans-2-enoyl-CoA reductase
QOR_RAT	Quinone oxidoreductase
Q5U362_RAT	Annexin A4
GNMT_HUMAN	Glycine N-methyltransferase
NIT2_RAT	Nitrilase homolog 2
HPT_RAT	Haptoglobin
PAHX_RAT	Phytanoyl-CoA dioxygenase, peroxisomal
Q2MHD9_RAT	17beta-hydroxysteroid dehydrogenase
MDHC_RAT	Malate dehydrogenase, cytoplasmic
LDHA_RAT	L-lactate dehydrogenase A chain
PNPH_RAT	Purine nucleoside phosphorylase

List of glycosylated proteins identified by mass-spectrometry

Eluted fraction from concanavalin A (ConA) column

P20029	RecName: Full=78 kDa glucose-regulated protein; Short=GRP-78;AltName: Full=Heat shock 70 kDa protein 5;AltNam
P09103	Protein disulfide-isomerase OS=Mus musculus GN=P4hb PE=1 SV=2 - [PDIA1_MOUSE]
P08113	RecName: Full=Endoplasmin;AltName: Full=Heat shock protein 90 kDa beta member 1;AltName: Full=94 kDa glucose-reg
P02535	RecName: Full=Keratin, type I cytoskeletal 10;AltName: Full=Cytokeratin-10; Short=CK-10;AltName: Full=Keratin-10
P14206	RecName: Full=40S ribosomal protein SA;AltName: Full=Laminin receptor 1; Short=LamR;AltName: Full=37/67 kDa
P08003	Protein disulfide-isomerase A4 OS=Mus musculus GN=Pdia4 PE=1 SV=3 - [PDIA4_MOUSE]
P62908	RecName: Full=40S ribosomal protein S3; - [RS3_MOUSE]
P04104	RecName: Full=Keratin, type II cytoskeletal 1;AltName: Full=Cytokeratin-1; Short=CK-1;AltName: Full=Keratin-1;
Q922R8	RecName: Full=Protein disulfide-isomerase A6; EC=5.3.4.1;AltName: Full=Thioredoxin domain-containing protein 7;F
Q6IFX2	RecName: Full=Keratin, type I cytoskeletal 42;AltName: Full=Cytokeratin-42; Short=CK-42;AltName: Full=Keratin-42
P14211	RecName: Full=Calreticulin;AltName: Full=CRP55;AltName: Full=Calregulin;AltName: Full=HACBP;AltName: Full=Endoplas
P50446	RecName: Full=Keratin, type II cytoskeletal 6A;AltName: Full=Cytokeratin-6A; Short=CK-6A;AltName: Full=Keratin-6
Q63880	RecName: Full=Liver carboxylesterase 31; Short=Esterase-31; EC=3.1.1.1;AltName: Full=ES-male;Flags: Precu
Q921I1	RecName: Full=Serotransferrin; Short=Transferrin;AltName: Full=Siderophilin;AltName: Full=Beta-1 metal-binding gl
Q8VCT4	RecName: Full=Carboxylesterase 3; EC=3.1.1.1; EC=3.1.1.67;AltName: Full=Triacylglycerol hydrolase; S
P01027	Complement C3 OS=Mus musculus GN=C3 PE=1 SV=3 - [CO3_MOUSE]
Q9QWL7	RecName: Full=Keratin, type I cytoskeletal 17;AltName: Full=Cytokeratin-17; Short=CK-17;AltName: Full=Keratin-17
Q8VCC2	RecName: Full=Liver carboxylesterase 1; EC=3.1.1.1;AltName: Full=Acyl-coenzyme A:cholesterol acyltransferase;Alt
Q6NXH9	RecName: Full=Keratin, type II cytoskeletal 73;AltName: Full=Cytokeratin-73; Short=CK-73;AltName: Full=Keratin-7
Q8VED5	RecName: Full=Keratin, type II cytoskeletal 79;AltName: Full=Cytokeratin-79; Short=CK-79;AltName: Full=Keratin-7
P11499	Heat shock protein HSP 90-beta OS=Mus musculus GN=Hsp90ab1 PE=1 SV=3 - [HS90B_MOUSE]
O08601	RecName: Full=Microsomal triglyceride transfer protein large subunit;Flags: Precursor; - [MTP_MOUSE]
P17717	RecName: Full=UDP-glucuronosyltransferase 2B5; Short=UDPGT 2B5; EC=2.4.1.17;AltName: Full=M-1;Flags:
Q78PY7	RecName: Full=Staphylococcal nuclease domain-containing protein 1;AltName: Full=p100 co-activator;AltName: Full=100
P68040	RecName: Full=Guanine nucleotide-binding protein subunit beta-2-like 1;AltName: Full=Receptor of activated protein kinas
P29341	Polyadenylate-binding protein 1 OS=Mus musculus GN=Pabpc1 PE=1 SV=2 - [PABP1_MOUSE]
P63017	RecName: Full=Heat shock cognate 71 kDa protein;AltName: Full=Heat shock 70 kDa protein 8; - [HSP7C_MOUSE]
Q8BHN3	RecName: Full=Neutral alpha-glucosidase AB; EC=3.2.1.84;AltName: Full=Glucosidase II subunit alpha;AltName: Fu
Q60817	RecName: Full=Nascent polypeptide-associated complex subunit alpha;AltName: Full=Alpha-NAC;AltName: Full=Alpha-NAC
P07901	RecName: Full=Heat shock protein HSP 90-alpha;AltName: Full=Heat shock 86 kDa; Short=HSP 86; Short=HSP
O08795	RecName: Full=Glucosidase 2 subunit beta;AltName: Full=Glucosidase II subunit beta;AltName: Full=Protein kinase C subs
Q8VCU1	RecName: Full=Liver carboxylesterase 31-like; EC=3.1.1.1;Flags: Precursor; - [ES31L_MOUSE]
P28665	RecName: Full=Murinoglobulin-1; Short=MuG1;Flags: Precursor; - [MUG1_MOUSE]
Q3TTY5	RecName: Full=Keratin, type II cytoskeletal 2 epidermal;AltName: Full=Cytokeratin-2e; Short=CK-2e;AltName: Full=
P56480	RecName: Full=ATP synthase subunit beta, mitochondrial; EC=3.6.3.14;Flags: Precursor; - [ATPB_MOUSE]
P60710	RecName: Full=Actin, cytoplasmic 1;AltName: Full=Beta-actin;Contains: RecName: Full=Actin, cytoplasmic 1, N-terminally
Q64176	RecName: Full=Liver carboxylesterase 22; Short=Esterase-22; Short=Es-22; EC=3.1.1.1;AltName: Full=E
Q9Z2U0	RecName: Full=Proteasome subunit alpha type-7; EC=3.4.25.1;AltName: Full=Proteasome subunit RC6-1; - [PSA7_M
Q8CFX1	GDH/6PGL endoplasmic bifunctional protein OS=Mus musculus GN=H6pd PE=2 SV=2 - [G6PE_MOUSE]
P07759	RecName: Full=Serine protease inhibitor A3K; Short=Serpin A3K;AltName: Full=Contrapsin;AltName: Full=SPI-2;Flag

P11589	RecName: Full=Major urinary protein 2; Short=MUP 2;Flags: Precursor; - [MUP2_MOUSE]
P57780	RecName: Full=Alpha-actinin-4;AltName: Full=Non-muscle alpha-actinin 4;AltName: Full=F-actin cross-linking protein; - [A
Q9EQK5	Major vault protein OS=Mus musculus GN=Mvp PE=1 SV=4 - [MVP_MOUSE]
P23953	Liver carboxylesterase N OS=Mus musculus GN=Es1 PE=1 SV=4 - [ESTN_MOUSE]
Q6P5E4	UDP-glucose:glycoprotein glucosyltransferase 1 OS=Mus musculus GN=Uggt1 PE=1 SV=4 - [UGGG1_MOUSE]
Q00897	RecName: Full=Alpha-1-antitrypsin 1-4;AltName: Full=Serine protease inhibitor 1-4;AltName: Full=Serine protease inhibito
Q01853	RecName: Full=Transitional endoplasmic reticulum ATPase; Short=TER ATPase;AltName: Full=15S Mg(2+)-ATPase p
P01029	Complement C4-B OS=Mus musculus GN=C4b PE=1 SV=3 - [CO4B_MOUSE]
P10126	RecName: Full=Elongation factor 1-alpha 1; Short=EF-1-alpha-1;AltName: Full=Eukaryotic elongation factor 1 A-1;
P63325	RecName: Full=40S ribosomal protein S10; - [RS10_MOUSE]
Q9QUM9	RecName: Full=Proteasome subunit alpha type-6; EC=3.4.25.1;AltName: Full=Proteasome iota chain;AltName: Full=
Q99KV1	RecName: Full=DnaJ homolog subfamily B member 11;AltName: Full=ER-associated dnaJ protein 3; Short=ERj3p;
Q9EQH2	Endoplasmic reticulum aminopeptidase 1 OS=Mus musculus GN=Erap1 PE=2 SV=2 - [ERAP1_MOUSE]
Q99PL5	RecName: Full=Ribosome-binding protein 1;AltName: Full=Ribosome receptor protein; Short=RRp; Short=mRR
Q8QZY1	RecName: Full=Eukaryotic translation initiation factor 3 subunit L; Short=eIF3l;AltName: Full=Eukaryotic translation
O08807	RecName: Full=Peroxiredoxin-4; EC=1.11.1.15;AltName: Full=Peroxiredoxin IV; Short=Prx-IV;AltName: Full=T
Q9D1Q6	RecName: Full=Endoplasmic reticulum resident protein 44; Short=ER protein 44; Short=ERp44;AltName: Full=
P27773	RecName: Full=Protein disulfide-isomerase A3; EC=5.3.4.1;AltName: Full=Disulfide isomerase ER-60;AltName: Full=
Q91W90	RecName: Full=Thioredoxin domain-containing protein 5;AltName: Full=Thioredoxin-like protein p46;AltName: Full=Endop
Q00898	RecName: Full=Alpha-1-antitrypsin 1-5;AltName: Full=Serine protease inhibitor 1-5;AltName: Full=Serine protease inhibito
P37040	RecName: Full=NADPH--cytochrome P450 reductase; Short=CPR; Short=P450R; EC=1.6.2.4; - [NCPR_M
O70435	RecName: Full=Proteasome subunit alpha type-3; EC=3.4.25.1;AltName: Full=Proteasome component C8;AltName:
P26443	RecName: Full=Glutamate dehydrogenase 1, mitochondrial; Short=GDH 1; EC=1.4.1.3;Flags: Precursor; - [DH
P21614	RecName: Full=Vitamin D-binding protein; Short=DBP; Short=VDB;AltName: Full=Group-specific component;A
P20918	Plasminogen OS=Mus musculus GN=Plg PE=1 SV=3 - [PLMN_MOUSE]
Q3UPL0	RecName: Full=Protein transport protein Sec31A;AltName: Full=SEC31-related protein A;AltName: Full=SEC31-like protein
P17897	RecName: Full=Lysozyme C-1; EC=3.2.1.17;AltName: Full=Lysozyme C type P;AltName: Full=1,4-beta-N-acetylmura
Q9D0F3	RecName: Full=Protein ERGIC-53;AltName: Full=ER-Golgi intermediate compartment 53 kDa protein;AltName: Full=Lectin
Q68FD5	RecName: Full=Clathrin heavy chain 1; - [CLH_MOUSE]
Q8R0Y6	RecName: Full=10-formyltetrahydrofolate dehydrogenase; Short=10-FTHFDH; EC=1.5.1.6;AltName: Full=Aldeh
Q9R1P4	RecName: Full=Proteasome subunit alpha type-1; EC=3.4.25.1;AltName: Full=Proteasome component C2;AltName:
Q8VDN2	RecName: Full=Sodium/potassium-transporting ATPase subunit alpha-1; Short=Na(+)/K(+) ATPase alpha-1 subunit;
P60843	RecName: Full=Eukaryotic initiation factor 4A-I; Short=eIF-4A-I; Short=eIF4A-I; EC=3.6.1.-;AltName: Fu
Q64514	RecName: Full=Tripeptidyl-peptidase 2; Short=TPP-2; EC=3.4.14.10;AltName: Full=Tripeptidyl-peptidase II;
Q63886	UDP-glucuronosyltransferase 1-1 OS=Mus musculus GN=Ugt1a1 PE=2 SV=2 - [UD11_MOUSE]
P24369	RecName: Full=Peptidyl-prolyl cis-trans isomerase B; Short=PPIase B; EC=5.2.1.8;AltName: Full=Rotamase B;A
P0CG49	Polyubiquitin-B OS=Mus musculus GN=Ubb PE=1 SV=1 - [UBB_MOUSE]
P24456	RecName: Full=Cytochrome P450 2D10; EC=1.14.14.1;AltName: Full=CYPIID10;AltName: Full=Cytochrome P450-16
P04939	RecName: Full=Major urinary protein 3; Short=MUP 3;AltName: Full=Non-group 1/group 2 MUP15;Flags: Precursor;
Q07456	RecName: Full=Protein AMBP;Contains: RecName: Full=Alpha-1-microglobulin;Contains: RecName: Full=Inter-alpha-tryp
Q8R180	RecName: Full=ERO1-like protein alpha; Short=ERO1-L-alpha; Short=ERO1-L; EC=1.8.4.-;AltName: Full=
P10518	RecName: Full=Delta-aminolevulinic acid dehydratase; Short=ALADH; EC=4.2.1.24;AltName: Full=Porphobilino
O55234	RecName: Full=Proteasome subunit beta type-5; EC=3.4.25.1;AltName: Full=Proteasome epsilon chain;AltName: Fu
Q8R0F3	Sulfatase-modifying factor 1 OS=Mus musculus GN=Sumf1 PE=1 SV=2 - [SUMF1_MOUSE]
Q3U2P1	RecName: Full=Protein transport protein Sec24A;AltName: Full=SEC24-related protein A; - [SC24A_MOUSE]
P63101	RecName: Full=14-3-3 protein zeta/delta;AltName: Full=Protein kinase C inhibitor protein 1; Short=KCIP-1;AltName:
P50580	RecName: Full=Proliferation-associated protein 2G4;AltName: Full=Proliferation-associated protein 1;AltName: Full=Protein
P62806	RecName: Full=Histone H4; - [H4_MOUSE]
Q64435	RecName: Full=UDP-glucuronosyltransferase 1-6; Short=UDPGT 1-6; Short=UGT1-06; Short=UGT1.6;
Q60692	RecName: Full=Proteasome subunit beta type-6; EC=3.4.25.1;AltName: Full=Proteasome delta chain;AltName: Full=

Q9DB77	RecName: Full=Cytochrome b-c1 complex subunit 2, mitochondrial;AltName: Full=Ubiquinol-cytochrome-c reductase comp
P62960	RecName: Full=Nuclease-sensitive element-binding protein 1;AltName: Full=Y-box-binding protein 1; Short=YB-1;Alt
O09159	Lysosomal alpha-mannosidase OS=Mus musculus GN=Man2b1 PE=2 SV=4 - [MA2B1_MOUSE]
Q9JKR6	RecName: Full=Hypoxia up-regulated protein 1; Short=GRP-170;AltName: Full=140 kDa Ca(2+)-binding protein;
P14824	Annexin A6 OS=Mus musculus GN=Anxa6 PE=1 SV=3 - [ANXA6_MOUSE]
Q5SW19	RecName: Full=Protein KIAA0664; - [K0664_MOUSE]
Q9WVJ3	RecName: Full=Plasma glutamate carboxypeptidase; EC=3.4.17.-;AltName: Full=Hematopoietic lineage switch 2;Flag
Q01405	RecName: Full=Protein transport protein Sec23A;AltName: Full=SEC23-related protein A; - [SC23A_MOUSE]
Q9ET22	Dipeptidyl peptidase 2 OS=Mus musculus GN=Dpp7 PE=2 SV=2 - [DPP2_MOUSE]
Q05117	RecName: Full=Tartrate-resistant acid phosphatase type 5; Short=TR-AP; EC=3.1.3.2;AltName: Full=Tartrate-r
Q921X9	RecName: Full=Protein disulfide-isomerase A5; EC=5.3.4.1;AltName: Full=Protein disulfide isomerase-related protein
Q9Z1Z2	RecName: Full=Serine-threonine kinase receptor-associated protein;AltName: Full=UNR-interacting protein; - [STRAP_MOU
Q9CYA0	RecName: Full=Cysteine-rich with EGF-like domain protein 2;Flags: Precursor; - [CREL2_MOUSE]
O09061	RecName: Full=Proteasome subunit beta type-1; EC=3.4.25.1;AltName: Full=Proteasome component C5;AltName: F
Q9R1P0	RecName: Full=Proteasome subunit alpha type-4; EC=3.4.25.1;AltName: Full=Proteasome component C9;AltName:
O08677	RecName: Full=Kininogen-1;Contains: RecName: Full=Kininogen-1 heavy chain;Contains: RecName: Full=Bradykinin;Con
P50172	RecName: Full=Corticosteroid 11-beta-dehydrogenase isozyme 1; EC=1.1.1.146;AltName: Full=11-beta-hydroxystero
P67984	RecName: Full=60S ribosomal protein L22;AltName: Full=Heparin-binding protein HBp15; - [RL22_MOUSE]
Q8R2E9	RecName: Full=ERO1-like protein beta; Short=ERO1-L-beta; EC=1.8.4.-;AltName: Full=Oxidoreductin-1-L-beta
Q6ZWX6	RecName: Full=Eukaryotic translation initiation factor 2 subunit 1;AltName: Full=Eukaryotic translation initiation factor 2 su
P14847	C-reactive protein OS=Mus musculus GN=Crp PE=2 SV=1 - [CRP_MOUSE]
P34927	RecName: Full=Asialoglycoprotein receptor 1; Short=ASGP-R 1; Short=ASGPR 1;AltName: Full=Hepatic lectin 1
Q9JM62	RecName: Full=Receptor expression-enhancing protein 6;AltName: Full=Polyposis locus protein 1-like 1;AltName: Full=TB2
Q9CZ13	Cytochrome b-c1 complex subunit 1, mitochondrial OS=Mus musculus GN=Uqcrc1 PE=1 SV=2 - [QCR1_MOUSE]
Q8CIM7	RecName: Full=Cytochrome P450 2D26; EC=1.14.14.1;AltName: Full=CYPIID26; - [CP2DQ_MOUSE]
Q91X72	Hemopexin OS=Mus musculus GN=Hpx PE=1 SV=2 - [HEMO_MOUSE]
P70195	RecName: Full=Proteasome subunit beta type-7; EC=3.4.25.1;AltName: Full=Proteasome subunit Z;AltName: Full=M
Q9DCH4	Eukaryotic translation initiation factor 3 subunit F OS=Mus musculus GN=Eif3f PE=1 SV=2 - [EIF3F_MOUSE]
Q61147	RecName: Full=Ceruloplasmin; EC=1.16.3.1;AltName: Full=Ferroxidase;Flags: Precursor; - [CERU_MOUSE]
Q5FW60	Major urinary protein 20 OS=Mus musculus GN=Mup20 PE=1 SV=1 - [MUP20_MOUSE]
Q91YQ5	RecName: Full=Dolichyl-diphosphooligosaccharide--protein glycosyltransferase subunit 1; EC=2.4.1.119;AltName: Fu
P51410	RecName: Full=60S ribosomal protein L9; - [RL9_MOUSE]
P61982	RecName: Full=14-3-3 protein gamma;Contains: RecName: Full=14-3-3 protein gamma, N-terminally processed; - [1433G
Q8K182	RecName: Full=Complement component C8 alpha chain;AltName: Full=Complement component 8 subunit alpha;Flags: Pre
Q91YW3	RecName: Full=DnaJ homolog subfamily C member 3;AltName: Full=Interferon-induced, double-stranded RNA-activated p
Q8BWY3	RecName: Full=Eukaryotic peptide chain release factor subunit 1; Short=Eukaryotic release factor 1; Short=eR
P32233	RecName: Full=Developmentally-regulated GTP-binding protein 1; Short=DRG-1;AltName: Full=Neural precursor cell
Q91Y97	RecName: Full=Fructose-bisphosphate aldolase B; EC=4.1.2.13;AltName: Full=Liver-type aldolase;AltName: Full=Ald
P99026	RecName: Full=Proteasome subunit beta type-4; Short=Proteasome beta chain; EC=3.4.25.1;AltName: Full=M
Q9WUU7	RecName: Full=Cathepsin Z; EC=3.4.18.1;Flags: Precursor; - [CATZ_MOUSE]
P97290	Plasma protease C1 inhibitor OS=Mus musculus GN=Serping1 PE=1 SV=3 - [IC1_MOUSE]
P35979	RecName: Full=60S ribosomal protein L12; - [RL12_MOUSE]
Q61646	RecName: Full=Haptoglobin;Contains: RecName: Full=Haptoglobin alpha chain;Contains: RecName: Full=Haptoglobin be
Q9CZX8	RecName: Full=40S ribosomal protein S19; - [RS19_MOUSE]
Q9WUZ9	RecName: Full=Ectonucleoside triphosphate diphosphohydrolase 5; Short=NTPDase 5; EC=3.6.1.6;AltName: F
Q9Z2U1	RecName: Full=Proteasome subunit alpha type-5; EC=3.4.25.1;AltName: Full=Proteasome zeta chain;AltName: Full=
O08573	RecName: Full=Galectin-9; Short=Gal-9; - [LEG9_MOUSE]
P99027	RecName: Full=60S acidic ribosomal protein P2; - [RLA2_MOUSE]
Q8BT60	RecName: Full=Copine-3;AltName: Full=Copine III; - [CPNE3_MOUSE]

Q9Z0N1	RecName: Full=Eukaryotic translation initiation factor 2 subunit 3, X-linked;AltName: Full=Eukaryotic translation initiation f
Q8BWQ1	RecName: Full=UDP-glucuronosyltransferase 2A3; Short=UDPGT 2A3; EC=2.4.1.17;Flags: Precursor; - [UD2A3
P70662	RecName: Full=LIM domain-binding protein 1; Short=LDB-1;AltName: Full=Nuclear LIM interactor;AltName: Full=Ca
Q9QZD9	RecName: Full=Eukaryotic translation initiation factor 3 subunit I; Short=eIF3i;AltName: Full=Eukaryotic translation i
P62264	RecName: Full=40S ribosomal protein S14; - [RS14_MOUSE]
P49935	Pro-cathepsin H OS=Mus musculus GN=Ctsh PE=2 SV=2 - [CATH_MOUSE]
Q9R1P3	RecName: Full=Proteasome subunit beta type-2; EC=3.4.25.1;AltName: Full=Proteasome component C7-I;AltName:
P06797	RecName: Full=Cathepsin L1; EC=3.4.22.15;AltName: Full=Major excreted protein; Short=MEP;AltName: Full=
P62270	RecName: Full=40S ribosomal protein S18;AltName: Full=Ke-3; Short=Ke3; - [RS18_MOUSE]
P62259	RecName: Full=14-3-3 protein epsilon; Short=14-3-3E; - [1433E_MOUSE]
Q8VCG4	Complement component C8 gamma chain OS=Mus musculus GN=C8g PE=1 SV=1 - [CO8G_MOUSE]
Q66JS6	RecName: Full=Eukaryotic translation initiation factor 3 subunit J; Short=eIF3j;AltName: Full=Eukaryotic translation
Q9D2G2	RecName: Full=Dihydrolipoyllysine-residue succinyltransferase component of 2-oxoglutarate dehydrogenase complex, mito
P28843	RecName: Full=Dipeptidyl peptidase 4; EC=3.4.14.5;AltName: Full=Dipeptidyl peptidase IV; Short=DPP IV;AltN
P35564	RecName: Full=Calnexin;Flags: Precursor; - [CALX_MOUSE]
Q61838	Alpha-2-macroglobulin OS=Mus musculus GN=A2m PE=1 SV=3 - [A2M_MOUSE]
Q5XJY5	Coatomer subunit delta OS=Mus musculus GN=Arcn1 PE=2 SV=2 - [COPD_MOUSE]
O70194	RecName: Full=Eukaryotic translation initiation factor 3 subunit D; Short=eIF3d;AltName: Full=Eukaryotic translation
Q9ERR7	15 kDa selenoprotein OS=Mus musculus GN=Sep15 PE=1 SV=3 - [SEP15_MOUSE]
Q61702	Inter-alpha-trypsin inhibitor heavy chain H1 OS=Mus musculus GN=Itih1 PE=1 SV=2 - [ITIH1_MOUSE]
P56395	RecName: Full=Cytochrome b5; - [CYB5_MOUSE]
Q8CDN6	RecName: Full=Thioredoxin-like protein 1;AltName: Full=32 kDa thioredoxin-related protein; - [TXNL1_MOUSE]
O70570	RecName: Full=Polymeric immunoglobulin receptor; Short=Poly-Ig receptor; Short=PIgR;Contains: RecName:
Q9R1P1	RecName: Full=Proteasome subunit beta type-3; EC=3.4.25.1;AltName: Full=Proteasome theta chain;AltName: Full=
Q8BYU6	RecName: Full=Torsin-1A-interacting protein 2; - [TOIP2_MOUSE]
P58252	RecName: Full=Elongation factor 2; Short=EF-2; - [EF2_MOUSE]
P38647	RecName: Full=Stress-70 protein, mitochondrial;AltName: Full=75 kDa glucose-regulated protein; Short=GRP-75;Alt
P23116	Eukaryotic translation initiation factor 3 subunit A OS=Mus musculus GN=Eif3a PE=1 SV=5 - [EIF3A_MOUSE]
Q505F5	RecName: Full=Leucine-rich repeat-containing protein 47; - [LRC47_MOUSE]
P14131	RecName: Full=40S ribosomal protein S16; - [RS16_MOUSE]
P29699	RecName: Full=Alpha-2-HS-glycoprotein;AltName: Full=Fetuin-A;AltName: Full=Countertrypin;Flags: Precursor; - [FETUA_
Q8BYB9	Protein O-glucosyltransferase 1 OS=Mus musculus GN=Poglut1 PE=2 SV=2 - [PGLT1_MOUSE]
P07724	RecName: Full=Serum albumin;Flags: Precursor; - [ALBU_MOUSE]
P63323	RecName: Full=40S ribosomal protein S12; - [RS12_MOUSE]
Q01279	RecName: Full=Epidermal growth factor receptor; EC=2.7.10.1;Flags: Precursor; - [EGFR_MOUSE]
P04186	RecName: Full=Complement factor B; EC=3.4.21.47;AltName: Full=C3/C5 convertase;Contains: RecName: Full=Com
O54782	RecName: Full=Epididymis-specific alpha-mannosidase; EC=3.2.1.24;AltName: Full=Mannosidase alpha class 2B mem
Q9D8N0	RecName: Full=Elongation factor 1-gamma; Short=EF-1-gamma;AltName: Full=eEF-1B gamma; - [EF1G_MOUSE]
Q6ZQI3	RecName: Full=Malectin;Flags: Precursor; - [MLEC_MOUSE]
Q99JX4	RecName: Full=Eukaryotic translation initiation factor 3 subunit M; Short=eIF3m;AltName: Full=PCI domain-containin
P19221	RecName: Full=Prothrombin; EC=3.4.21.5;AltName: Full=Coagulation factor II;Contains: RecName: Full=Activation
P07356	RecName: Full=Annexin A2;AltName: Full=Annexin-2;AltName: Full=Annexin II;AltName: Full=Lipocortin II;AltName: Full=
P80314	RecName: Full=T-complex protein 1 subunit beta; Short=TCP-1-beta;AltName: Full=CCT-beta; - [TCPB_MOUSE]
P97821	Dipeptidyl peptidase 1 OS=Mus musculus GN=Ctsc PE=2 SV=1 - [CATC_MOUSE]
P62082	RecName: Full=40S ribosomal protein S7; - [RS7_MOUSE]
Q9D1M0	RecName: Full=Protein SEC13 homolog;AltName: Full=SEC13-related protein;AltName: Full=SEC13-like protein 1; - [SEC1
Q9CR57	RecName: Full=60S ribosomal protein L14; - [RL14_MOUSE]
P62900	RecName: Full=60S ribosomal protein L31; - [RL31_MOUSE]
P16406	RecName: Full=Glutamyl aminopeptidase; Short=EAP; EC=3.4.11.7;AltName: Full=Aminopeptidase A; Sh
P47962	RecName: Full=60S ribosomal protein L5; - [RL5_MOUSE]
P47754	RecName: Full=F-actin-capping protein subunit alpha-2;AltName: Full=CapZ alpha-2; - [CAZA2_MOUSE]
P97351	RecName: Full=40S ribosomal protein S3a;AltName: Full=Protein TU-11; - [RS3A_MOUSE]
Q8R146	RecName: Full=Acylamino-acid-releasing enzyme; Short=AARE; EC=3.4.19.1;AltName: Full=Acyl-peptide hydro

Q8BM72	Heat shock 70 kDa protein 13 OS=Mus musculus GN=Hspa13 PE=2 SV=1 - [HSP13_MOUSE]
P25444	RecName: Full=40S ribosomal protein S2;AltName: Full=40S ribosomal protein S4;AltName: Full=Protein LLRep3; - [RS2_M
P01942	RecName: Full=Hemoglobin subunit alpha;AltName: Full=Hemoglobin alpha chain;AltName: Full=Alpha-globin; - [HBA_MO
Q9QXC1	Fetuin-B OS=Mus musculus GN=Fetub PE=1 SV=1 - [FETUB_MOUSE]
Q9D7N9	RecName: Full=Adipocyte plasma membrane-associated protein;AltName: Full=Protein DD16; - [APMAP_MOUSE]
Q8JZQ9	RecName: Full=Eukaryotic translation initiation factor 3 subunit B; Short=eIF3b;AltName: Full=Eukaryotic translation
P15105	RecName: Full=Glutamine synthetase; Short=GS; EC=6.3.1.2;AltName: Full=Glutamate--ammonia ligase;AltNa
Q9CXW4	RecName: Full=60S ribosomal protein L11; - [RL11_MOUSE]
Q8BI84	RecName: Full=Melanoma inhibitory activity protein 3;AltName: Full=Transport and Golgi organization protein 1; Sho
Q64459	RecName: Full=Cytochrome P450 3A11; EC=1.14.14.1;AltName: Full=CYPIIIA11;AltName: Full=Cytochrome P-450II
P68433	RecName: Full=Histone H3.1; - [H31_MOUSE]
Q6AW46	RecName: Full=Carboxylesterase 7; EC=3.1.1.1;AltName: Full=Carboxylesterase-like urinary excreted protein homolo
P62852	RecName: Full=40S ribosomal protein S25; - [RS25_MOUSE]
Q9CY58	RecName: Full=Plasminogen activator inhibitor 1 RNA-binding protein;AltName: Full=PAI1 RNA-binding protein 1; Sh
O54734	Dolichyl-diphosphooligosaccharide--protein glycosyltransferase 48 kDa subunit OS=Mus musculus GN=Ddost PE=1 SV=2 -
P62281	RecName: Full=40S ribosomal protein S11; - [RS11_MOUSE]

Eluted fraction from wheat germ agglutinin (WGA) column

P08113	RecName: Full=Endoplasmin;AltName: Full=Heat shock protein 90 kDa beta member 1;AltName: Full=94 kDa glucose-reg
P02535	RecName: Full=Keratin, type I cytoskeletal 10;AltName: Full=Cytokeratin-10; Short=CK-10;AltName: Full=Keratin-10
P20029	RecName: Full=78 kDa glucose-regulated protein; Short=GRP-78;AltName: Full=Heat shock 70 kDa protein 5;AltNam
P09103	Protein disulfide-isomerase OS=Mus musculus GN=P4hb PE=1 SV=2 - [PDIA1_MOUSE]
P62908	RecName: Full=40S ribosomal protein S3; - [RS3_MOUSE]
P14206	RecName: Full=40S ribosomal protein SA;AltName: Full=Laminin receptor 1; Short=LamR;AltName: Full=37/67 kDa
P04104	RecName: Full=Keratin, type II cytoskeletal 1;AltName: Full=Cytokeratin-1; Short=CK-1;AltName: Full=Keratin-1;
Q922R8	RecName: Full=Protein disulfide-isomerase A6; EC=5.3.4.1;AltName: Full=Thioredoxin domain-containing protein 7;F
P14211	RecName: Full=Calreticulin;AltName: Full=CRP55;AltName: Full=Calregulin;AltName: Full=HACBP;AltName: Full=Endoplas
Q3UPL0	RecName: Full=Protein transport protein Sec31A;AltName: Full=SEC31-related protein A;AltName: Full=SEC31-like protein
P68040	RecName: Full=Guanine nucleotide-binding protein subunit beta-2-like 1;AltName: Full=Receptor of activated protein kinas
Q6IFX2	RecName: Full=Keratin, type I cytoskeletal 42;AltName: Full=Cytokeratin-42; Short=CK-42;AltName: Full=Keratin-42
Q78PY7	RecName: Full=Staphylococcal nuclease domain-containing protein 1;AltName: Full=p100 co-activator;AltName: Full=100
O08601	RecName: Full=Microsomal triglyceride transfer protein large subunit;Flags: Precursor; - [MTP_MOUSE]
P08003	Protein disulfide-isomerase A4 OS=Mus musculus GN=Pdia4 PE=1 SV=3 - [PDIA4_MOUSE]
P28665	RecName: Full=Murinoglobulin-1; Short=MuG1;Flags: Precursor; - [MUG1_MOUSE]
P11499	Heat shock protein HSP 90-beta OS=Mus musculus GN=Hsp90ab1 PE=1 SV=3 - [HS90B_MOUSE]
Q9JKR6	RecName: Full=Hypoxia up-regulated protein 1; Short=GRP-170;AltName: Full=140 kDa Ca(2+)-binding protein;
Q8BHN3	RecName: Full=Neutral alpha-glucosidase AB; EC=3.2.1.84;AltName: Full=Glucosidase II subunit alpha;AltName: Fu
Q91ZX7	RecName: Full=Prolow-density lipoprotein receptor-related protein 1; Short=LRP-1;AltName: Full=Alpha-2-macroglob
Q8VDN2	RecName: Full=Sodium/potassium-transporting ATPase subunit alpha-1; Short=Na(+)/K(+) ATPase alpha-1 subunit;
P17717	RecName: Full=UDP-glucuronosyltransferase 2B5; Short=UDPGT 2B5; EC=2.4.1.17;AltName: Full=M-1;Flags:
Q8VED5	RecName: Full=Keratin, type II cytoskeletal 79;AltName: Full=Cytokeratin-79; Short=CK-79;AltName: Full=Keratin-7
P07901	RecName: Full=Heat shock protein HSP 90-alpha;AltName: Full=Heat shock 86 kDa; Short=HSP 86; Short=HSP
P29341	Polyadenylate-binding protein 1 OS=Mus musculus GN=Pabpc1 PE=1 SV=2 - [PABP1_MOUSE]

Q6P5E4	UDP-glucose:glycoprotein glucosyltransferase 1 OS=Mus musculus GN=Uggt1 PE=1 SV=4 - [UGGG1_MOUSE]
Q9D1Q6	RecName: Full=Endoplasmic reticulum resident protein 44; Short=ER protein 44; Short=ERp44;AltName: Full=
P57780	RecName: Full=Alpha-actinin-4;AltName: Full=Non-muscle alpha-actinin 4;AltName: Full=F-actin cross-linking protein; - [A
Q60817	RecName: Full=Nascent polypeptide-associated complex subunit alpha;AltName: Full=Alpha-NAC;AltName: Full=Alpha-NA
P28666	Murinoglobulin-2 OS=Mus musculus GN=Mug2 PE=2 SV=2 - [MUG2_MOUSE]
Q3TTY5	RecName: Full=Keratin, type II cytoskeletal 2 epidermal;AltName: Full=Cytokeratin-2e; Short=CK-2e;AltName: Full=
P24456	RecName: Full=Cytochrome P450 2D10; EC=1.14.14.1;AltName: Full=CYPIID10;AltName: Full=Cytochrome P450-16
O08795	RecName: Full=Glucosidase 2 subunit beta;AltName: Full=Glucosidase II subunit beta;AltName: Full=Protein kinase C sub
P11714	Cytochrome P450 2D9 OS=Mus musculus GN=Cyp2d9 PE=1 SV=2 - [CP2D9_MOUSE]
P63325	RecName: Full=40S ribosomal protein S10; - [RS10_MOUSE]
Q9D0F3	RecName: Full=Protein ERGIC-53;AltName: Full=ER-Golgi intermediate compartment 53 kDa protein;AltName: Full=Lectin
Q91W90	RecName: Full=Thioredoxin domain-containing protein 5;AltName: Full=Thioredoxin-like protein p46;AltName: Full=Endop
O08807	RecName: Full=Peroxiredoxin-4; EC=1.11.1.15;AltName: Full=Peroxiredoxin IV; Short=Prx-IV;AltName: Full=T
P01029	Complement C4-B OS=Mus musculus GN=C4b PE=1 SV=3 - [CO4B_MOUSE]
P60710	RecName: Full=Actin, cytoplasmic 1;AltName: Full=Beta-actin;Contains: RecName: Full=Actin, cytoplasmic 1, N-terminally
P56480	RecName: Full=ATP synthase subunit beta, mitochondrial; EC=3.6.3.14;Flags: Precursor; - [ATPB_MOUSE]
P34927	RecName: Full=Asialoglycoprotein receptor 1; Short=ASGP-R 1; Short=ASGPR 1;AltName: Full=Hepatic lectin 1
Q61147	RecName: Full=Ceruloplasmin; EC=1.16.3.1;AltName: Full=Ferroxidase;Flags: Precursor; - [CERU_MOUSE]
P0CG49	Polyubiquitin-B OS=Mus musculus GN=Ubb PE=1 SV=1 - [UBB_MOUSE]
P63017	RecName: Full=Heat shock cognate 71 kDa protein;AltName: Full=Heat shock 70 kDa protein 8; - [HSP7C_MOUSE]
Q01853	RecName: Full=Transitional endoplasmic reticulum ATPase; Short=TER ATPase;AltName: Full=15S Mg(2+)-ATPase p
Q91X72	Hemopexin OS=Mus musculus GN=Hpx PE=1 SV=2 - [HEMO_MOUSE]
Q8R0Y6	RecName: Full=10-formyltetrahydrofolate dehydrogenase; Short=10-FTHFDH; EC=1.5.1.6;AltName: Full=Aldeh
Q9Z2U0	RecName: Full=Proteasome subunit alpha type-7; EC=3.4.25.1;AltName: Full=Proteasome subunit RC6-1; - [PSA7_M
Q64514	RecName: Full=Tripeptidyl-peptidase 2; Short=TPP-2; EC=3.4.14.10;AltName: Full=Tripeptidyl-peptidase II;
P35951	RecName: Full=Low-density lipoprotein receptor; Short=LDL receptor;Flags: Precursor; - [LDLR_MOUSE]
P04938	RecName: Full=Major urinary proteins 11 and 8;AltName: Full=MUP11 and MUP8;Flags: Fragment; - [MUP8_MOUSE]
Q8JZR0	RecName: Full=Long-chain-fatty-acid--CoA ligase 5; EC=6.2.1.3;AltName: Full=Long-chain acyl-CoA synthetase 5;
Q9WUZ9	RecName: Full=Ectonucleoside triphosphate diphosphohydrolase 5; Short=NTPDase 5; EC=3.6.1.6;AltName: F
Q8R1B4	RecName: Full=Eukaryotic translation initiation factor 3 subunit C; Short=eIF3c;AltName: Full=Eukaryotic translation
Q8VCM7	RecName: Full=Fibrinogen gamma chain;Flags: Precursor; - [FIBG_MOUSE]
Q9R1P4	RecName: Full=Proteasome subunit alpha type-1; EC=3.4.25.1;AltName: Full=Proteasome component C2;AltName:
Q9QZW0	RecName: Full=Probable phospholipid-transporting ATPase 11C; EC=3.6.3.1;AltName: Full=ATPase class VI type 11C
P07759	RecName: Full=Serine protease inhibitor A3K; Short=Serpin A3K;AltName: Full=Contrapsin;AltName: Full=SPI-2;Flag
Q8VDJ3	RecName: Full=Vigilin;AltName: Full=High density lipoprotein-binding protein; Short=HDL-binding protein; - [VIGLN_
Q9QUM9	RecName: Full=Proteasome subunit alpha type-6; EC=3.4.25.1;AltName: Full=Proteasome iota chain;AltName: Full=
Q5SW19	RecName: Full=Protein KIAA0664; - [K0664_MOUSE]
Q6GQT9	Nodal modulator 1 OS=Mus musculus GN=Nomo1 PE=1 SV=1 - [NOMO1_MOUSE]
Q64435	RecName: Full=UDP-glucuronosyltransferase 1-6; Short=UDPGT 1-6; Short=UGT1-06; Short=UGT1.6;
Q9DB77	RecName: Full=Cytochrome b-c1 complex subunit 2, mitochondrial;AltName: Full=Ubiquinol-cytochrome-c reductase comp
Q01405	RecName: Full=Protein transport protein Sec23A;AltName: Full=SEC23-related protein A; - [SC23A_MOUSE]
Q8CIM7	RecName: Full=Cytochrome P450 2D26; EC=1.14.14.1;AltName: Full=CYPIID26; - [CP2DQ_MOUSE]
P60843	RecName: Full=Eukaryotic initiation factor 4A-I; Short=eIF-4A-I; Short=eIF4A-I; EC=3.6.1.-;AltName: Fu
P62259	RecName: Full=14-3-3 protein epsilon; Short=14-3-3E; - [1433E_MOUSE]
Q9CZX8	RecName: Full=40S ribosomal protein S19; - [RS19_MOUSE]
Q91YQ5	RecName: Full=Dolichyl-diphosphooligosaccharide--protein glycosyltransferase subunit 1; EC=2.4.1.119;AltName: Fu
P17897	RecName: Full=Lysozyme C-1; EC=3.2.1.17;AltName: Full=Lysozyme C type P;AltName: Full=1,4-beta-N-acetylmura
P61982	RecName: Full=14-3-3 protein gamma;Contains: RecName: Full=14-3-3 protein gamma, N-terminally processed; - [1433G

P20918	Plasminogen OS=Mus musculus GN=Plg PE=1 SV=3 - [PLMN_MOUSE]
P28843	RecName: Full=Dipeptidyl peptidase 4; EC=3.4.14.5;AltName: Full=Dipeptidyl peptidase IV; Short=DPP IV;AltN
Q07113	RecName: Full=Cation-independent mannose-6-phosphate receptor; Short=CI Man-6-P receptor; Short=CI-MP
O70435	RecName: Full=Proteasome subunit alpha type-3; EC=3.4.25.1;AltName: Full=Proteasome component C8;AltName:
O09061	RecName: Full=Proteasome subunit beta type-1; EC=3.4.25.1;AltName: Full=Proteasome component C5;AltName: F
P37040	RecName: Full=NADPH--cytochrome P450 reductase; Short=CPR; Short=P450R; EC=1.6.2.4; - [NCPR_M
P01027	Complement C3 OS=Mus musculus GN=C3 PE=1 SV=3 - [CO3_MOUSE]
Q3U2P1	RecName: Full=Protein transport protein Sec24A;AltName: Full=SEC24-related protein A; - [SC24A_MOUSE]
P26443	RecName: Full=Glutamate dehydrogenase 1, mitochondrial; Short=GDH 1; EC=1.4.1.3;Flags: Precursor; - [DH
P99026	RecName: Full=Proteasome subunit beta type-4; Short=Proteasome beta chain; EC=3.4.25.1;AltName: Full=M
Q99KV1	RecName: Full=DnaJ homolog subfamily B member 11;AltName: Full=ER-associated dnaJ protein 3; Short=ERj3p;
Q68FD5	RecName: Full=Clathrin heavy chain 1; - [CLH_MOUSE]
P21614	RecName: Full=Vitamin D-binding protein; Short=DBP; Short=VDB;AltName: Full=Group-specific component;A
P27773	RecName: Full=Protein disulfide-isomerase A3; EC=5.3.4.1;AltName: Full=Disulfide isomerase ER-60;AltName: Full=
O08705	RecName: Full=Sodium/bile acid cotransporter;AltName: Full=Na(+)/bile acid cotransporter;AltName: Full=Na(+)/taurocho
Q03265	RecName: Full=ATP synthase subunit alpha, mitochondrial;Flags: Precursor; - [ATPA_MOUSE]
Q01279	RecName: Full=Epidermal growth factor receptor; EC=2.7.10.1;Flags: Precursor; - [EGFR_MOUSE]
Q9D1M0	RecName: Full=Protein SEC13 homolog;AltName: Full=SEC13-related protein;Full=SEC13-like protein 1; - [SEC1
Q921X9	RecName: Full=Protein disulfide-isomerase A5; EC=5.3.4.1;AltName: Full=Protein disulfide isomerase-related protein
P11679	RecName: Full=Keratin, type II cytoskeletal 8;AltName: Full=Cytokeratin-8; Short=CK-8;AltName: Full=Keratin-8;
Q5FW60	Major urinary protein 20 OS=Mus musculus GN=Mup20 PE=1 SV=1 - [MUP20_MOUSE]
Q64176	RecName: Full=Liver carboxylesterase 22; Short=Esterase-22; Short=Es-22; EC=3.1.1.1;AltName: Full=E
Q3UPH1	RecName: Full=Protein PRRC1; - [PRRC1_MOUSE]
Q60692	RecName: Full=Proteasome subunit beta type-6; EC=3.4.25.1;AltName: Full=Proteasome delta chain;AltName: Full=
P14246	RecName: Full=Solute carrier family 2, facilitated glucose transporter member 2;AltName: Full=Glucose transporter type 2
P10126	RecName: Full=Elongation factor 1-alpha 1; Short=EF-1-alpha-1;AltName: Full=Eukaryotic elongation factor 1 A-1;
P80318	RecName: Full=T-complex protein 1 subunit gamma; Short=TCP-1-gamma;AltName: Full=CCT-gamma;AltName: Ful
P62960	RecName: Full=Nuclease-sensitive element-binding protein 1;AltName: Full=Y-box-binding protein 1; Short=YB-1;Alt
Q9DBH5	Vesicular integral-membrane protein VIP36 OS=Mus musculus GN=Lman2 PE=2 SV=2 - [LMAN2_MOUSE]
Q61830	Macrophage mannose receptor 1 OS=Mus musculus GN=Mrc1 PE=1 SV=2 - [MRC1_MOUSE]
P63101	RecName: Full=14-3-3 protein zeta/delta;AltName: Full=Protein kinase C inhibitor protein 1; Short=KCIP-1;AltName:
Q8QZY1	RecName: Full=Eukaryotic translation initiation factor 3 subunit L; Short=eIF3l;AltName: Full=Eukaryotic translation
P10518	RecName: Full=Delta-aminolevulinic acid dehydratase; Short=ALADH; EC=4.2.1.24;AltName: Full=Porphobilino
Q63886	UDP-glucuronosyltransferase 1-1 OS=Mus musculus GN=Ugt1a1 PE=2 SV=2 - [UD11_MOUSE]
Q9R1P0	RecName: Full=Proteasome subunit alpha type-4; EC=3.4.25.1;AltName: Full=Proteasome component C9;AltName:
P11276	RecName: Full=Fibronectin; Short=FN;Contains: RecName: Full=Anastellin;Flags: Precursor; - [FINC_MOUSE]
Q61702	Inter-alpha-trypsin inhibitor heavy chain H1 OS=Mus musculus GN=Itih1 PE=1 SV=2 - [ITIH1_MOUSE]
P11438	RecName: Full=Lysosome-associated membrane glycoprotein 1; Short=Lysosome-associated membrane protein 1;
P62281	RecName: Full=40S ribosomal protein S11; - [RS11_MOUSE]
P42932	RecName: Full=T-complex protein 1 subunit theta; Short=TCP-1-theta;AltName: Full=CCT-theta; - [TCPQ_MOUSE]
Q8CFX1	GDH/6PGL endoplasmic bifunctional protein OS=Mus musculus GN=H6pd PE=2 SV=2 - [G6PE_MOUSE]
Q9Z2U1	RecName: Full=Proteasome subunit alpha type-5; EC=3.4.25.1;AltName: Full=Proteasome zeta chain;AltName: Full=
P67984	RecName: Full=60S ribosomal protein L22;AltName: Full=Heparin-binding protein HBp15; - [RL22_MOUSE]
Q8BI84	RecName: Full=Melanoma inhibitory activity protein 3;AltName: Full=Transport and Golgi organization protein 1; Sho
Q9CZ13	Cytochrome b-c1 complex subunit 1, mitochondrial OS=Mus musculus GN=Uqcrc1 PE=1 SV=2 - [QCR1_MOUSE]
Q8R2E9	RecName: Full=ERO1-like protein beta; Short=ERO1-L-beta; EC=1.8.4.-;AltName: Full=Oxidoreductin-1-L-beta
P32261	RecName: Full=Antithrombin-III; Short=ATIII;AltName: Full=Serpin C1;Flags: Precursor; - [ANT3_MOUSE]
Q9JM62	RecName: Full=Receptor expression-enhancing protein 6;AltName: Full=Polyposis locus protein 1-like 1;AltName: Full=TB2
P51410	RecName: Full=60S ribosomal protein L9; - [RL9_MOUSE]
P97290	Plasma protease C1 inhibitor OS=Mus musculus GN=Serping1 PE=1 SV=3 - [IC1_MOUSE]
Q9QY30	Bile salt export pump OS=Mus musculus GN=Abcb11 PE=1 SV=2 - [ABCBB_MOUSE]
P70194	RecName: Full=C-type lectin domain family 4 member F;AltName: Full=C-type lectin superfamily member 13; Short=
Q05117	RecName: Full=Tartrate-resistant acid phosphatase type 5; Short=TR-AP; EC=3.1.3.2;AltName: Full=Tartrate-r
P68510	RecName: Full=14-3-3 protein eta; - [1433F_MOUSE]

Q6ZWX6	RecName: Full=Eukaryotic translation initiation factor 2 subunit 1;AltName: Full=Eukaryotic translation initiation factor 2 su
Q8BWQ1	RecName: Full=UDP-glucuronosyltransferase 2A3; Short=UDPGT 2A3; EC=2.4.1.17;Flags: Precursor; - [UD2A3
Q61838	Alpha-2-macroglobulin OS=Mus musculus GN=A2m PE=1 SV=3 - [A2M_MOUSE]
P62245	RecName: Full=40S ribosomal protein S15a; - [RS15A_MOUSE]
P99027	RecName: Full=60S acidic ribosomal protein P2; - [RLA2_MOUSE]
O54734	Dolichyl-diphosphooligosaccharide--protein glycosyltransferase 48 kDa subunit OS=Mus musculus GN=Ddost PE=1 SV=2 -
O08573	RecName: Full=Galectin-9; Short=Gal-9; - [LEG9_MOUSE]
Q8K182	RecName: Full=Complement component C8 alpha chain;AltName: Full=Complement component 8 subunit alpha;Flags: Pre
P11983	RecName: Full=T-complex protein 1 subunit alpha; Short=TCP-1-alpha;AltName: Full=CCT-alpha;AltName: Full=Tail
O08677	RecName: Full=Kininogen-1;Contains: RecName: Full=Kininogen-1 heavy chain;Contains: RecName: Full=Bradykinin;Con
P35564	RecName: Full=Calnexin;Flags: Precursor; - [CALX_MOUSE]
P24369	RecName: Full=Peptidyl-prolyl cis-trans isomerase B; Short=PPIase B; EC=5.2.1.8;AltName: Full=Rotamase B;A
Q9CYA0	RecName: Full=Cysteine-rich with EGF-like domain protein 2;Flags: Precursor; - [CREL2_MOUSE]
P50580	RecName: Full=Proliferation-associated protein 2G4;AltName: Full=Proliferation-associated protein 1;AltName:
Q91XD7	RecName: Full=Cysteine-rich with EGF-like domain protein 1;Flags: Precursor; - [CREL1_MOUSE]
P35979	RecName: Full=60S ribosomal protein L12; - [RL12_MOUSE]
P62852	RecName: Full=40S ribosomal protein S25; - [RS25_MOUSE]
P56395	RecName: Full=Cytochrome b5; - [CYB5_MOUSE]
Q63880	RecName: Full=Liver carboxylesterase 31; Short=Esterase-31; EC=3.1.1.1;AltName: Full=ES-male;Flags: Precu
Q8R4U0	RecName: Full=Stabilin-2;AltName: Full=Fasciclin, EGF-like, laminin-type EGF-like and link domain-containing scavenger re
P16406	RecName: Full=Glutamyl aminopeptidase; Short=EAP; EC=3.4.11.7;AltName: Full=Aminopeptidase A; Sh
Q8VCG4	Complement component C8 gamma chain OS=Mus musculus GN=C8g PE=1 SV=1 - [CO8G_MOUSE]
P04939	RecName: Full=Major urinary protein 3; Short=MUP 3;AltName: Full=Non-group 1/group 2 MUP15;Flags: Precursor;
P50172	RecName: Full=Corticosteroid 11-beta-dehydrogenase isozyme 1; EC=1.1.1.146;AltName: Full=11-beta-hydroxystero
Q61559	RecName: Full=IgG receptor FcRn large subunit p51; Short=FcRn;AltName: Full=Neonatal Fc receptor;AltName: Full
P23116	Eukaryotic translation initiation factor 3 subunit A OS=Mus musculus GN=Eif3a PE=1 SV=5 - [EIF3A_MOUSE]
O55234	RecName: Full=Proteasome subunit beta type-5; EC=3.4.25.1;AltName: Full=Proteasome epsilon chain;AltName: Fu
Q9D8N0	RecName: Full=Elongation factor 1-gamma; Short=EF-1-gamma;AltName: Full=eEF-1B gamma; - [EF1G_MOUSE]
Q64459	RecName: Full=Cytochrome P450 3A11; EC=1.14.14.1;AltName: Full=CYPIIIA11;AltName: Full=Cytochrome P-450II
Q9DCN2	RecName: Full=NADH-cytochrome b5 reductase 3; Short=Cytochrome b5 reductase; Short=B5R; EC=1.6
Q4LDG0	RecName: Full=Bile acyl-CoA synthetase; Short=BACS; EC=6.2.1.7;AltName: Full=Bile acid-CoA ligase; S
Q5XJY5	Coatomer subunit delta OS=Mus musculus GN=Arcn1 PE=2 SV=2 - [COPD_MOUSE]
Q9QZD9	RecName: Full=Eukaryotic translation initiation factor 3 subunit I; Short=eIF3i;AltName: Full=Eukaryotic translation i
P50285	RecName: Full=Dimethylaniline monooxygenase [N-oxide-forming] 1; EC=1.14.13.8;AltName: Full=Hepatic flavin-co
P32233	RecName: Full=Developmentally-regulated GTP-binding protein 1; Short=DRG-1;AltName: Full=Neural precursor cell
Q2VLH6	Scavenger receptor cysteine-rich type 1 protein M130 OS=Mus musculus GN=Cd163 PE=1 SV=2 - [C163A_MOUSE]
P80315	RecName: Full=T-complex protein 1 subunit delta; Short=TCP-1-delta;AltName: Full=CCT-delta;AltName: Full=A45;
Q9EQH2	Endoplasmic reticulum aminopeptidase 1 OS=Mus musculus GN=Erap1 PE=2 SV=2 - [ERAP1_MOUSE]
Q8C129	RecName: Full=Leucyl-cystinyl aminopeptidase; Short=Cystinyl aminopeptidase; EC=3.4.11.3;AltName: Full=O
Q8VEK3	RecName: Full=Heterogeneous nuclear ribonucleoprotein U; Short=hnRNP U;AltName: Full=Scaffold attachment fact
Q9DD20	RecName: Full=Methyltransferase-like protein 7B; EC=2.1.1.-;Flags: Precursor; - [MET7B_MOUSE]
P23953	Liver carboxylesterase N OS=Mus musculus GN=Es1 PE=1 SV=4 - [ESTN_MOUSE]
Q9Z1Z2	RecName: Full=Serine-threonine kinase receptor-associated protein;AltName: Full=UNR-interacting protein; - [STRAP_MOU
Q8BM72	Heat shock 70 kDa protein 13 OS=Mus musculus GN=Hspa13 PE=2 SV=1 - [HSP13_MOUSE]
Q7TMK9	RecName: Full=Heterogeneous nuclear ribonucleoprotein Q; Short=hnRNP Q;AltName: Full=Synaptotagmin-binding,
Q9CR57	RecName: Full=60S ribosomal protein L14; - [RL14_MOUSE]
Q61129	Complement factor I OS=Mus musculus GN=Cfi PE=1 SV=3 - [CFAI_MOUSE]
P08226	RecName: Full=Apolipoprotein E; Short=Apo-E;Flags: Precursor; - [APOE_MOUSE]
Q9EPU0	RecName: Full=Regulator of nonsense transcripts 1; EC=3.6.1.-;AltName: Full=ATP-dependent helicase RENT1;AltNa
Q99JX4	RecName: Full=Eukaryotic translation initiation factor 3 subunit M; Short=eIF3m;AltName: Full=PCI domain-

	containi
Q9EQK5	Major vault protein OS=Mus musculus GN=Mvp PE=1 SV=4 - [MVP_MOUSE]
P07356	RecName: Full=Annexin A2;AltName: Full=Annexin-2;AltName: Full=Annexin II;AltName: Full=Lipocortin II;AltName: Full=
O08547	RecName: Full=Vesicle-trafficking protein SEC22b;AltName: Full=SEC22 vesicle-trafficking protein homolog B;AltName: Fu
Q8BWY3	RecName: Full=Eukaryotic peptide chain release factor subunit 1; Short=Eukaryotic release factor 1; Short=eR
Q9DBW0	RecName: Full=Cytochrome P450 4V3; EC=1.14.-.-; - [CP4V3_MOUSE]
P56657	Cytochrome P450 2C40 OS=Mus musculus GN=Cyp2c40 PE=2 SV=2 - [CP240_MOUSE]
Q91VS7	RecName: Full=Microsomal glutathione S-transferase 1; Short=Microsomal GST-1; EC=2.5.1.18;AltName: Full=
P60867	RecName: Full=40S ribosomal protein S20; - [RS20_MOUSE]
Q9DBZ5	RecName: Full=Eukaryotic translation initiation factor 3 subunit K; Short=eIF3k;AltName: Full=Eukaryotic translation
Q9R1P1	RecName: Full=Proteasome subunit beta type-3; EC=3.4.25.1;AltName: Full=Proteasome theta chain;AltName: Full=
Q9WVJ3	RecName: Full=Plasma glutamate carboxypeptidase; EC=3.4.17.-;AltName: Full=Hematopoietic lineage switch 2;Flag
P47740	Fatty aldehyde dehydrogenase OS=Mus musculus GN=Aldh3a2 PE=2 SV=2 - [AL3A2_MOUSE]
P10853	RecName: Full=Histone H2B type 1-F/J/L;AltName: Full=H2B 291A; - [H2B1F_MOUSE]
P62082	RecName: Full=40S ribosomal protein S7; - [RS7_MOUSE]
Q9DBG6	RecName: Full=Dolichyl-diphosphooligosaccharide--protein glycosyltransferase subunit 2; EC=2.4.1.119;AltName: Fu
Q61703	RecName: Full=Inter-alpha-trypsin inhibitor heavy chain H2; Short=Inter-alpha-inhibitor heavy chain 2; Short=
Q8R146	RecName: Full=Acylamino-acid-releasing enzyme; Short=AARE; EC=3.4.19.1;AltName: Full=Acyl-peptide hydro
Q9D662	RecName: Full=Protein transport protein Sec23B;AltName: Full=SEC23-related protein B; - [SC23B_MOUSE]
O88451	RecName: Full=Retinol dehydrogenase 7; EC=1.1.1.105;AltName: Full=Cis-retinol/androgen dehydrogenase type 2;
Q921G7	RecName: Full=Electron transfer flavoprotein-ubiquinone oxidoreductase, mitochondrial; Short=ETF-ubiquinone oxido
Q8BT60	RecName: Full=Copine-3;AltName: Full=Copine III; - [CPNE3_MOUSE]
Q9EQH3	RecName: Full=Vacuolar protein sorting-associated protein 35;AltName: Full=Vesicle protein sorting 35;AltName: Full=Mat
O89079	RecName: Full=Coatomer subunit epsilon;AltName: Full=Epsilon-coat protein; Short=Epsilon-COP; - [COPE_MOUSE]
Q8VCR2	RecName: Full=17-beta-hydroxysteroid dehydrogenase 13; Short=17-beta-HSD 13; EC=1.1.-.-;AltName: Full=
P62900	RecName: Full=60S ribosomal protein L31; - [RL31_MOUSE]
Q9D7N9	RecName: Full=Adipocyte plasma membrane-associated protein;AltName: Full=Protein DD16; - [APMAP_MOUSE]
P55302	RecName: Full=Alpha-2-macroglobulin receptor-associated protein; Short=Alpha-2-MRAP;AltName: Full=Low density
Q9D379	Epoxide hydrolase 1 OS=Mus musculus GN=Ephx1 PE=1 SV=2 - [HYEP_MOUSE]
Q91WK2	RecName: Full=Eukaryotic translation initiation factor 3 subunit H; Short=eIF3h;AltName: Full=Eukaryotic translation
Q62186	RecName: Full=Translocon-associated protein subunit delta; Short=TRAP-delta;AltName: Full=Signal sequence recep
P60229	RecName: Full=Eukaryotic translation initiation factor 3 subunit E; Short=eIF3e;AltName: Full=Eukaryotic translation
Q9R0E2	RecName: Full=Procollagen-lysine,2-oxoglutarate 5-dioxygenase 1; EC=1.14.11.4;AltName: Full=Lysyl hydroxylase 1
P97872	Dimethylaniline monooxygenase [N-oxide-forming] 5 OS=Mus musculus GN=Fmo5 PE=2 SV=4 - [FMO5_MOUSE]
Q9CY58	RecName: Full=Plasminogen activator inhibitor 1 RNA-binding protein;AltName: Full=PAI1 RNA-binding protein 1; Sh
Q7TMS5	RecName: Full=ATP-binding cassette sub-family G member 2;AltName: Full=Breast cancer resistance protein 1 homolog;A
Q8JZZ0	RecName: Full=UDP-glucuronosyltransferase 3A2; Short=UDPGT 3A2; EC=2.4.1.17;Flags: Precursor; - [UD3A2
Q8VEK0	RecName: Full=Cell cycle control protein 50A;AltName: Full=Transmembrane protein 30A; - [CC50A_MOUSE]
Q64458	Cytochrome P450 2C29 OS=Mus musculus GN=Cyp2c29 PE=1 SV=2 - [CP2CT_MOUSE]
P12970	RecName: Full=60S ribosomal protein L7a;AltName: Full=Surfeit locus protein 3; - [RL7A_MOUSE]
P33267	RecName: Full=Cytochrome P450 2F2; EC=1.14.14.-;AltName: Full=CYPIIF2;AltName: Full=Naphthalene dehydroge
Q8VCC2	RecName: Full=Liver carboxylesterase 1; EC=3.1.1.1;AltName: Full=Acyl-coenzyme A:cholesterol acyltransferase;Alt
Q91YW3	RecName: Full=DnaJ homolog subfamily C member 3;AltName: Full=Interferon-induced, double-stranded RNA-activated p
Q9ERR7	15 kDa selenoprotein OS=Mus musculus GN=Sep15 PE=1 SV=3 - [SEP15_MOUSE]
Q9DCH4	Eukaryotic translation initiation factor 3 subunit F OS=Mus musculus GN=Eif3f PE=1 SV=2 - [EIF3F_MOUSE]
Q8JZQ9	RecName: Full=Eukaryotic translation initiation factor 3 subunit B; Short=eIF3b;AltName: Full=Eukaryotic translation
P62806	RecName: Full=Histone H4; - [H4_MOUSE]
P26043	Radixin OS=Mus musculus GN=Rdx PE=1 SV=3 - [RADI_MOUSE]

Q9R1P3	RecName: Full=Proteasome subunit beta type-2; EC=3.4.25.1;AltName: Full=Proteasome component C7-I;AltName:
Q9ESP1	RecName: Full=Stromal cell-derived factor 2-like protein 1; Short=SDF2-like protein 1;Flags: Precursor; - [SDF2L_MO
O70251	RecName: Full=Elongation factor 1-beta; Short=EF-1-beta; - [EF1B_MOUSE]
P97855	RecName: Full=Ras GTPase-activating protein-binding protein 1; Short=G3BP-1; EC=3.6.1.-;AltName: Full=AT
O55143	RecName: Full=Sarcoplasmic/endoplasmic reticulum calcium ATPase 2; Short=SR Ca(2+)-ATPase 2; Short=SER
Q99PG0	RecName: Full=Arylacetamide deacetylase; EC=3.1.1.3; - [AAAD_MOUSE]
P47962	RecName: Full=60S ribosomal protein L5; - [RL5_MOUSE]
Q9CRC0	RecName: Full=Vitamin K epoxide reductase complex subunit 1; EC=1.1.4.1;AltName: Full=Vitamin K1 2,3-epoxide r
Q9R0E1	Procollagen-lysine,2-oxoglutarate 5-dioxygenase 3 OS=Mus musculus GN=Plod3 PE=1 SV=1 - [PLOD3_MOUSE]
Q9Z0N1	RecName: Full=Eukaryotic translation initiation factor 2 subunit 3, X-linked;AltName: Full=Eukaryotic translation initiation f
O70570	RecName: Full=Polymeric immunoglobulin receptor; Short=Poly-Ig receptor; Short=PIgR;Contains: RecName
P24668	RecName: Full=Cation-dependent mannose-6-phosphate receptor; Short=CD Man-6-P receptor; Short=CD-MPR
O89020	RecName: Full=Afamin;AltName: Full=Alpha-albumin; Short=Alpha-Alb;Flags: Precursor; - [AFAM_MOUSE]
Q07456	RecName: Full=Protein AMBP;Contains:Full=Alpha-1-microglobulin;Contains: RecName: Full=Inter-alpha-tryp
P68433	RecName: Full=Histone H3.1; - [H31_MOUSE]
Q99PE8	ATP-binding cassette sub-family G member 5 OS=Mus musculus GN=Abcg5 PE=1 SV=1 - [ABCG5_MOUSE]
Q9JIL4	RecName: Full=Na(+)/H(+) exchange regulatory cofactor NHE-RF3; Short=NHERF-3;AltName: Full=PDZ domain-con
P18572	RecName: Full=Basigin;AltName: Full=Basic immunoglobulin superfamily;AltName: Full=Membrane glycoprotein gp42;AltN
Q9D2G2	RecName: Full=Dihydrolipoyllysine-residue succinyltransferase component of 2-oxoglutarate dehydrogenase complex, mito
P52479	RecName: Full=Ubiquitin carboxyl-terminal hydrolase 10; EC=3.1.2.15;AltName: Full=Ubiquitin thioesterase 10;AltNa
Q8CDN6	RecName: Full=Thioredoxin-like protein 1;AltName: Full=32 kDa thioredoxin-related protein; - [TXNL1_MOUSE]
P62264	RecName: Full=40S ribosomal protein S14; - [RS14_MOUSE]
P47963	RecName: Full=60S ribosomal protein L13;AltName: Full=A52; - [RL13_MOUSE]
P57776	RecName: Full=Elongation factor 1-delta; Short=EF-1-delta; - [EF1D_MOUSE]
P62702	RecName: Full=40S ribosomal protein S4, X isoform; - [RS4X_MOUSE]
P33587	RecName: Full=Vitamin K-dependent protein C; EC=3.4.21.69;AltName: Full=Autoprothrombin IIA;AltName: Full=An
Q9DCG2	CD302 antigen OS=Mus musculus GN=Cd302 PE=2 SV=2 - [CD302_MOUSE]
P97461	RecName: Full=40S ribosomal protein S5;Contains: RecName: Full=40S ribosomal protein S5, N-terminally processed; - [R
O88587	RecName: Full=Catechol O-methyltransferase; EC=2.1.1.6; - [COMT_MOUSE]
Q8BSY0	RecName: Full=Aspartyl/asparaginyl beta-hydroxylase; EC=1.14.11.16;AltName: Full=Aspartate beta-hydroxylase;
P06909	RecName: Full=Complement factor H;AltName: Full=Protein beta-1-H;Flags: Precursor; - [CFAH_MOUSE]
P28063	Proteasome subunit beta type-8 OS=Mus musculus GN=Psmb8 PE=1 SV=2 - [PSB8_MOUSE]
P68373	RecName: Full=Tubulin alpha-1C chain;AltName: Full=Tubulin alpha-6 chain;AltName: Full=Alpha-tubulin 6;AltName: Full=
Q8VBT0	RecName: Full=Thioredoxin-related transmembrane protein 1;AltName: Full=Thioredoxin domain-containing protein 1;Flag
Q7SIG6	RecName: Full=Arf-GAP with SH3 domain, ANK repeat and PH domain-containing protein 2;AltName: Full=Development an
P14131	RecName: Full=40S ribosomal protein S16; - [RS16_MOUSE]
Q8K297	RecName: Full=Procollagen galactosyltransferase 1; EC=2.4.1.50;AltName: Full=Hydroxylysine galactosyltransferase
P61164	RecName: Full=Alpha-centractin; Short=Centractin;AltName: Full=Centrosome-associated actin homolog;AltName: F
Q505F5	RecName: Full=Leucine-rich repeat-containing protein 47; - [LRC47_MOUSE]
Q6ZQI3	RecName: Full=Malectin;Flags: Precursor; - [MLEC_MOUSE]
Q60872	RecName: Full=Eukaryotic translation initiation factor 1A; Short=eIF-1A;AltName: Full=Eukaryotic translation initiatio
Q9D1D4	RecName: Full=Transmembrane emp24 domain-containing protein 10;AltName: Full=21 kDa transmembrane-trafficking pr
P97351	RecName: Full=40S ribosomal protein S3a;AltName: Full=Protein TU-11; - [RS3A_MOUSE]
P40336	RecName: Full=Vacuolar protein sorting-associated protein 26A;AltName: Full=Vesicle protein sorting 26A; Short=mV
P10605	RecName: Full=Cathepsin B; EC=3.4.22.1;AltName: Full=Cathepsin B1;Contains: RecName: Full=Cathepsin B light c
Q920A5	Retinoid-inducible serine carboxypeptidase OS=Mus musculus GN=Scpep1 PE=2 SV=2 - [RISC_MOUSE]
Q99L45	RecName: Full=Eukaryotic translation initiation factor 2 subunit 2;AltName: Full=Eukaryotic translation initiation factor 2 su
P28798	RecName: Full=Granulins;AltName: Full=Proepithelin; Short=PEPI;AltName: Full=PC cell-derived growth factor;

P47753	RecName: Full=F-actin-capping protein subunit alpha-1;AltName: Full=CapZ alpha-1; - [CAZA1_MOUSE]
P49722	RecName: Full=Proteasome subunit alpha type-2; EC=3.4.25.1;AltName: Full=Proteasome component C3;AltName:
P24668	RecName: Full=Cation-dependent mannose-6-phosphate receptor; Short=CD Man-6-P receptor; Short=CD-MPR
O89020	RecName: Full=Afamin;AltName: Full=Alpha-albumin; Short=Alpha-Alb;Flags: Precursor; - [AFAM_MOUSE]
Q07456	RecName: Full=Protein AMBP;Contains: RecName: Full=Alpha-1-microglobulin;Contains: RecName: Full=Inter-alpha-tryp
P68433	RecName: Full=Histone H3.1; - [H31_MOUSE]
Q99PE8	ATP-binding cassette sub-family G member 5 OS=Mus musculus GN=Abcg5 PE=1 SV=1 - [ABCG5_MOUSE]
Q9JIL4	RecName: Full=Na(+)/H(+) exchange regulatory cofactor NHE-RF3; Short=NHERF-3;AltName: Full=PDZ domain-con
P18572	RecName: Full=Basigin;AltName: Full=Basic immunoglobulin superfamily;AltName: Full=Membrane glycoprotein gp42;AltN
Q9D2G2	RecName: Full=Dihydrolipoyllysine-residue succinyltransferase component of 2-oxoglutarate dehydrogenase complex, mito
P52479	RecName: Full=Ubiquitin carboxyl-terminal hydrolase 10; EC=3.1.2.15;AltName: Full=Ubiquitin thioesterase 10;AltNa
Q8CDN6	RecName: Full=Thioredoxin-like protein 1;AltName: Full=32 kDa thioredoxin-related protein; - [TXNL1_MOUSE]
P62264	RecName: Full=40S ribosomal protein S14; - [RS14_MOUSE]
P47963	RecName: Full=60S ribosomal protein L13;AltName: Full=A52; - [RL13_MOUSE]
P57776	RecName: Full=Elongation factor 1-delta; Short=EF-1-delta; - [EF1D_MOUSE]
P62702	RecName: Full=40S ribosomal protein S4, X isoform; - [RS4X_MOUSE]
P33587	RecName: Full=Vitamin K-dependent protein C; EC=3.4.21.69;AltName: Full=Autoprothrombin IIA;AltName: Full=An
Q9DCG2	CD302 antigen OS=Mus musculus GN=Cd302 PE=2 SV=2 - [CD302_MOUSE]
P97461	RecName: Full=40S ribosomal protein S5;Contains: RecName: Full=40S ribosomal protein S5, N-terminally processed; - [R
O88587	RecName: Full=Catechol O-methyltransferase; EC=2.1.1.6; - [COMT_MOUSE]
Q8BSY0	RecName: Full=Aspartyl/asparaginyl beta-hydroxylase; EC=1.14.11.16;AltName: Full=Aspartate beta-hydroxylase;
P06909	RecName: Full=Complement factor H;AltName: Full=Protein beta-1-H;Flags: Precursor; - [CFAH_MOUSE]
P28063	Proteasome subunit beta type-8 OS=Mus musculus GN=Psmb8 PE=1 SV=2 - [PSB8_MOUSE]
P68373	RecName: Full=Tubulin alpha-1C chain;AltName: Full=Tubulin alpha-6 chain;AltName: Full=Alpha-tubulin 6;AltName: Full=
Q8VBT0	RecName: Full=Thioredoxin-related transmembrane protein 1;AltName: Full=Thioredoxin domain-containing protein 1;Flag
Q7SIG6	RecName: Full=Arf-GAP with SH3 domain, ANK repeat and PH domain-containing protein 2;AltName: Full=Development an
P14131	RecName: Full=40S ribosomal protein S16; - [RS16_MOUSE]
Q8K297	RecName: Full=Procollagen galactosyltransferase 1; EC=2.4.1.50;AltName: Full=Hydroxylysine galactosyltransferase
P61164	RecName: Full=Alpha-centractin; Short=Centractin;AltName: Full=Centrosome-associated actin homolog;AltName: F
Q505F5	RecName: Full=Leucine-rich repeat-containing protein 47; - [LRC47_MOUSE]
Q6ZQI3	RecName: Full=Malectin;Flags: Precursor; - [MLEC_MOUSE]
Q60872	RecName: Full=Eukaryotic translation initiation factor 1A; Short=eIF-1A;AltName: Full=Eukaryotic translation initiatio
Q9D1D4	RecName: Full=Transmembrane emp24 domain-containing protein 10;AltName: Full=21 kDa transmembrane-trafficking pr
P97351	RecName: Full=40S ribosomal protein S3a;AltName: Full=Protein TU-11; - [RS3A_MOUSE]
P40336	RecName: Full=Vacuolar protein sorting-associated protein 26A;AltName: Full=Vesicle protein sorting 26A; Short=mV
P10605	RecName: Full=Cathepsin B; EC=3.4.22.1;AltName: Full=Cathepsin B1;Contains: RecName: Full=Cathepsin B light c
Q920A5	Retinoid-inducible serine carboxypeptidase OS=Mus musculus GN=Scpep1 PE=2 SV=2 - [RISC_MOUSE]
Q99L45	RecName: Full=Eukaryotic translation initiation factor 2 subunit 2;AltName: Full=Eukaryotic translation initiation factor 2 su
P28798	RecName: Full=Granulins;AltName: Full=Proepithelin; Short=PEPI;AltName: Full=PC cell-derived growth factor;
P47753	RecName: Full=F-actin-capping protein subunit alpha-1;AltName: Full=CapZ alpha-1; - [CAZA1_MOUSE]
P49722	RecName: Full=Proteasome subunit alpha type-2; EC=3.4.25.1;AltName: Full=Proteasome component C3;AltName:

Curriculum Vitae

Name: Balázs Legeza

E-mail: balazs.legeza@unibas.ch

Place and date of birth: Nyíregyháza, March 24, 1982.

Education:

1995-2001 Budapesti Piarista Gimnázium, Budapest Hungary

2001-2009 Semmelweis University, Faculty of Medicine, Budapest Hungary

2009- PhD student at the Division of Molecular and Systems Toxicology, Department of Pharmaceutical Sciences at University of Basel under the supervision of Prof. Alex Odermatt DSc, PhD

Publications:

Kardon T., Senesi S., Marcolongo P., **Legeza B.**, Bánhegyi G., Mandl J., Fulceri R., Benedetti A.: Maintenance of luminal NADPH in the endoplasmic reticulum promotes the survival of human neutrophil granulocytes. FEBS Lett. 2008 Jun 11;582(13):1809-15

Atanasov AG., Nashev LG., Gelman L., **Legeza B**., Sack R., Portmann R., Odermatt A.: Direct protein-protein interaction of 11beta-hydroxysteroid dehydrogenase type 1 and hexose-6-phosphate dehydrogenase in the endoplasmic reticulum lumen. Biochim Biophys Acta Molecular Cell Research 2008 Aug;1783(8):1536-43.

Senesi S.,* **Legeza B**.,* Balázs Z.,* Csala M., Marcolongo P., Kereszturi E., Szelényi P., Egger C., Fulceri R., Mandl J., Giunti R., Odermatt A., Bánhegyi G., Benedetti A.: Contribution of Fructose-6-Phosphate to Glucocorticoid Activation in the Endoplasmic Reticulum: Possible Implication in the Metabolic Syndrome. Endocrinology. 2010 Oct;151(10):4830-9. (*Translational Highlight, J Clin Endocrinol Metab 2010 95: 4478*)

Legeza B., Balázs Z., Nashev LG., Odermatt A.: The microsomal enzyme 17β-hydroxysteroid dehydrogenase 3 faces the cytoplasm and utilizes NADPH generated by glucose-6-phosphate dehydrogenase. Endocrinology. 2013 Jan;154(1):205-13.

Acknowledgments

I thank Professor Alex Odermatt the head of the Division of Molecular and Systems Toxicology, Department of Pharmaceutical Sciences at University of Basel for affording me the opportunity to archieve my PhD study. Being my mentor and supervisor, I admire his wide knowledge of science, his way of analyzing scientific problems from all sides, and his ability to come up with new intriguing ideas and approaches.

I wish to thank Professor Martin Spiess and Professor Jörg Huwyler for devoting time being members of my PhD committee and for their guidance during reviewing my PhD thesis.

I wish to thank Professor József Mandl, the former head of the Department of Medical Chemistry, Molecular Biology and Pathobiochemistry at Semmelweis University, and Professor Angelo Benedetti, the former head of the Department of Pathophysiology, Experimental Medicine, and Public Health at University of Siena for providing the opportunity to participate in the scientific work of the Institutes at Budapest and Siena. I am grateful for the way they have supported and encouraged me in every possible way.

I would like to express my deep gratitude and special thank Professor Gábor Bánhegyi, I am most grateful for his encouragement and for mentorship during my early years as a junior scientist. I could always rely on his advice when needed.

I wish to express my gratitude to my friend and mentor Tamás Kardon for the careing support during my first steps as a junior scientist. He tought me with great passion and was always available to answer all my questions no matter what the issue.

Many thanks are directed to Zoltán Balázs and Lyubomir Nashev my friends and co-authors, their mentorship, encouragement and friendship were vital for me both in the laboratory and far away from work.

I owe my warm thanks to my colleagues and friends, Boonrat Chantong and Aurélie Egert for their great support; I could always rely on their friendship and care when needed.

I wish to thanks Pascal Detampel for huge assistance during protein chromatography, and Dr. Reto Portmann, Suzanne Moes and Dr. Paul Jenö for the protein identification by mass-spectrometry, kindly performed by them.

I want to thank my colleagues Denise Kratschmar, Cornelia Fürstenberger, Julia Birk, Mariangela Meyer, Julia Seibert, Evelyne Aubry, Anna Dzyakanchuk, Christel Gumy, Thierry Da Cunha, Carlos A. Penno, Arne Meyer, Munindra Ruwali, Adam Lister, Orlando Mani, Thomas Ramming, Christian Appenzeller for the cheerful days in the MolTox laboratory and formerly in Bern and for having had the opportunity to work with them.

I owe my warm thanks to my old colleagues in the Department of Medical Chemistry, Molecular Biology and Pathobiochemistry at Semmelweis University. I always felt their support and encouragement during my first steps as a junior student in Budapest, as well as from distance during my PhD study later.

Furthermore, I would like to express my truthful gratitude and special thank all my friend who lend a hand during these years, some with a calm word, some with a reassuring remark, one with a future picture. It was bound to happen.

Probably my warmest thoughts are devoted to my parents and family. I thank you for your constant love, support and encouragement during these years far from home.